ANCHORAGE ZONE DESIGN FOR PRETENSIONED BULB-TEE BRIDGE GIRDERS IN VIRGINIA

By

Eric D. Crispino

Thesis submitted to the faculty of the

Virginia Polytechnic Institute and State University

in partial fulfillment of the requirements for the degree of

MASTER OF SCIENCE

In

CIVIL ENGINEERING

Approved:

Dr. Thomas E. Cousins

Dr. Carin L. Roberts-Wollmann

Dr. Rodney T. Davis

March 1, 2007

Blacksburg, Virginia

Keywords: Anchorage Zone, Pretensioned Bridge Girder, Strut-and-Tie Model

ANCHORAGE ZONE DESIGN FOR PRETENSIONED BULB-TEE BRIDGE GIRDERS IN VIRGINIA

by

Eric D. Crispino

ABSTRACT

Precast/Prestressed concrete girders are commonly used in bridge construction in the United States. The application and diffusion of the prestress force in a pretensioned girder causes a vertical tension force to develop near the end of the beam. Field surveys of the beam ends of pretensioned bridge girders indicate that many of the PCBT beams used in the Commonwealth of Virginia develop cracks within the anchorage zone region. The lengths and widths of these cracks range from acceptable to poor and in need of repair. Field observations also indicate deeper cross sections, very heavily prestressed sections, and girders with lightweight concrete tend to be most susceptible to crack formation.

This research examined a new strut-and-tie based design approach to the anchorage zone design of the PCBT bridge girders used in Virginia. Case study girders surveyed during site visits are discussed and used to illustrate the nature of the problem and support the calibration of the strut-and-tie based model. A parametric study was conducted using this proposed design model and the results of this study were consolidated into anchorage zone design tables. The results of the parametric study were compared to the results obtained using existing anchorage zone design models, international bridge codes, and standard anchorage zone details used by other states. A set of new standard details was developed for the PCBT girders which incorporates elements of the new design approach and is compatible with the anchorage zone design aids.

A 65 ft PCBT-53 girder was fabricated to verify the new strut-and-tie based design model. This girder contained anchorage zone details designed with the new model. The new anchorage zone details were successful at controlling the development of anchorage zone cracks. The new design approach is recommended for implementation by the Virginia Department of Transportation.

Acknowledgements

I would like to thank the members of my committee for the opportunity to conduct this research. Dr. Rodney Davis provided with me endless insight on the nature of the problem and was always available to assist me with questions. Dr. Wollmann and Dr. Cousins provided me with excellent mentorship not only in these research aspects, but in the classroom as well. My sincerest gratitude goes to all of you. This research was possible thanks to the support of the Virginia Transportation Research Council. Over the course of this research project I have had the opportunity to work with several members of this outstanding organization. I extend my gratitude to Dr. Ozyildirim, Bernard Kassner, and Bill Ordel. I was fortunate to have the dedicated support of Ben Dymond, Dennis Huffman, and Brett Farmer, who were all crucial to the success of this project.

My wife Amy provided me with unlimited support over these last two years. You have read through all of my work and offered constructive suggestions no matter how foreign the topics may have been to you. My children, Patrick and Anna, have given me numerous reasons for study breaks and moments of joy during this journey. Finally I would like to thank the Civil and Mechanical Engineering Department at West Point for providing me the opportunity to educate and train the leaders of tomorrow.

Table Of Contents

List of Figures

List of Tables

Chapter 1. Introduction

1.1 Background

1.1.1 Prestressed Concrete Overview

The principle concept behind prestressed concrete is simple: preload a member in such a manner to eliminate or reduce tensile stresses that would occur under anticipated service loads. This idea was first proposed in the United States as early as 1886; however, it was the French engineer Eugene Freyssinet who made prestressed concrete become a reality in the 1930s with numerous advances that are still commonly used today in the prestressed concrete industry (Nilson 1987). In addition to reducing service load stresses, prestressed concrete has other advantages. Cracks can be eliminated or limited to a desired degree and deflections can be controlled. These factors result in improved serviceability of the structure. Prestressed concrete also enables the economical use of high strength concrete and high strength steel. As a result, span length can be increased and smaller and lighter members can be used. Prestressed concrete has a wide range of applications and new uses continue to evolve.

Prestressed concrete is generally grouped into two categories: pretensioned and post-tensioned. During the construction of a pretensioned concrete member, a prestressing strand is stretched between two permanent abutments. Then forms are placed about the tensioned strands and concrete is poured into the forms. As the concrete cures it bonds to the steel. When the concrete reaches a specified compressive strength the strands are cut, typically with an acetylene torch, which permanently transfers the force in the steel to the concrete. During the construction of a post-tensioned concrete member, hollow conduits are placed in the forms before concrete is poured. After the member has been cast and the concrete reaches a specified compressive strength, prestressing strands or rods are placed in the hollow conduits. These steel elements are anchored at one end of the member and tensioned at the other to some specified stress level. Later the steel may be permanently bonded to the inside of the conduit by pumping grout through the conduit.

1.1.2 Anchorage Zone Definition

An anchorage zone refers to the region of the structure in which the prestress force is transferred from the prestressing steel to the concrete and distributed more widely to the member. In post-tensioned structures the anchorage zone is subdivided into the local zone and general zone. The local zone refers to the volume of concrete surrounding and immediately ahead of a mechanical anchorage device which transfers the prestress force to the member. The general zone is the region in which the prestress force spreads out into a linear stress distribution over the entire cross section of the member. The local zone is subjected to very high compressive stresses. These compressive stresses propagate into the member in a curved pattern until a linear stress distribution develops at a distance approximately equal to the member height. As these compressive stresses change direction, tensile stresses develop normal to the axis of the prestress force. These tensile stresses, known as bursting stresses, can be large enough to cause cracking in the member.

In pretensioned structures the local zone term is not applicable since these members do not contain a mechanical anchorage device. The prestress force is introduced gradually by bond between the steel and concrete over a distance known as the transfer length. This force creates compressive stresses which propagate into the member in a curved pattern until a linear stress distribution results. Just as in post-tensioned concrete members the dispersion of the prestress force causes tensile stresses to develop normal to the direction of the prestress force. The stress conditions for pretensioned beams are usually less severe than those for post-tensioned beams because the prestress force is introduced gradually; however, the tensile stresses which develop are often large enough to cause cracks in the member. The relatively thin webs of I-shaped girders in particular are very vulnerable to the development of cracks from the prestress force.

1.1.3 Anchorage Zone Cracking

Field surveys of the beam ends of numerous pretensioned bridge girders indicate that many of the precast bulb-tee (PCBT) beams used in the Commonwealth of Virginia develop cracks within the anchorage zone region. The lengths and widths of these cracks range from acceptable to poor and in need of repair. A diagram of a typical crack pattern

in a PCBT anchorage zone is shown in Figure 1-1. It is common for a horizontal crack to develop at the intersection between the bottom flange and the web. This crack may extend longitudinally 12 to 18 in. into the beam. It is also very common for a diagonal crack to develop in the upper portion of the web. This crack will generally start several inches in from the end of the beam; close to the location where the harped strands first enter the web region and will extend on a downward angle. In many cases this diagonal crack may extend several feet into the girder. Occasionally additional horizontal cracks develop throughout the depth of the web.

Cracks such as those shown in Figure 1-1 generally form at the time of prestress release or within a few days of release. The diagonal crack will typically form as the member is lifted off the precast bed. During the lifting process the self weight of the girder is acting on the lifting provisions located several feet in from the end of the beam which enables cracks to open and propagate further. As the self weight acts on the lifting provision it is removed from the general zone which eliminates the clamping action that helps prevent cracks from propagating. Field observations indicate deeper cross sections tend to be more susceptible to crack formation than shallow cross sections. Additionally, beams cast with lightweight concrete tend to display more cracks due to the reduced tensile strength of the lightweight concrete and reduced modulus of elasticity. The cracking shown in Figure 1-1 represents a worst case scenario. Some beams may develop one crack or none at all while in extreme cases several cracks may form as shown in Figure 1-1.

The general zone of a prestressed bridge girder is a region of complex stress behavior. This region has a very high negative moment caused by the prestress force which creates shear distortion of the girder web. This shear distortion is evident from field observations of girders which have anchorage zone cracking as shown in Figure 1-1. From these observations it has been noted that there is also slip along the crack lines in girders with extensive anchorage zone cracking problems. This slippage suggests the stirrups crossing these cracks are carrying tension force and shear force (or dowel action) as well.

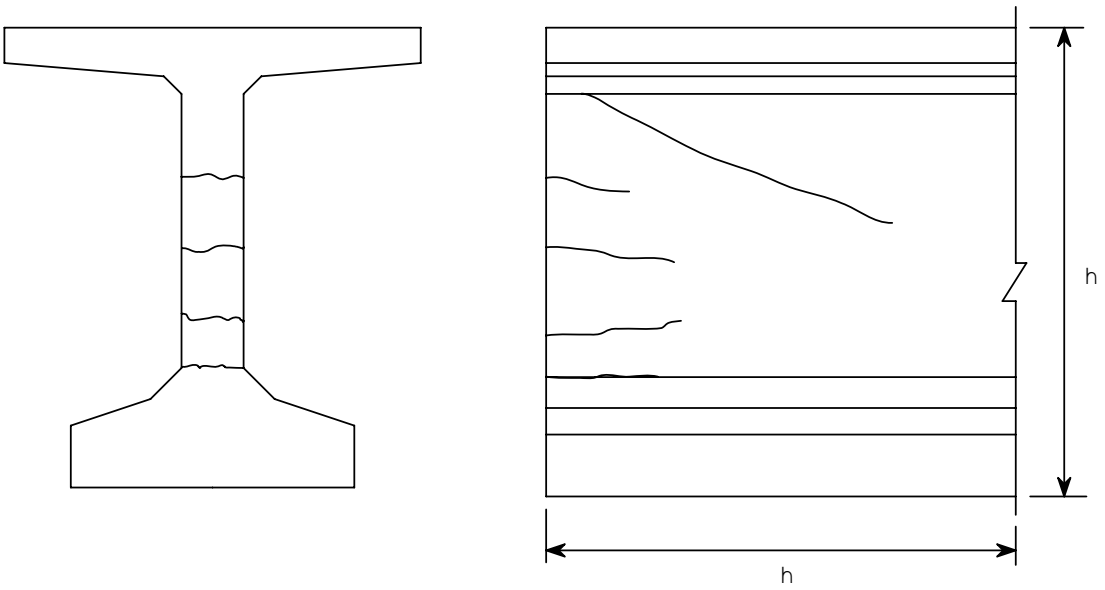

Figure 1-1. Common crack pattern in PCBT anchorage zone

1.1.4 Serviceability and Structural Issues

The presence of cracks in an anchorage zone can be important to the serviceability of the beam. If the crack widths are large enough, moisture can penetrate the section and lead to corrosion of the reinforcement. In some cases a beam end may be enclosed in a cast-in-place diaphragm limiting the exposure to moisture and the cracks may not be a cause for concern. In other cases the beam end may remain exposed to de-icing salts and moisture throughout the service life of the member. An example of such a condition would be a beam end that is adjacent to an expansion joint within a bridge. Beams in bridges which are located in marine environments must be held to a higher standard with respect to beam end cracking, than beams in inland bridges due to the corrosive nature of the salt water.

Repair of these cracks can be costly and time consuming and few repair options exist. One commonly used method of crack repair is epoxy injection. During this procedure an epoxy solution is injected into the crack and on the surface of the member along the length of the crack. This type of crack repair; however, can detract from the appearance of the member when it is applied, is expensive, and can result in production

delays. A photo of a repaired PCBT girder which had severe end cracking is shown in Figure 1-2.

Figure 1-2. Photo of a repaired 95 in. PCEF bulb-tee girder from Davis, et al. (2005)

The cracks shown in Figure 1-1 and Figure 1-2 will typically not pose a problem to the structural performance of the girder. If a girder with this type of cracking is used in a simply supported structure, or a simply supported structure made continuous for live load a diagonal compressive strut carrying the shear force to the bearing should intersect these cracks. The additional dead load from the deck may also help to close these cracks. Cracking in the beam end region requires attention if the cracks are very close to the strands or cross the path of the strands. In this case the cracking may reduce the bond of the steel to the concrete and will affect the transfer of prestress force from the steel to the concrete.

Another scenario for concern is cracking in the ends of haunched girders used for spliced girder applications. Cracks in this situation may open and close under normal service conditions which would be detrimental to the performance of the structure. An illustration of a haunched girder with cracking is shown in Figure 1-3. Cracking in the ends of the drop-in girders is also a cause for concern as these cracks may also open and close under service load.

From an ownership and inspection standpoint it is highly desirable to have only minimal crack formation. This will allow the structure to achieve the highest possible rating when it is new and first enters service. This will also ensure that anchorage zone cracks do not become an issue which must be monitored periodically.

Figure 1-3. End cracking in a splice girder pier segment

1.1.5 Anchorage Zone Crack Control Methods

It is important to control the formation of anchorage zone cracks during the design phase by providing adequate vertical reinforcement. The presence of vertical reinforcement will most likely not eliminate cracking, but it can control the widths and lengths of the cracks. Current bridge design specifications prescribe a minimum area of reinforcement; however, field experience in Virginia suggests this minimum is not sufficient to control cracks in many of the large PCBT girders used by the Virginia Department of Transportation (VDOT).

Another method to control crack formation is to debond some number of strands near the end of the beam. Debonding some strands distributes the transfer of prestress force to the concrete over a greater length. Currently no method exists to determine the amount of debonding needed to control cracking. Debonding may also affect the shear capacity of the member and debonded strands may be vulnerable to corrosion. Applying a vertical pretension force at the end of a girder would eliminate the formation of

anchorage zone cracks, but this technique is not an economical solution (Castrodale, et al. 2002). Given the relatively small region vulnerable to these cracks, the most practical solution is to provide enough mild steel reinforcement placed in such a manner to ensure the crack lengths and widths are controlled even if the concrete quality at the beam end is slightly lower than anticipated. The cost of additional reinforcement in the anchorage zone is offset by the advantages for the owner.

A variety of methods have been developed to predict the magnitude of the tensile force at the beam end and enable a designer to develop appropriate reinforcement details. These methods include both experimental and analytical solutions. A recent study conducted by Davis, et al. (2005) proposed a strut-and-tie based analytical model, calibrated from field observations of VDOT PCBT girders to control crack widths and lengths. This new model served as the basis for this research project.

1.2 Objectives and Scope

The main objective of this project was to develop a series of design tables for the anchorage zones of the VDOT PCBT girders. To achieve this goal, a parametric study was conducted using over 270 sample PCBT girders of varying size and prestress force arrangement and magnitude. The results of the parametric study were consolidated into anchorage zone design tables. Additionally the results of the parametric study were compared to other design models, international bridge codes, and to case study girders surveyed during visits to precast manufacturing facilities.

The second objective of this project was to verify the strut-and-tie based model and operational stress recommendations proposed by Davis, et al. (2005) for use in the anchorage zone design of VDOT PCBT bridge girders through a full scale test. To accomplish this objective, a 65 ft PCBT-53 girder was constructed using anchorage zone reinforcement details designed with the new model. The stirrups within the anchorage zone were instrumented to measure stirrup strains, and to verify the strut-and-tie model calibration. The crack patterns of these anchorage zones were recorded and compared to the anchorage zone crack patterns of multiple case study PCBT girders designed in accordance with current specifications.

The final objective was to develop new standard details for the anchorage zones of the VDOT PCBT girders. The new standard details were developed to incorporate elements of the new design model, to control crack formation in the anchorage zone, facilitate potential deck removal or replacement, and to improve field safety for workers during bridge construction. Comparisons of the new VDOT standard details and standard details used by others states were also made. These stirrup details and anchorage zone details are recommended for incorporation in the VDOT standard details for bridges.

1.3 Organization of Thesis

Chapter 2 presents a literature review of previous analytical and experimental methods developed for the design of pretensioned anchorage zones. An overview of strut-and-tie modeling is also included. Chapter 3 presents a series of case studies used to illustrate the calibration of the proposed strut-and-tie model. This chapter then outlines the procedure for the parametric study and presents the results. The results of the parametric study are incorporated into design tables for girders with normal weight concrete and girders with lightweight concrete. Finally Chapter 3 discusses the new standard details for VDOT and provides comparisons of the proposed details to details used by other states. Chapter 4 explains the experimental design, instrumentation, fabrication, and testing of the full scale bridge girder and analysis of the beam performance. The final chapter provides conclusions and recommendations for anchorage zone design and future research.

Chapter 2. Literature Review

2.1 Introduction

A combination of analytical and experimental research has been conducted to develop methods to control cracking in the anchorage zone of pretensioned concrete beams. These various studies have proposed design methods to determine the reinforcement requirement in the beam end region. As pretensioned concrete gained popularity in the United States during the 1950's and 1960's, designers began to take note of the horizontal cracks in the ends of these girders. This problem was first addressed in an experimental study conducted by Marshall and Mattock in 1962. Since this study other researchers have employed strut-and-tie models, finite element analysis, and experimental research programs to attempt to control anchorage zone crack widths and crack lengths in pretensioned bridge girders.

2.2 Current AASHTO Provisions

Article 5.10.10.1 in the *AASHTO LRFD Bridge Design Specifications* (AASHTO, 2004) addresses the design of the anchorage zone in pretensioned concrete girders. This specification requires the placement of enough vertical reinforcement in the end zone to resist a force equivalent to at least 4 percent of the total prestress force at transfer. The maximum working stress in the stirrups is limited to 20 ksi and the specification requires the steel to be evenly distributed within a distance equal to 25 percent of the member height, h. The *AASHTO Standard Specifications for Highway Bridges* (AASHTO, 2003) contains almost the same requirement. Article 9.22.1 in this document requires the same area of reinforcement, but specifies this steel be evenly distributed within a distance equal to 25 percent of the member effective depth. Currently the Virginia Department of Transportation is in the process of converting from the *AASHTO Standard Specifications for Highway Bridges* to the *AASHTO LRFD Bridge Design Specifications*; however, the impact on anchorage zone design will be minimal.

The use of a stirrup working stress of 24 ksi has been proposed, but has not been approved (Castrodale, et al. 2002). Tuan, et al. (2004) recommended increasing the stress

limit to 30 ksi or even 36 ksi following proper experimental justification. These two stress limits are sometimes used for crack control during flexural design. Using a higher working stress limit would result in larger crack widths when the tensile stress in the beam end is large enough to cause cracking.

2.3 International Bridge Code Provisions

2.3.1 Canadian Bridge Code

The *Canadian Highway Bridge Design Code* (CHBDC, 2000) discusses reinforcement design for pretensioned anchorage zones in section 8.16.3.2. This section provides Equation 2-1 for computing a required area of anchorage zone reinforcement.

$$A_{st} \geq \frac{0.08 F_{pu}}{\phi_s f_y} \qquad (2\text{-}1)$$

Where:

F_{pu} = Total specified breaking strength of tendons, N

φ_s = Resistance factor for reinforcing bars, 0.9 for stirrups

f_y = Specified yield strength of reinforcing bars, MPa

The *Canadian Highway Bridge Design Code* (CHBDC, 2000) specifies the area of steel computed with Equation 2-1 shall be uniformly distributed over a distance equal to 0.25*h* from the end of the member. This provision is approximately equivalent to providing a bursting resistance of 3.95 percent of the jacking force and using a stirrup working stress of 20 ksi.

2.3.2 Australian Bridge Code

The *Australian Standard for Bridge Design* (Australian Standard, 2005) addresses anchorage zones in pretensioned members in section 12.2.7. These provisions are almost identical to the AASHTO LRFD provisions. The maximum stress in the stirrups allowed by the Australian Code is 150 MPa which is equal to 21.8 ksi. This difference results in a very slightly smaller area of vertical reinforcement than that required by AASHTO LRFD. The *Australian Standard for Bridge Design* recommends distributing the reinforcement over the same distance as AASHTO LRFD.

2.4 Analytical Methods

2.4.1 General

The stress distribution in the anchorage zone of a pretensioned beam is complicated and can depend on several factors such as the location of prestress force, the magnitude of prestress force, the transfer length, the quantity and arrangement of stirrups, presence of cracks, and the size of the beam cross section. Several authors have used analytical methods such as the cracked beam model, finite element analysis, and strut-and-tie models to approximate this stress distribution.

2.4.2 Gergely and Sozen Cracked Beam Model

Gergely and Sozen (1967) presented an analytical method to design the transverse reinforcement to restrain anchorage zone cracks. The method outlined in the study was based on the equilibrium conditions of a cracked anchorage zone and proposed a method for estimating the position of the first crack. The Gergely and Sozen method assumed that the end region of a prestressed member will have a horizontal crack. With this assumption the authors then analyzed the forces needed to maintain equilibrium within the cracked section.

A free body diagram of a cracked end zone section is shown in Figure 2-1. The beam end, base, and horizontal crack define the boundaries of the free body diagram shown in Figure 2-1 (a). The distance at which the stress distribution caused by the prestress force becomes linear defines the total length of the free body diagram. The forces acting on the free body diagram are shown in Figure 2-1 (b). The applied prestress force P creates a linear stress distribution at a distance L from the beam end. When a horizontal crack forms at a height c from the base of the beam, a moment and a shear force develop on the top surface of the free body diagram. A resisting moment M develops from the tensile force T in the reinforcement and the compression force C in the concrete to maintain equilibrium.

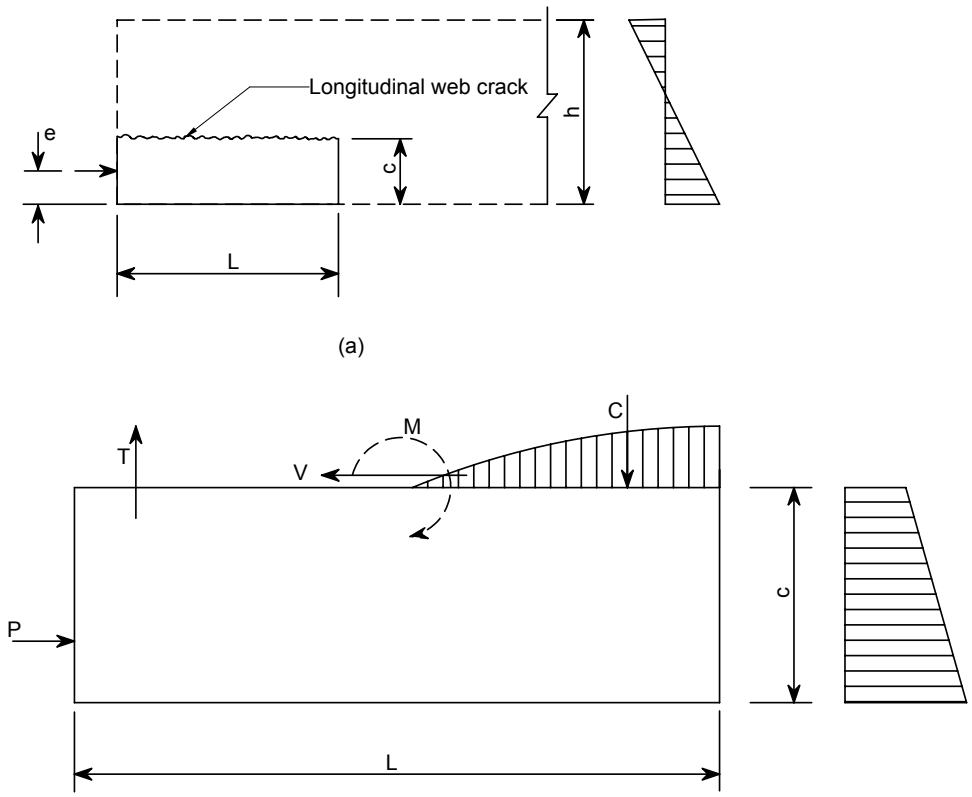

Figure 2-1. Gergely and Sozen cracked section model.

As the height of the free body diagram c changes, the magnitude of the resisting moment also changes. The height c which corresponds to the maximum moment on the section represents the location where the first longitudinal crack is most likely to form. By computing the maximum moment, a designer can determine the forces T and C by estimating a distance between these two forces. The tensile force, T, is located at the center of the anchorage zone stirrup group. The compressive force, C, will act some place between the end of the crack and the end of the free body diagram. Since knowing the exact length of the crack is difficult, Gergely and Sozen positioned this force at a distance *h* from the end face of the beam which represented an upper limit on the distance between the force T and C.

The Gergely and Sozen study also presented a method to control crack widths. Using bond-slip relationships developed from experimental research, Gergely and Sozen presented Equation 2-2 for the limit on the stress in the stirrups to obtain a desired crack width.

$$f_s = \sqrt{\frac{4E\sqrt{f_c^{`}}w}{A}} \qquad (2\text{-}2)$$

Where:

f_s = stress in the stirrups (psi)

E = modulus of elasticity of stirrup (psi)

$f^{`}_c$ = concrete compressive strength at transfer (psi)

A = area of steel of one stirrup (in^2)

w = desired crack width (in)

From equation 2-2 one can determine a stirrup stress based on a desired crack width, and compare this to some maximum allowable stress for the steel. Using the lower of these two values, and knowing the tension force T, the engineer can then determine an area of reinforcement.

The main challenge with this method was determining the value of the maximum moment on the section. The process is relatively straightforward for a rectangular cross section, but it is very complex for I-shaped members. Gergely and Sozen presented a series of equations and tables to assist designers in determining the maximum moment for I-shaped sections. Once the moment is known, the process of computing the tensile force and area of stirrups is straightforward. An experimental study conducted by Tuan, et al. (2004) used the Gergely and Sozen model to predict the location of cracks in their experimental anchorage zone details. This study reported the method was successful at locating the position of crack formation.

The Gergely and Sozen model is very similar to the strut-and-tie based model which is used in this research. The main difference is that the proposed strut-and-tie based model has been calibrated based on the cracks observed to occur in the field. This calibration impacts the location of the ties in the strut-and-tie based model.

2.4.3 Finite Element Modeling

2.4.3.1 General

A finite element analysis can provide useful insight on the flow and diffusion of prestress force into the beam end. Finite element computer programs are widely

available; however, this method of analysis is somewhat impractical for typical design use. Using a linear elastic analysis will indicate locations where cracks are likely to form, but it is difficult to translate these results into the design of reinforcement. Before the reinforcement becomes effective the concrete must crack; however, the presence of a crack will invalidate the linear elastic state and the assumptions used for the analysis. A non-linear analysis may be more effective in the design of reinforcement, but this process is substantially more involved. The anchorage zone design of a pretensioned beam constitutes a relatively small portion of the overall beam design and the time required to create a finite element model is not justified. Additionally early age concrete properties are not known well enough to justify a method with an implied level of accuracy.

2.4.3.2 Kannel, et al. (1997)

Kannel, et al. used a finite element model to investigate the affect of strand cutting pattern on the formation of cracks in pretensioned girders. Their finite element model was relatively simple and was based only on an elastic state. Kannel, et al. did not intend for their model to accurately represent the complex stress distribution in the beam end region; however, they used the model to examine trends in the stress pattern under various strand cutting sequences. While this technique is not useful for the design of pretensioned anchorage zones, the authors did provide some recommendations to help reduce anchorage zone cracking.

Kannel, et al. recommended precutting some of the straight strands before cutting all of the draped strands. The rule of thumb they proposed was to precut one pair of straight strands for every three pairs of draped strands. The study also recommended cutting the straight strands in alternating columns from the interior of the cross section to the outside face of the flange. Finally, they found debonding several strands was effective at controlling cracking. During an experimental portion of the study, Kannel, et al. used plastic sheaths to debond selected strands. The sheaths were placed a few inches in front of the beam end face to create a short plug of bonded concrete to reduce the risk of corrosion of the debonded strands. The combination of debonding and precutting some straight strands was very effective at reducing anchorage zone cracking.

2.4.4 Strut-and-Tie Modeling

2.4.4.1 General

The strut-and-tie model is another useful tool in the analysis of members with a complex stress distribution such as a pretensioned beam end. In a pretensioned anchorage zone the normal assumption for beam theory that plane sections remain plane is not applicable. This type of region is commonly referred to as a disturbed zone or D-region. A strut-and-tie model is a truss model of a D-region made up of struts (compression members) and ties (tension members) connected together at nodes. The compressive forces in the truss are carried by concrete struts and the tensile forces are carried by ties made of mild reinforcement and/or prestresssing steel. The truss model is capable of transferring forces from the D-region at the end of the beam, to the region of the beam where normal beam theory assumptions are applicable. Normally, the length of a D-region for a pretensioned beam end is equal to the total depth of the member. At this length it is assumed that the stress distribution has become linear, and therefore the plane sections remain plane assumption for beam theory is applicable.

An extensive study of strut-and-tie modeling was completed by Schlaich, et al. (1987). This study presented the load path method for developing strut-and-tie models. This method is illustrated in Figure 2-2, which represents a deep beam with a uniformly distributed load applied. In the load path method, stress contours from an elastic analysis are overlaid on the section in Figure 2-2(a). As the forces flow through the member, the contours show that tensile stresses form along the bottom of the member, and compressive stresses form within the member as shown in Figure 2-2(b). The struts and ties of the truss model can be placed near the centroids of these tensile and compressive stresses. The result is the strut and tie model of the member in Figure 2-2(c). The longitudinal struts which exit the model are equal to the applied load and the model satisfies equilibrium. This same model, if rotated 90°, is similar to the scenario within a pretensioned beam anchorage zone.

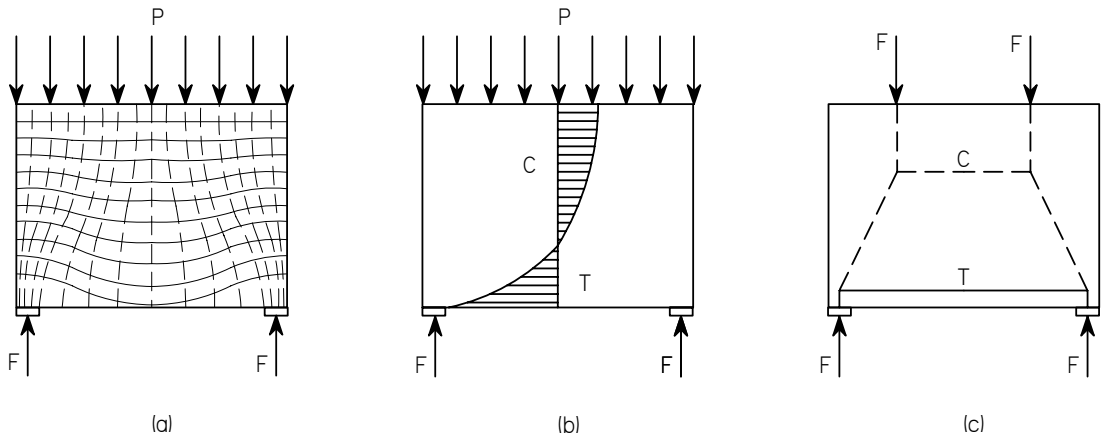

Figure 2-2. Load path method for developing a strut-and-tie model

A strut-and-tie model represents a strength limit state. This implies that the concrete has no tensile capacity. For a given scenario, a variety of strut-and-tie models can be developed. A designer is free to pick the arrangement of the truss model, but some models may yield more conservative results than others. In general, the arrangement of the truss model should follow the flow of elastic force through a section. A designer must be aware however, that when a section begins to crack, the elastic model begins to lengthen. To determine the best arrangement of the strut-and-tie model, a designer must also imagine the flow of forces through a cracked section to ensure the reinforcement is placed properly. A strut-and-tie model must be in equilibrium with all applied loads and reactions; however, a strut-and-tie model does not have to satisfy compatibility. To ensure that crack widths do not become too large, limits are often placed on the stress in the steel.

This type of analysis is commonly used in the design of post-tensioned anchorage zones. The main difference between a post-tensioned anchorage zone and a pretensioned anchorage zone is the method in which the prestress force is applied. In a post-tensioned anchorage zone the prestress forces are applied directly to the concrete at the beam end face by a bearing plate. In a pretensioned anchorage zone the prestress force is applied gradually over the transfer length to the concrete through the bond between the prestress strand and the surrounding concrete. In a strut-and-tie model for a pretensioned beam end the prestress force is assumed to act as a point load on the end surface of the member. This assumption causes strut-and-tie models to typically yield conservative results for

pretensioned anchorage zone design. Despite these conservative results, a strut-and-tie model is a valid method to select the quantity and placement of reinforcement within the beam end to provide adequate strength. Stress limits can also be imposed on the reinforcement to control crack lengths and widths.

2.4.4.2 Castrodale, et al. (2002)

Castrodale, et al. presented a strut-and-tie model to estimate the tension force which develops in the beam end of a pretensioned girder at release. The model was designed to analyze girders with draped strands. The authors applied this model to several girder designs and found the results to suggest that the AASHTO LRFD design requirements for pretensioned anchorage zones may be inadequate for some beams.

The geometry of the strut-and-tie model developed by Castrodale, et al. shown in Figure 2-3, was arranged to reflect the requirements in the 1998 edition of AASHTO LRFD Section 5.10.10.1. The older edition of AASHTO LRFD required the anchorage zone reinforcement be placed within $h/5$ (or $0.2h$) from the end of the girder. Based on this requirement, the center of the reinforcement was located at $0.1h$ which corresponds to the placement of the tie in Figure 2-3. Castrodale, et al. assumed the remainder of the D region from $0.2h$ to h to be in compression. As a result, the compression strut is placed in the center of this compression region at a distance of $0.5h$ from the tie. This strut and tie model ignored the effect of transfer length and applied the prestress force to the end of the beam as a concentrated force. It also applied the prestress force from the draped strands (P1) horizontally, even though it was slightly inclined.

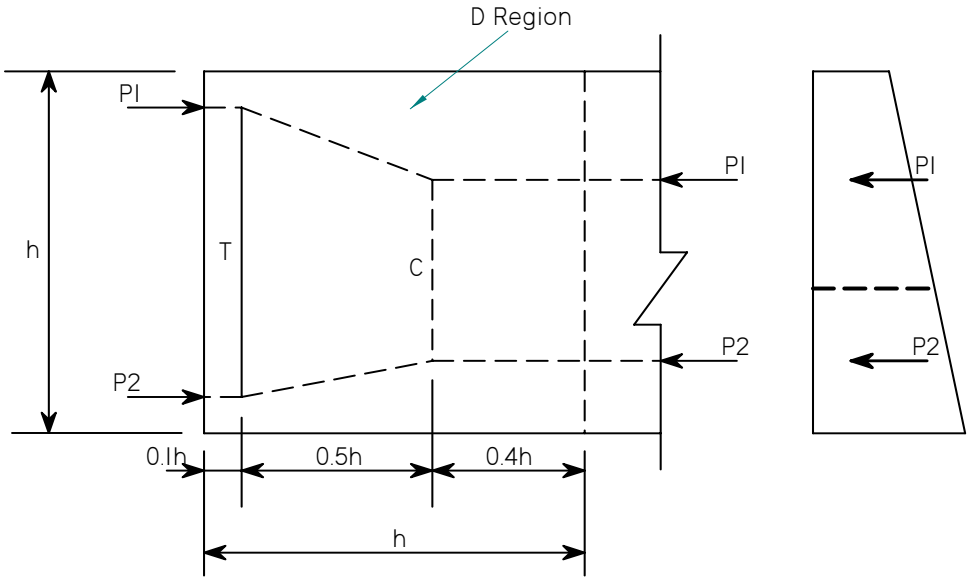

Figure 2-3. Strut-and-tie model for pretensioned beam end

After setting the geometry for the strut-and-tie model, Castrodale, et al. analyzed 20 sample girders of varying cross section. By computing the force in the tie, the authors determined an area of steel required to resist cracking. The authors assumed a working stress for the steel during this analysis of 20 ksi. A sample of the results from the parametric study is shown in Table 2-1.

Table 2-1. Results of parametric study conducted by Castrodale, et al. (2002)

Girder	Total strands	# Draped Strands	# Straight Strands	Prestress force (k)	T (k)	T/Prestress force (%)
Type II	30	12	18	930	45.8	4.93
Type II	14	6	8	434	47.7	11.0
Type IV	68	18	50	2,988	145	4.84
Type IV	32	8	24	1,406	163	11.6
Type VI	80	20	60	3,515	209	5.96
Type VI	40	10	30	1,758	203	11.5
PCI BT-54	40	12	28	1,758	127	7.23
PCI BT-54	20	6	14	879	94.4	10.7
PCI BT-72	40	12	28	1,758	176	10.0
PCI BT-72	20	6	14	879	111	12.6
NEBT 1400	54	12	42	2,373	142	5.98
NEBT 1400	26	6	20	1,143	113	9.86
NEBT 1800	54	12	42	2,373	197	8.28
NEBT 1800	26	6	20	1,143	129	11.3

The results of this analysis showed the magnitude of the tensile force to be quite high in most cases. The ratio of the tensile force to the total prestress force varied from 4.84 percent to 12.6 percent suggesting the current requirement in AASHTO LRFD of a ratio of 4 percent is inadequate. The area of steel required to resist some of these large tension forces would be impossible to provide when using an average working stress of 20 ksi. The results also showed that shallow sections tend to have lower tensile forces suggesting they would be less susceptible to cracking. The authors recognized the results of this model were probably overly conservative and recommended further calibration of the model to better represent actual beam performance.

Castrodale, et al. also used their model to examine various strategies for controlling anchorage zone cracks. These strategies included lowering the height of the draped strands, reducing the number of draped strands, debonding several strands, and using a wider spacing of strands at the end of the girder. By applying one or several of these strategies, they used the strut-and-tie model to evaluate the effect on the magnitude of the tension force. While all of these strategies proved successful at reducing the tensile force, they could also affect other aspects of the overall girder design such as the shear capacity. Castrodale, et al. concluded their model would produce very conservative results when used to predict the reinforcement requirement to control anchorage zone cracking. They also concluded this simple strut-and-tie model was useful at evaluating various strategies to control cracking.

One of the main shortcomings of this strut-and-tie model is that the vertical strut is placed very close to the beam end. This very short model gives a high area of reinforcement required near the end of the beam. This arrangement does not reflect the true stress distribution in the anchorage zone when the member begins to crack. As cracks develop in the anchorage zone, the length of the general zone begins to lengthen and the bars are not properly distributed to control crack propagation.

2.5 Experimental Methods

2.5.1 General

Measuring the complex stress distribution in the anchorage zone of a pretensioned beam is challenging. Several studies have attempted to measure strains in the concrete

and reinforcement in the anchorage zone to develop a method to predict the location and magnitude of the tension force. The design methods which are discussed in the next two sections were developed from experimental studies and have proven successful in controlling crack formation in some cases.

2.5.2 Marshall and Mattock (1962)

Marshall and Mattock conducted one of the earliest experimental investigations into the tensile stresses in the anchorage zones of pretensioned girders at transfer. The study proposed an equation for the design of stirrups to restrict the formation of horizontal cracks. The test program consisted of two series of tests. The first series measured the concrete stresses in the anchorage zones of ten pretensioned girders without stirrups, and the second series measured the strain in the stirrups at the end of 25 pretensioned girders.

The test girders were all less than 25 in. deep which is relatively small in comparison to girders typically used today in bridge construction. During the first test series, strain gages were mounted on the girder surface after the forms were removed. The gages measured vertical tension strain in the concrete over the end region of the girder. The second series of test girders contained stirrups. Strain gages attached to the stirrups measured the vertical tension strains. Using these strains the authors computed the total stirrup force.

From the results of the experimental program, Marshall and Mattock proposed Equation 2-3 to compute the amount of reinforcement to control cracking.

$$A_t = 0.021 \frac{T}{f_s} \frac{h}{l_t} \qquad (2\text{-}3)$$

Where:

A_t = area of stirrup reinforcement (in^2)

T = total prestress force (k)

f_s = maximum working stress in the stirrups (ksi)

h = member depth (in)

l_t = transfer length (in)

Marshall and Mattock recommended distributing the area of steel computed with Equation 2-3 uniformly over a length equal to $h/5$ measured from the end face of the girder and placing the first stirrup as close to the end face as possible.

The study suggested that Equation 2-3 is applicable for a range of values such that $h/l_t \leq 2$. As the ratio of h/l_t increases beyond 2, then Equation 2-3 produces conservative results. Assuming a transfer length of 50 times the strand diameter and a girder with ½ in. diameter strands, then this equation would be applicable for girders 50 in. deep or smaller. Out of the nine standard bulb-tee cross sections used in Virginia, six are larger than 50 in. As a result, Equation 2-3 is not particularly useful for the design of modern day bridge girders in its current form. The provisions for pretensioned anchorage zone design presented in both AASHTO LRFD and *AASHTO Standard Specifications for Highway Bridges* appear to be a simplified form of Equation 2-3. By taking the h/l_t ratio as a constant value of 2, then the equation simplifies to 4 percent of the total prestress force divided by some maximum working stress. Finally, Equation 2-3 was developed from tests on girders which all had two groups of strands, one near the top of the beam and one near the bottom. For beams with other end-loading conditions, such as strands grouped near mid-depth, Equation 2-3 could yield misleading results.

2.5.3 Tuan, et al. (2004)

Tuan, et al. conducted an experimental study into end zone cracking and end zone reinforcement design using actual bridge girders commonly used in construction today. This study consisted of two parts. The first part measured the strains in the end zone stirrups of several girder shapes made in accordance with AASHTO LRFD Section 5.10.10.1. For the second phase of the study, the authors designed and tested new end zone details based upon the observations and measured test results from the first series of tests. The goal of the second phase of the study was to develop new details which could reduce end zone cracking and reduce end zone reinforcement congestion.

During the first phase, Tuan, et al. evaluated the stresses in the anchorage zone reinforcement at release in 12 pretensioned girders designed in accordance with AASHTO LRFD specifications. The girders consisted of six I-shaped cross sections and six inverted tee cross sections. All members used ½ in. diameter strands. Using strain

gages mounted on stirrups in the anchorage zone, the study measured strain in the reinforcement as the strands were released. The results showed the first stirrup had the highest strain, and the strain rapidly decreased as the distance from the end face increased. The strain had totally dissipated at a distance approximately equal to the girder depth from the end face. The maximum stress in any stirrup in the end zone was less than the allowable working stress of 20 ksi prescribed in AASHTO LRFD. Using the sum of the forces in the anchorage zone reinforcement, Tuan, et al. estimated the total tension force in the beam end to be approximately 2 percent of the prestressing force. The beams in this phase typically had several small horizontal cracks in the web which extended longitudinally 8 to 12 in. into the beam.

Based on the results and observations from the first portion of the study, the authors developed new end zone details. The new details were designed from a working stress of 20 ksi in the steel, and the anchorage zone reinforcement was designed to resist only 2 percent of the prestress force. This reinforcement was distributed over a distance of *h/8* from the beam end. The new reinforcement detail used for an I-shaped member is shown in Figure 2-4. The detail included grade 60 deformed bars welded to a steel plate on the bottom of the girder. Small steel plates were also welded to the tops of the deformed bars to help provide enough anchorage. Strain gages were applied in a manner similar to the first phase, and strains were recorded during the release process.

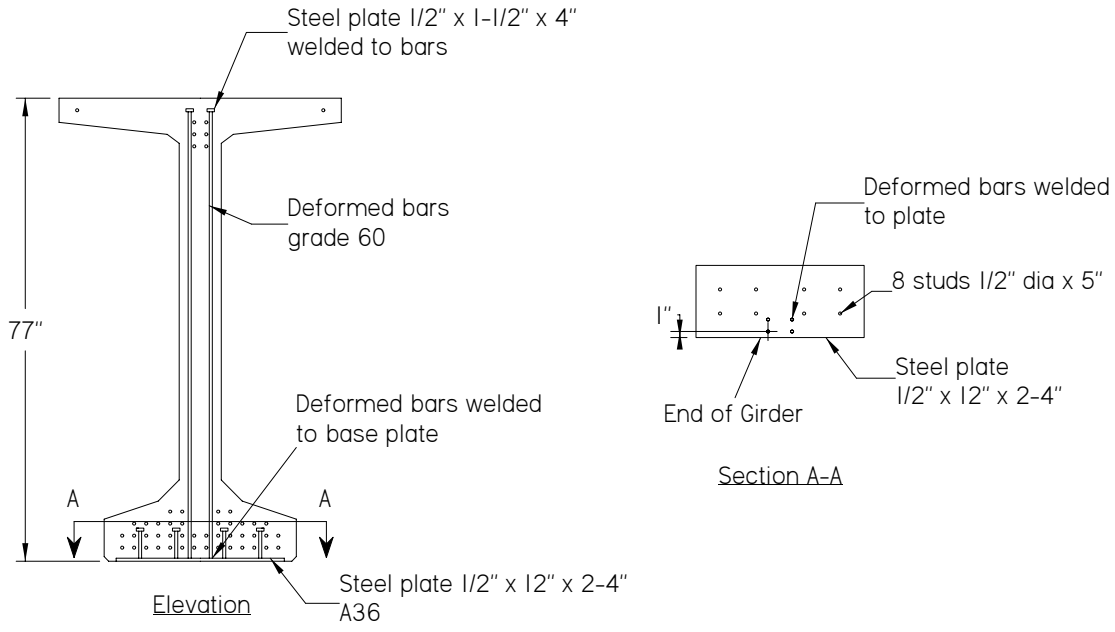

Figure 2-4. Example of experimental details developed by Tuan, et al. (2004)

The strains measured using the new details were smaller than the strains from the first test phase. While cracking still occurred in the girders with the new details, the crack lengths were smaller. The tensile strain distribution over the anchorage zone length followed the same trend as the authors observed in the first test phase, with the first bar having the highest strain. The tensile stress in the stirrups varied from 0.4 to 25.8 ksi. From these results, Tuan, et al. developed a relationship between stirrup stress and the distance from the member end. This relationship is presented graphically in Figure 2-5.

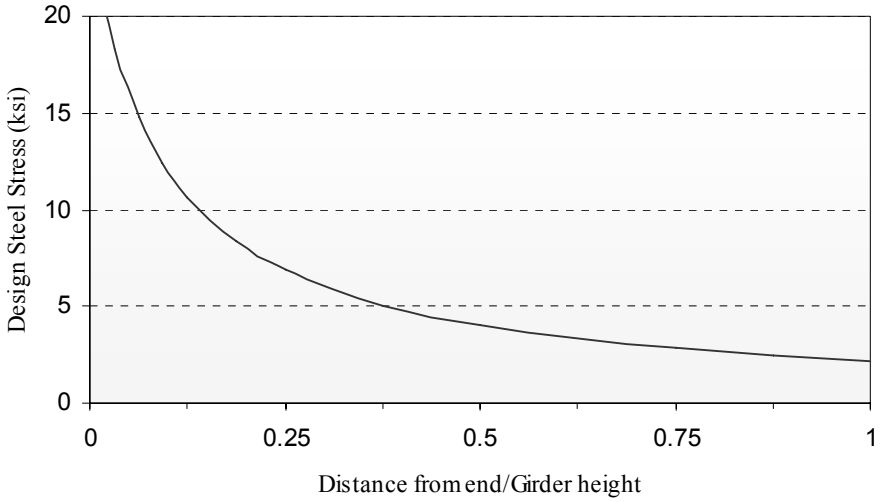

Figure 2-5. Proposed design stress distribution in end zone reinforcement by Tuan, et al. (2004)

Tuan, et al. estimated the total tensile force in the stirrups based upon the tensile stress distribution in the beam end. For stirrups which were not instrumented the authors used linear regression to predict the stress for these bars. The ratio of the tension force to the prestress force for girders from both tests ranged from 0.69 to 3.02 percent. Based on these findings, the authors proposed Equation 2-4 to determine the total area of steel required to resist cracking.

$$A_s = 0.04\frac{P_i}{f_s} \qquad (2\text{-}4)$$

Where:

A_s = total area of reinforcement (in^2)

P_i = initial prestress force before release (k)

f_s = limit for the steel stress (ksi)

The study recommended placing 50 percent of the area of steel computed with Equation 2-4 within a distance of *h/8* from the member end. The authors also recommended using bars welded to the bearing plate within this region as done in the detail shown in Figure 2-4. Finally, they recommended evenly distributing the remainder of the steel over a distance between *h/8* and *h/2* from the end. Beyond this zone, reinforcement shall be provided as required by the shear design. Although the area of steel from Equation 2-4 is the same as required currently by AASHTO LRFD, the

arrangement of the steel and the study found new detailing proved better at controlling cracks.

The anchorage zone cracks in this study were well controlled. It is standard practice in Nebraska to us a gradual release with hydraulic jacks as opposed to flame cutting strands. The authors believed this practice is important to minimize end zone cracking. The average compressive strength of the concrete at transfer was 7,560 psi for the experimental girders in phase two and the average modulus of elasticity at transfer was 5,040 ksi. These values are somewhat higher than the typical values for girders manufactured in Virginia which would also help minimize anchorage zone cracking. The study did not discuss if cracks opened or propagated further when the girder was lifted from the casting bed which is something that has been frequently observed in Virginia.

2.6 Proposed Model for Anchorage Zone Design

2.6.1 General

Davis, et al. (2005) presented a strut-and-tie based model to use for the design of pretensioned anchorage zones. Using case studies of actual bridge girders cast for the Virginia Department of Transportation, the authors calibrated the locations of the struts and ties in the model. From these case studies, Davis, et al. concluded that a group of dense reinforcement placed close to the beam end will not be able to control the diagonal cracks that will form in the beam web of the VDOT PCBT girders. They also concluded that the vertical stiffness of the reinforcement was directly related to crack widths as well as the length of the general zone. The basic design process involves using two strut-and-tie models which are solved separately. One strut-and-tie model is arranged to control cracks at the bulb-to-web interface typically observed in VDOT's PCBT girders. The second strut-and-tie model is arranged to control the formation of diagonal cracks in the web which also commonly form in VDOT PCBT girders.

2.6.2 Method

A generic layout of the strut-and-tie models is shown in Figure 2-6. These two models only consider the forces due to the prestress force. Self weight and the effect of the reaction are neglected to represent the worst case of when the beam is lifted from the

casting bed. The force from the lower strand group is found from integrating the stress over the strand area and is applied as an external force to the beam end. The force in the upper strand group is computed the same way. It is also applied as an external force to the beam end and is assumed to act horizontally, even though it is slightly inclined due to the draping. The locations and magnitudes of the resultant forces are computed by performing a transformed section analysis at a distance equal to *h* from the beam end, and integrating the concrete stress over the concrete area. Once the resultant forces are located, the magnitude of the tension force is computed by summing the moments about points A and B for the upper and lower models respectively. If the analysis is completed correctly, the unbalanced moment is the same in the upper and lower strut-and-tie model.

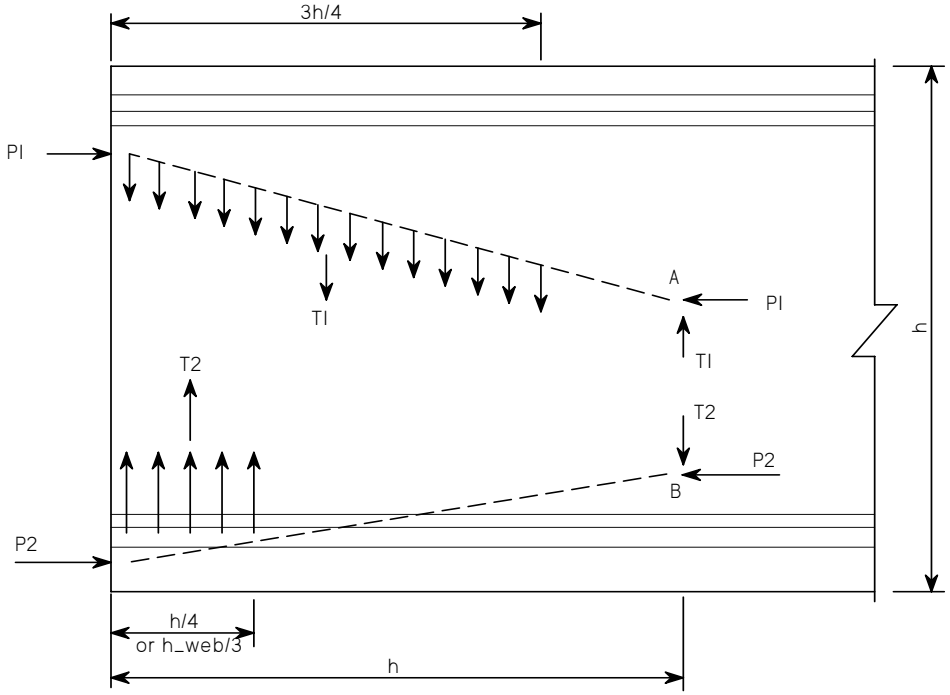

Figure 2-6. Strut-and-tie models proposed by Davis, et al. (2005)

The tension force from the upper strut-and-tie model is assumed to act uniformly over a length equal to *3h/4*. This distance is based upon the lengths of diagonal cracks observed in numerous case studies of PCBT girders made by VDOT. The tension force in the lower strut-and-tie model is assumed to act evenly over a length of *h/4* for small depth sections, and $h_{web}/3$ for larger depth sections, which is also based upon field observations. To compute the area of reinforcement, the authors recommended three options for the working stress in the steel. For normal weight concrete beams in non-

aggressive environments, Davis, et al. recommended a stress of 18 ksi. For lightweight concrete beams or girders exposed to saltwater environments the authors recommended a stress of 12 ksi based upon the tensile strength of lightweight concrete being approximately 20 percent less than that of normal weight concrete and based upon lightweight concrete having a lower modulus of elasticity. Finally for extreme cases, such as splice girder ends, they proposed a stress of 8 ksi. These operating stress levels were selected in order to ensure crack widths were less than 0.012 in. after transfer.

Davis, et al. conducted an initial parametric study using Virginia PCBT girders and the proposed strut-and-tie model. The parametric study found that in short beams, the reinforcement requirement near the beam end is very close to the current requirement of 4 percent of the total prestress force. In larger depth beams, the requirement near the beam end was closer to 5 percent of the total prestress force. Most notably, the study suggested that the stirrup requirement away from the beam end ranged between 4 to 5 percent of the prestress force for larger depth beams. This finding is important as larger depth beams and higher prestress forces become more common and based on the extensive diagonal cracking noted in these beams. The results from this parametric study are shown graphically in Figure 2-7.

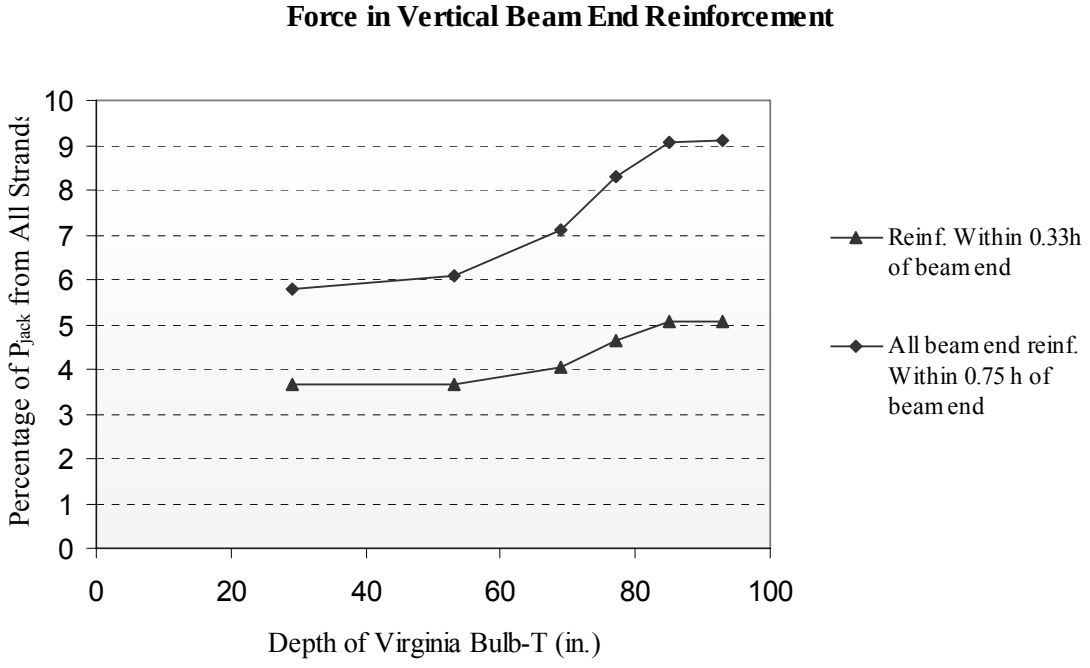

Figure 2-7. Results of parametric study by Davis, et al. (2005)

2.7 Summary of Literature Review

This chapter has summarized previous research conducted on pretensioned anchorage zones. While a large volume of work has been conducted on post-tensioned anchorage zones, relatively little work has been done on pretensioned anchorage zones. This is due primarily to the fact that the prestress force is introduced gradually in a pretensioned anchorage zone and the magnitude of the tension force near the beam end is smaller. Nevertheless, the research outlined above suggests that the current provisions for pretensioned anchorage zone design are inadequate and perhaps outdated. This research will attempt to verify a new design method for the anchorage zones of VDOT's standard PCBT girders.

Chapter 3. Development of Design Aids and Standard Details

3.1 Introduction

This chapter begins with a presentation of case study girders surveyed during several trips to a precast yard in Virginia. These case studies illustrate some of the deficiencies of anchorage zones in girders designed with the current AASHTO LRFD provisions. The theory and goals of the proposed model are discussed and a design example is completed using the full strut-and-tie based model. The next portion of this chapter discusses the procedure and results from the parametric study which was conducted using this model. The results from the parametric study were consolidated into anchorage zone design tables, and these tables are compared to other design models, international bridge codes, and to the case study girders. The last portion of the chapter discusses how the aspects of the proposed design model are incorporated into new standard anchorage zone details for Virginia. The new details for Virginia are compared to the standard details used by several states throughout the country.

3.2 Beam End Case Studies

3.2.1 General Field Observations

To begin this research several trips were made to Bayshore Concrete Products Corporation (Bayshore) located in Cape Charles, VA. This facility manufactures many of the PCBT girders for bridges used throughout Virginia. During the visits to this facility, the ends of numerous PCBT girders were studied to measure crack lengths and crack widths. In general the PCBT-37, 45, 53, and 61 girders displayed minimal anchorage zone cracking when designed in accordance with AASHTO LRFD provisions, and the larger girders such as the PCBT-77 and 93 displayed a high level of cracking. The PCBT-69 and 85 girders were not observed during the site visits; however, it can be assumed they would perform similarly to the other large girders.

Crack widths were measured using a crack comparator card. All of the girders observed had been hand rubbed with a mortar mixture to minimize surface defects. The cracks in the end region, however, were still visible and the widths could be reasonably

estimated with a crack comparator. The length of the cracks were also measured and recorded. Photographs of the girders were taken and are shown in the following sections. The cracks in the photographs have been highlighted for emphasis.

3.2.2 Fair Beam Ends

The girder shown in Figure 3-1 is a 53 in. bulb-tee with 44, ½ in. strands with six of the strands harped. The total prestress force was 1,368 kips at the time the strands were tensioned. The crack pattern shown in Figure 3-1 was typical of eight other beams with the same magnitude of prestress force and stirrup arrangement. The area of vertical reinforcement within a distance of $h/4$ from the end of the girder was 3.1 in^2 and this region was free of cracks. A diagonal crack formed near the top flange-web interface several inches in from the end of the beam and extended a length of almost 60 percent of the girder height. The widest portion of this crack measured approximately 0.010 in. This crack width would be acceptable for most bridge girders not exposed to salt water environments.

This case study illustrates that the dense reinforcement close to the beam end required by AASHTO LRFD, will not control diagonal cracks that can form in the web. It also suggests that the length of the general zone is longer than $h/4$ and the vertical reinforcement for the anchorage zone should extend farther into the beam. This girder was classified as fair because of the length of the diagonal crack. It is desired for any diagonal cracks which develop near the top flange to terminate within $h/2$. Diagonal cracks which terminate within h/2 often tighter and are less of a concern to bridge inspectors. The diagonal crack in this girder was not repaired.

Figure 3-1. PCBT-53 anchorage zone case study – fair condition

The girder shown in Figure 3-2 is a 107 ft long PCBT-61 which contained a total of 48, ½ in. diameter strands. Forty of the strands were straight and 8 strands were harped. The top row of harped strands was raised to 8-¾ in. below the surface of the top flange at the beam end. The total prestress force at the time the strands were tensioned was 1,490 kips. The stirrup detail at the beam end was robust. Within a length of *h*/4 from the beam end, seven No. 4 stirrups were provided at 2 in. spacing for a stirrup area of 2.8 in^2.

Figure 3-2 shows the cracks which formed in the girder. This cracking was typical of four other girders with the same prestress pattern and stirrup arrangement also studied. A diagonal crack opened and extended longitudinally into the beam for a length of almost 50 percent of the beam height. This crack formed close to the harped strands and extended on a downward angle slightly steeper than these strands. The diagonal crack did not appear to cross the path of the harped strands. The presence of the two columns of holes near the beam end created stress concentrations and most likely contributed to this crack propagation. Additionally, the harped strands in this girder were not raised to full height at the beam end which resulted in a slightly larger eccentricity of the prestress force. This factor was also likely to have contributed to crack development and propagation. Two horizontal cracks formed in the lower portion of the web. The

lowest crack extended longitudinally 16 in. which is approximately 26 percent of the beam height. The middle crack extended only about 8 in. into the beam. All cracks widths were less than 0.008 in. which is an acceptable width for girders in most bridges. This girder is classified as fair because of the lengths of the cracks in the lower portion of the web. It is desired for longitudinal web cracks to terminate in a length less than $h/4$ and for diagonal cracks to terminate in a length less than $h/2$. The crack lengths in the lower portion of the web in this case study girder slightly exceeded these limits.

Figure 3-2. PCBT-61 anchorage zone case study – fair condition

3.2.3 Poor Beam Ends

The case study beam shown in Figure 3-3 is a PCBT-77 bridge girder stressed with 34, 0.6 in. diameter prestress strands. The total jacking force was 1,509 kips. The cracking in this girder was typical of five other beams surveyed which all had identical prestress force and stirrup arrangement at the beam end. The girders all displayed numerous cracks near the beam end. The longest diagonal crack started near the top flange and extended a distance of 70 percent of the girder height. Several of the cracks in the lower portion of the web extended longitudinally a distance of over 40 percent of the girder height. The maximum width of all cracks measured 0.010 in. which again is acceptable for girders located in inland structures. The area of vertical reinforcement

within a distance of $h/4$ from the beam end was 2.8 in^2, which met the minimum requirements from AASHTO LRFD. This case study girder is classified as poor because of the lengths of the diagonal cracks that developed near the top flange and throughout the depth of the web. This case study effectively illustrates that deep girders with high levels of prestress force are prone to cracking in the end region. It also illustrates that the current minimum area of steel required by AASHTO LRFD clearly is not sufficient in deep girders. Finally, this girder also emphasizes that the length of the general zone is longer than a length of $h/4$. The cracks in this girder were not repaired.

Figure 3-3. PCBT-77 anchorage zone case study – poor condition

Another example of a poor beam end is shown in Figure 3-4. This girder is also a PCBT-77. It was 106 ft. long and contained a total of 30, 0.6 in. diameter strands.

Twenty-four of the strands were straight and six were harped. The magnitude of prestress force at the time the strands were tensioned was 1,320 kips. The area of vertical reinforcement provided within $h/4$ from the beam end was 2.0 in^2. This is slightly below the minimum reinforcement requirement outlined in AASHTO LRFD. The cracking at the end of the girder was severe and is shown below in Figure 3-4. The cracks in this girder were surveyed after it was placed on the bearing pads of a bridge recently constructed in Virginia. This span of the bridge contained five girders and all of them exhibited a similar crack pattern. The composite deck was not poured at the time the cracks were surveyed.

Figure 3-4. PCBT-77 anchorage zone – poor condition

The longest diagonal crack extended longitudinally into the beam almost 70 percent of the girder height. The horizontal crack near the bottom flange extended over 50 percent of the girder height into the beam. The maximum crack width measured was 0.01 in. The anchorage zone in this girder is classified as poor because of the lengths of the cracks which developed. This case study illustrates the level of damage that can occur in the beam end region if the anchorage zone is not correctly designed. The

uppermost diagonal crack is very close to the path of the harped strands. If these cracks cross the path of the strands the bond between the steel and concrete may be reduced and the structural performance of the girder may be adversely affected. Just as the previous PCBT-77 girder, this beam highlights the shortcomings of the current AASHTO LRFD anchorage zone design requirements.

3.2.4 Poor Beam End With Repairs

The next case study shows a girder which experienced severe anchorage zone cracking and was subsequently repaired by epoxy injection. The girder in Figure 3-5 is a 95.5 in. PCEF Bulb-Tee girder constructed from lightweight concrete. The unit weight of the concrete was about 120 lb/ft^3 and the tensile strength of the concrete was approximately two-thirds that of normal weight concrete with the same design strength. It contained 56, ½ in. diameter strands with eight of the strands harped. The area of reinforcement within a distance of $h/4$ from the beam end slightly exceeded the minimum requirement from AASHTO LRFD.

The reinforcement pattern was not sufficient to control crack lengths and widths. The diagonal crack near the upper flange extended 69 in. in length and had a width up to 0.025 in. As a result of the large crack widths, the girder was repaired by epoxy injection as seen in Figure 3-5. An important factor which affects the level of cracking in the beam end is the tensile strength of the concrete. As split-cylinder tests demonstrated for this girder, the splitting tensile strength of the concrete at transfer was approximately two-thirds that of normal weight concrete with similar design strength. Current AASHTO LRFD provisions for anchorage zone design do not consider the concrete material properties. This case study shows that girders made from lightweight concrete are particularly prone to anchorage zone cracking. This case study is also presented to illustrate the severity of cracking that can occur in very large, heavily prestressed girders.

Figure 3-5. 95.5 in. PBCT beam ends with repairs. Photograph from Davis, et al. (2005)

3.2.5 Drop-in Girders and Pier Segments

The final case study shown in Figure 3-6 is a 95.5 in. lightweight bulb-tee girder used as a "drop-in" segment in a splice girder bridge. This girder was lightly stressed with 16, 0.6 in. diameter strands to provide a jacking force of 656 kips. The member had no harped strands. The vertical reinforcement within $h/4$ from the beam end was 1.24 in^2. As Figure 3-6 shows, several longitudinal cracks developed in the web of the girder. These cracks were measured to be 0.010 in. or less and extended a length of almost 30 percent of girder height. Also, it is important to note the proximity of these cracks to the post tensioning ducts. This case study girder is classified as poor because of the lengths of the horizontal cracks which developed. This case study again illustrates the shortcomings in the current AASHTO LRFD provisions when applied to deep girders.

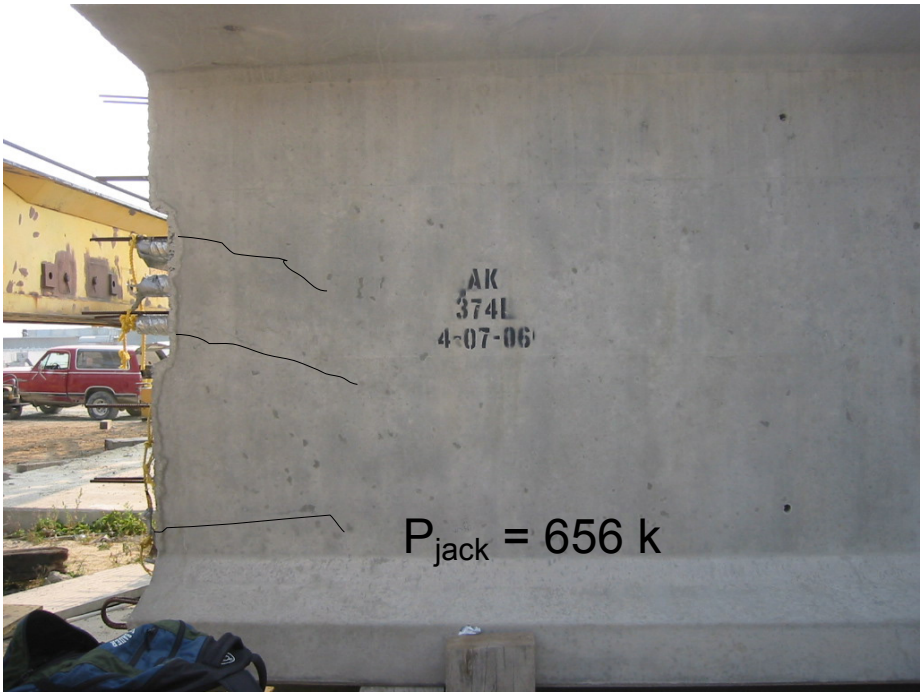

Figure 3-6. Drop in girder with anchorage zone cracking

Pier segments with anchorage zone cracking are also an area of concern. During site visits to Bayshore, diagonal and horizontal cracks were observed on deep haunched girders as shown in Figure 3-7. Cracking of this type could be detrimental to girder strength. When a girder with this type of cracking is in service, tension must cross the crack. As a result the crack could open and close as traffic crosses the bridge.

An example of this exact type of problem is shown in Figure 3-8. This photograph shows the connection between a pier segment and a drop in girder from a project recently completed in Virginia. The pier segment rests on the pier bent and is in the right hand portion of the photograph. A drop in girder is on the left portion of the photograph. The cracking at the ends of these two girders is clear in the photograph and have not been highlighted for emphasis. It was observed that these cracks open and close under traffic loads as evident from flaking along the crack edges.

Figure 3-7. Anchorage zone cracking observed in deep haunched girders

Figure 3-8. Anchorage zone cracking of in-service haunched girder and "drop-in" girder (photograph by Rodney T. Davis)

3.2.6 Summary of Field Observations

As these case studies illustrate, anchorage zone cracking in VDOT PCBT girders is a common problem and additional research is required. The requirements outlined in the AASHTO LRFD specifications are not sufficient to control crack formation in most large girders. Horizontal cracks were typically seen to form at the bottom flange-web interface and extend longitudinally up to 25 percent of the girder height. Diagonal cracks would frequently develop several inches in from the end of the beam and would propagate longitudinally as far as 75 percent of the girder height. Anchorage zones in deep girders developed the most cracks and anchorage zones in girders such as the PCBT-61 and the smaller sections usually performed adequately when designed by AASHTO LRFD. Girders which have too little reinforcement at the end often have longer and worse diagonal cracking. Girders which have ample reinforcement near the end, may have little cracking within the first few inches, but diagonal cracking may still develop.

3.3 New Design Model Theory and Goals

3.3.1 General

The basic goal of this new strut-and-tie based design approach is to provide enough stirrup area, correctly distributed within the anchorage zone, to provide a path for the vertical forces and distortional tensile stresses to follow without causing excessive anchorage zone cracking. This will reduce concerns from inspectors and owners as girders are placed into service. It is clear from the field observations that many of the girder ends designed with AASHTO LRFD do not provide sufficient vertical resistance to control cracking. Additionally, the region of dense reinforcement within $h/4$ will not provide enough resistance to control the formation and propagation of diagonal cracks in the upper portion of the web since this crack will typically form several inches from the end of the beam (between $h/8$ and $h/4$). This new design model will consider the region from $h/4$ to $3h/4$ as part of the anchorage zone. Current provisions do not consider this region as part of the anchorage zone, however; field observations suggest this region is highly affected by the diffusion of the prestress force. The following section will relate

the field observations from the previous case studies to the calibration of the strut-and-tie model.

3.3.2 Calibration of the Strut-and-Tie Model

The basic layout of the strut-and-tie models are shown in Figure 3-9. The placement of the vertical struts and ties within the upper and lower strut-and-tie models was developed from the field observations made in the beginning of this chapter. In the lower strut-and-tie model, the tie is centered at a distance of $h/8$ from the end of the beam. The reinforcement for this force is uniformly distributed over a distance of $h/4$ from the beam end. This placement relates to the observation that horizontal cracks within the web typically extended out a distance of 25 percent of the total girder depth. In the upper strut-and-tie model, the tie is centered at a distance of $3h/8$ from the end of the beam. The reinforcement for this force is uniformly distributed over a distance of $3h/4$ from the beam end. The placement of this tie relates to the observation of diagonal cracks in the upper portion of the web that may extend out to a distance of 75 percent of the total girder depth as seen in lightly reinforced beams. This calibration will dictate the stirrup density or distribution in the anchorage zone.

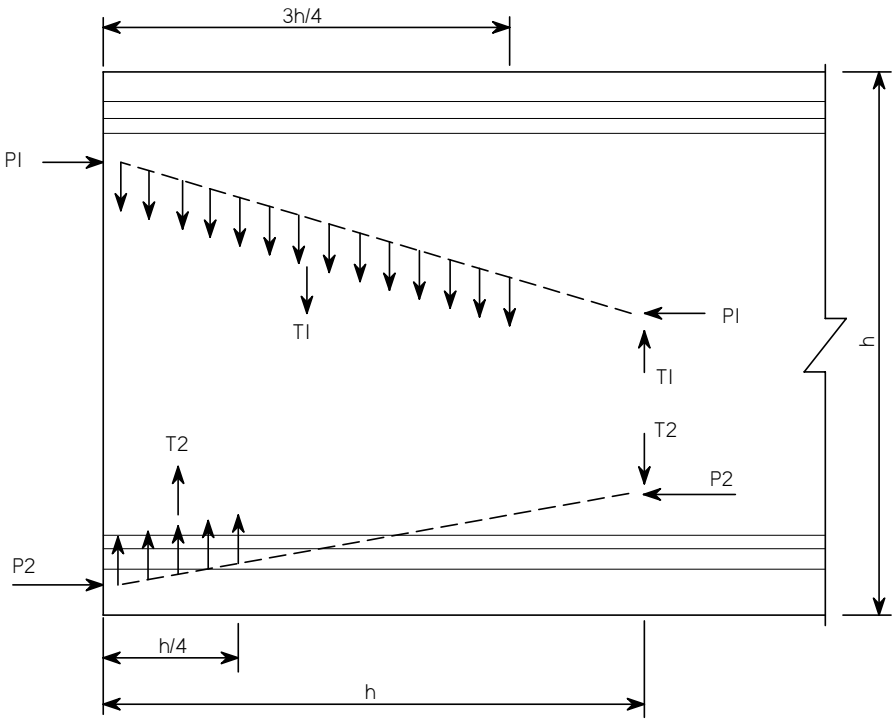

Figure 3-9. Calibration of the proposed strut-and-tie based model

The placement of the vertical compression strut in both the upper and lower strut-and-tie model is at a distance equal to the girder height from the end of the beam. This is a very important calibration of the model as the location of this strut will greatly influence the magnitude of the forces in the ties. If the vertical strut was located too close to the beam end, the magnitude of the force and subsequently the area of reinforcement will become too high and the anchorage zone would not be feasible to fabricate. It will also result in more reinforcement than necessary and at the wrong place. If this strut was placed too far from the beam end, the resulting area of steel will be too low to properly control crack lengths and widths. By placing the vertical compression strut at a distance equal to *h* from the beam end, the magnitude of the tension force for girders around 50 in. or less in height obtained by using the model was similar to bursting resistance computed in section 5.10.10.1 in AASHTO LRFD. This corresponded to field observations in which smaller girders tended to perform adequately when designed according to the current AASHTO LRFD provisions.

Another aspect of the model calibration was the selection of the stirrup working stresses. The selected working stress will affect the area of steel required to resist the

tension force and will affect the crack widths and lengths. A maximum working stress of 20 ksi has traditionally been used for both *AASHTO Standard Specifications* and AASHTO LRFD. The new design model proposes a stepped approach to selecting a working stress.

For girders with normal weight concrete, located in non-aggressive environments a working stress of 18 ksi is proposed. A working stress of 12 ksi is proposed for girders with lightweight concrete and normal weight concrete girders in overpass structures which are exposed to de-icing salts spraying up from the road below, and normal weight concrete girders located in marine environments. These working stresses are selected for simplicity since the splitting tensile strength of lightweight concrete is less than normal weight concrete and the modulus of elasticity is usually two-thirds the modulus of elasticity of normal weight concrete. Finally, the new design approach proposes a working stress of 8 ksi for splice girders or lightweight concrete beams in aggressive or marine environments. This scaled approach to the working stress selection allows flexibility for the designer to customize the anchorage zone design for various conditions. The working stress which is selected will affect the distribution of the vertical reinforcement and therefore the length of the general zone.

3.3.3 Acceptable Crack Widths and Crack Lengths

The calibration of the strut-and-tie models discussed in the previous two paragraphs was based on field observation and was selected to ensure the design method will reliably produce beam ends with cracks below a specific level. The goal of this model is to ensure that longitudinal web cracks will terminate within a length of 25 percent of the girder height and diagonal web cracks will terminate within a length of 50 percent of the girder height. These lengths are acceptable to bridge inspectors and are considered normal.

Acceptable crack widths for a girder depend upon the environment in which the girder will be exposed over the service life. The type of structure in which a girder is placed will also affect the environmental exposure of the girder. For example a girder end which is enclosed in a cast-in-place diaphragm will not be exposed to de-icing chemicals from the road deck, but may be exposed to de-icing chemical from below if it

is in an overpass structure. Girder ends which are adjacent to an expansion joint in a bridge will be very exposed to de-icing chemicals draining from the road deck if a joint seal leaks.

The acceptable crack widths for this model are as follows:

- 0.005 in. for concrete exposed to seawater spray
- 0.008 in. for concrete exposed to deicing chemicals
- 0.010 in. for concrete in dry environments

As a general note, cracks less than 0.008 in. are considered fine upon visual inspection and cracks that are 0.005 in. are of little concern by bridge inspectors. Cracks which are greater than 0.012 in. are an indicator of a design problem and are usually noted and recorded by bridge inspectors. These cracks must be continuously monitored over the life of the structure. Cracks which are 0.012 in. are also an indication of a design problem or low concrete strength at transfer. The proposed design model is calibrated to give crack lengths and crack widths that are of little concern to a bridge inspector even if the concrete strength is slightly less than predicted.

3.4 Design Example

3.4.1 Overview

The design model which is the subject of this research is significantly different from the current procedures outlined by AASHTO LRFD. A sample PCBT beam is used in the following section to illustrate the design process and steps involved in this model. The full calculations of this example are provided in Appendix A.

3.4.2 PCBT-77 Design Example Using Strut-and-Tie Models

The design example uses the case study girder shown in Figure 3-3. This girder was a 143 ft long PCBT-77. The beam was prestressed with a total of 34, 0.6 in. diameter strands. Six of these strands were harped. The harp points were located at 0.4 L and 0.6 L, where L is the total beam length. The beam was cast with normal weight concrete and had a design release strength of 5,800 psi. This analysis included the prestress force from the two courtesy strands located in the top flange of the girder.

These strands were stressed to 1 kip each and were located 2 in. down from the surface of the top flange of the girder.

The first step in the design process was to compute transformed section properties for the girder at a distance 77 in. from the end. Using these transformed section properties, the linear stress distribution at this location was computed. The force in the straight strand group after elastic shortening was computed by finding the stress in the concrete at the centroid of the strand group and using the modular ratio at transfer. The forces in the draped strand group and courtesy strand group were calculated in a similar manner. The forces and stress distribution acting on the beam end are shown in Figure 3-10. In this figure the resultant force of the draped strands and courtesy strands is shown at the top of the member.

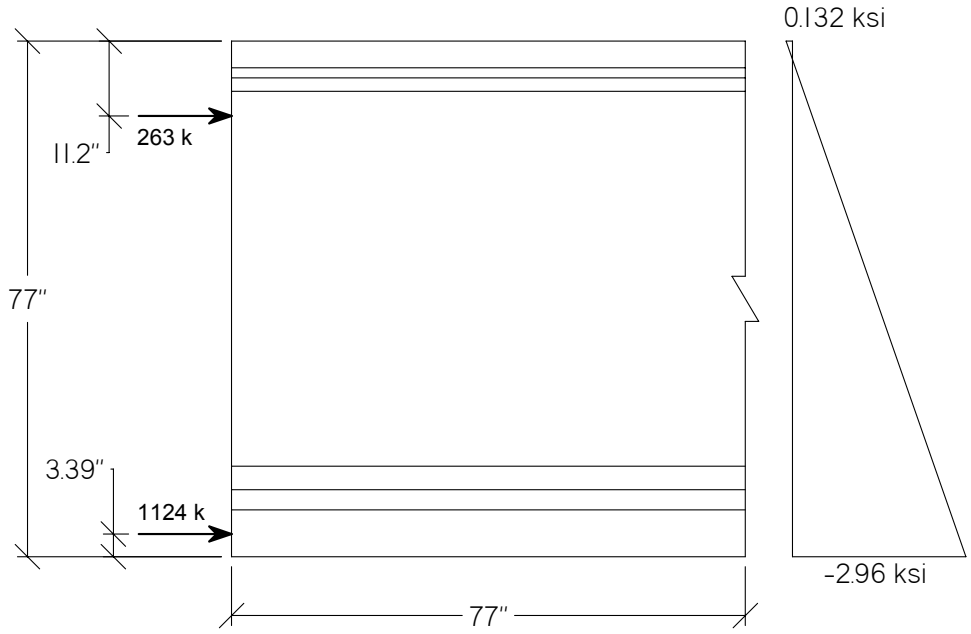

Figure 3-10. Beam end with stress distribution and prestress forces

The next step in the process was to solve the upper and lower strut-and-tie models. The process of solving the lower strut-and-tie model is illustrated with Figure 3-11. To solve the lower strut-and-tie model, the stress in the concrete was integrated over the area of concrete from the bottom up until the resultant force in the concrete was equal to the applied force in the straight strand group. The action of the resultant force in the concrete and the applied force in the straight strands created an unbalanced moment on the section. To maintain equilibrium within the section, this moment must be

balanced by a couple created from the force in the tie and the force in the vertical strut. The force in the tie for the lower strut-and-tie model was computed by summing moments about the location of the vertical strut which is labeled as Point A in Figure 3-11. The force in the tie and the force in the vertical strut are equal which maintains static equilibrium for the lower strut-and-tie model.

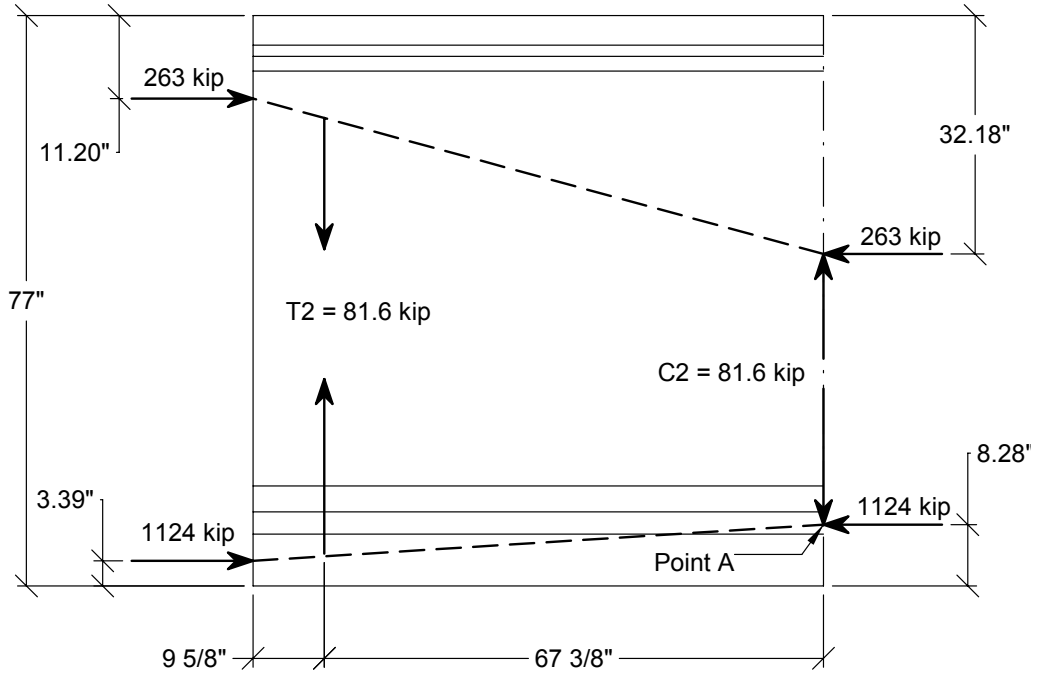

Figure 3-11. Lower strut-and-tie model example

The upper strut-and-tie model was solved in a similar manner. To solve this model the stress in the concrete was integrated over the area of concrete from the top down until the resultant force in the concrete was equal to the applied force in the harped and courtesy strands. The resultant force in the concrete and the applied prestress force in the upper strand group will create an unbalanced moment on the section. If the integration is performed correctly this unbalanced moment is equal to the unbalanced moment determined previously when integrating from the bottom up. In this example the step of integrating from the top down was skipped, and the unbalanced moment from the lower strut-and-tie model was used to solve the upper strut-and-tie model. Figure 3-12 illustrates the forces in the upper strut-and-tie model. The final results from solving the two strut-and-tie models are shown in Figure 3-13.

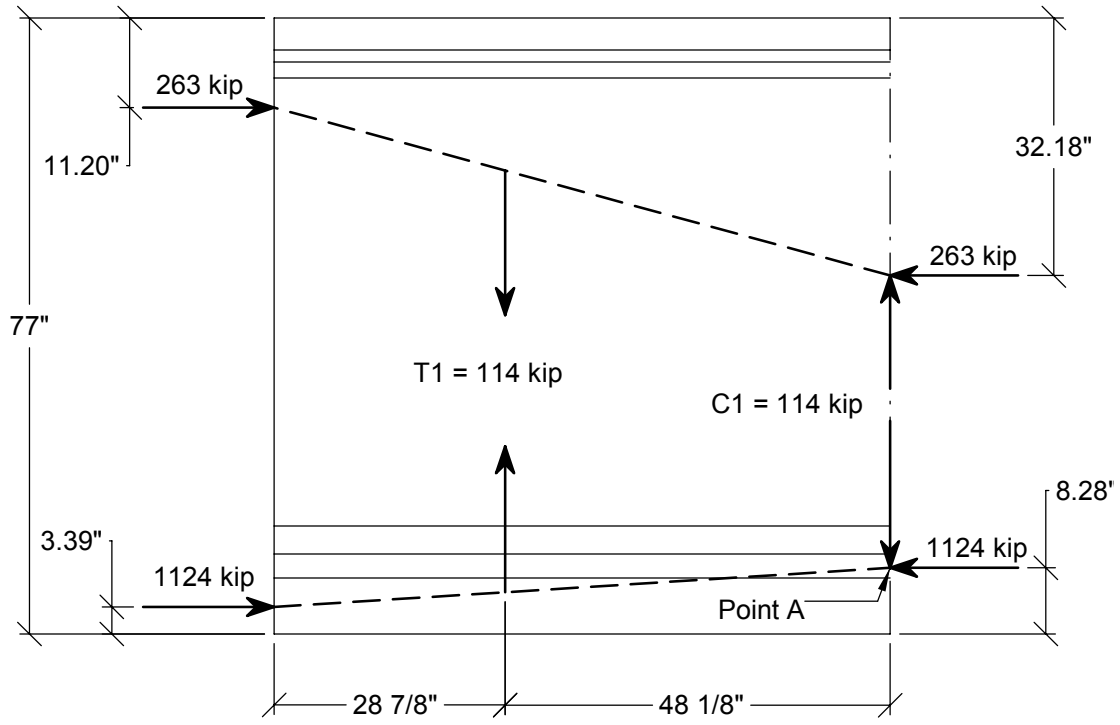

Figure 3-12. Upper strut-and-tie model example

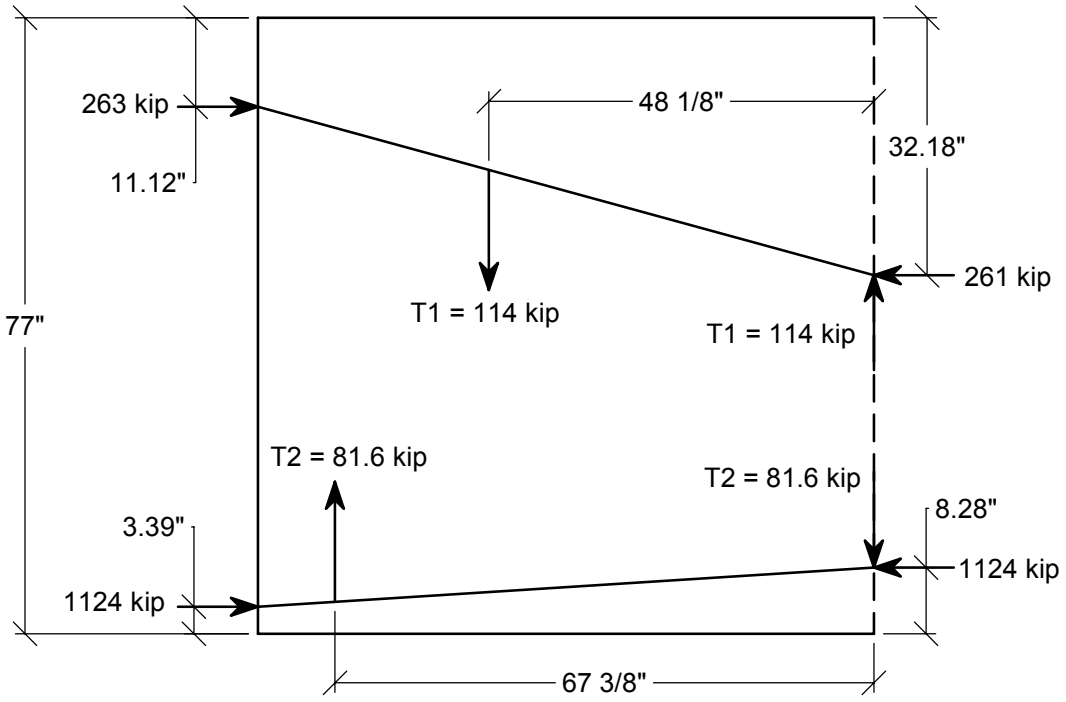

Figure 3-13. Results of both strut-and-tie models

The final step in the design process was to design the reinforcement details based on the forces from the strut-and-tie model. This girder was cast with normal weight concrete so an average stirrup working stress of 18 ksi was selected. The area of reinforcement required to resist the force T2 was 4.53 in^2, and the area of reinforcement required to resist the force T1 was 6.33 in^2. The model assumes the area of stirrups for the force T1 is uniformly distributed from the end of the beam to 3*h*/4 even though the stirrups within *h*/4 to resist T2 will be more closely spaced. The area of steel to place between *h*/4 and 3*h*/4 was 4.22 in^2. The region of the beam from *h*/4 to 3*h*/4 is typically not considered as part of the anchorage zone design as in this model. This region should also be checked for the area of steel required for horizontal shear transfer and vertical shear strength. The larger steel requirement shall control; however, it is unlikely the stirrup requirement for either the horizontal shear or vertical shear design will control over the anchorage zone requirement. In this particular example the model is used to get a stirrup spacing between *h*/4 and 3*h*/4 of No. 5 stirrups at 5 ½ in. An example of the anchorage zone stirrup detailing is show in Figure 3-14.

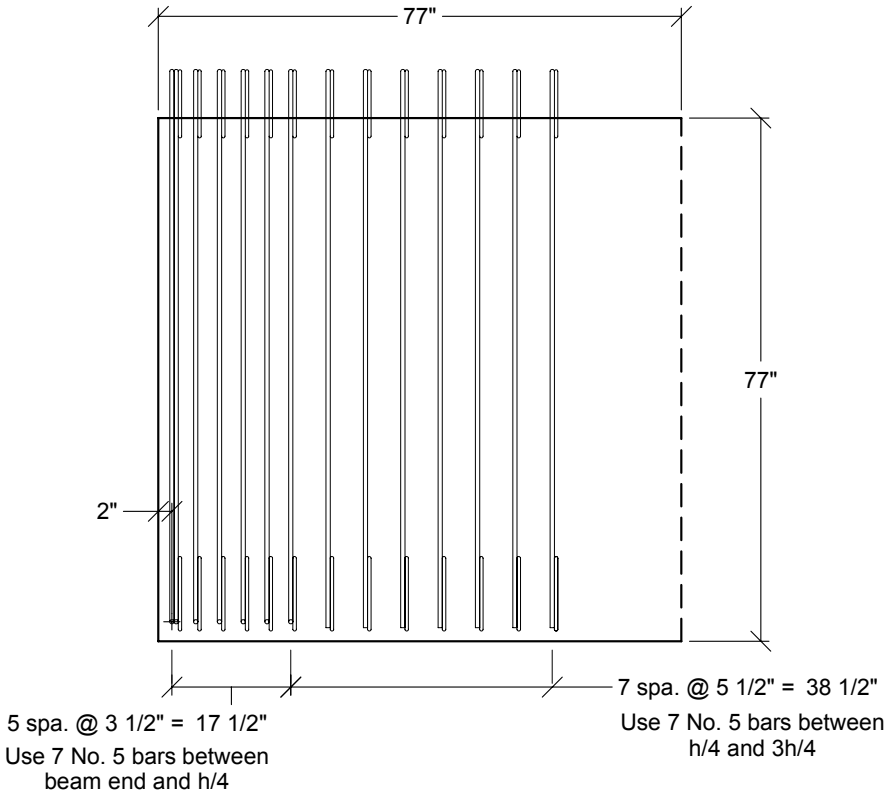

Figure 3-14. Example of proposed stirrup detailing

The details developed using this design approach result in a significantly greater area of stirrups compared to the details in the actual case study beam shown in Figure 3-3. In the actual case study girder, the region between the beam end and $h/4$ contained a stirrup area of 2.8 in^2. The example detail in Figure 3-14 contains 4.34 in^2 within this same region. This design provides a vertical resistance of 5.22 percent of the jacking force.

In the case study girder the region between $h/4$ and $3h/4$ contained a stirrup area of 2.8 in^2. The example detail in Figure 3-14 contains 4.34 in^2 in this region. It is clear from the photograph of the anchorage zone cracking in this case study, the area of stirrups provided was not sufficient to control the cracks. The new design model results in a 55 percent increase in the stirrup area in the region from the end to $h/4$ and a 55 percent increase from $h/4$ to $3h/4$ compared to the original stirrup detail. By using No. 5 stirrups as opposed to No. 4 stirrups used in the original design, a stirrup spacing can be used which will provide adequate clear spacing to ensure good concrete consolidation.

3.5 Parametric study

The primary objective of this research project was to develop a simplified approach to beam end design to use for most typical PCBT applications in Virginia. To accomplish this objective, two parametric studies using the proposed design model were conducted. One parametric study included members cast with normal weight concrete, and the second study included members cast with lightweight concrete. The results from these two parametric studies were consolidated into design aids to provide designers a quick method to determine the area of stirrups to use within the anchorage zone of the beam. The following sections discuss the assumptions, procedures, and results from the two parametric studies.

3.5.1 Parametric Study Assumptions

Several assumptions about material properties were made before conducting the parametric study. For all sample beams in the study, the release strength of the concrete was assumed to be 5,500 psi. The unit weight of the normal weight concrete was taken to be 150 lb/ft^3 and the unit weight of the lightweight concrete was assumed to be 120 lb/ft^3. Together, the unit weight of the concrete and release strength affect the modulus of

elasticity of the concrete at transfer. The modulus of elasticity of the concrete at transfer was computed using Equation 3-1.

$$E_{ci} = 33w^{1.5}\sqrt{f_{ci}^{`}} \qquad (3\text{-}1)$$

Where:

E_{ci} = modulus of elasticity at transfer in psi

w = unit weight of concrete in lb/ft^3

$f_{ci}^{`}$ = compressive strength of concrete at release in psi

The modulus of elasticity of the prestress steel was assumed to be 28,000 ksi. This value affects the modular ratio which was used in computing transformed section properties as part of the analysis. The ultimate strength of the prestress steel was 270 ksi, and the initial stress in the strand at the time of tensioning was $0.75f_{pu}$ or 202.5 ksi. The prestress force applied in the courtesy strands was also considered in the models for the parametric studies. A total of 1 kip per strand was assumed to act in each of the four courtesy strands located in the top flange of the girder. This resulted in 4 kips of force in addition to the force applied by the straight and harped strands. The parametric study included girders with ½ in. strand and 0.6 in. strand. Girders in the parametric study which contained ½ in. strand also included ½ in. diameter courtesy strands. Girders which used 0.6 in. strand had 0.6 in. diameter courtesy strands. The harping points for all draped strands were assumed to be at 0.4 L and 0.6 L, where L was the total length of the beam. The model assumes that there are no debonded strands.

One final assumption pertained to the strand pattern of the sample beams for the parametric study. The top row of harped strands was raised to a height 2 in. below the surface of the top flange of the girder. At the beam end, each row available for prestress strands was filled from the bottom up. The number of pairs of harped strands was equal to the number of rows filled at the bottom of the beam. All holes for the prestress strands were located on a 2 in. center-to-center spacing.

3.5.2 Parametric Study Procedure

The lightweight and normal weight concrete parametric studies looked at sample girders of all nine PCBT cross sections used by VDOT. For each cross section shape, the design model was applied to multiple girders of varying length and level of prestress

force. The span-to-depth ratio of the sample girders varied from 15 to 20. For each shape, as the lengths of the sample girders increased, the level of prestress force also increased. The maximum number of ½ in. diameter strands which would fit in the PCBT bottom flange was 48. For the PCBT-29 and PCBT-37 cross sections, the model was run for sample beams with ½ in. diameter strands only. For the PCBT-45 through PCBT-93 cross sections, the model was run for sample girders with both ½ in. and 0.6 in. strands. For these sections there was some overlap in prestress force between the sample girders with ½ in. strands and the sample girders with 0.6 in. strands.

The number of harped strands was determined by the allowable stresses at transfer in the top and bottom of the beam. This check neglected any loss of prestress force caused by steel relaxation between tensioning and prestress release. The allowable stresses at transfer were computed using transformed section properties and the jacking force. The stresses were computed at the harping point in the extreme tension fiber and extreme compression fiber of the member. The computed stresses were compared to the allowable concrete stress limits in section 5.9.4 of AASHTO LRFD.

An Excel spreadsheet was developed which could execute the computations required to solve the strut-and-tie models. Using the spreadsheet, the girder section properties, material properties of the concrete and steel, and strand pattern could be input. The spreadsheet automatically computed the transformed section properties at the harping point and at a section located a distance h from the beam end; and the tension and compression stresses in the top and bottom at these locations. Using the Goal Seek function in Excel, the integration of concrete stress was performed and the strut-and-tie models could be solved quickly.

The beam end design model was applied to a total of 134 sample beams for the normal weight concrete parametric study, and 137 test beams for the lightweight concrete parametric study. The end results of each analysis were the forces in the ties for both strut-and-tie models. This information was converted into an area of steel using the stirrup working stress appropriate for the type of concrete. The forces in the ties were also expressed as a percentage of the jacking force for comparison purposes. The results for each sample girder were recorded and another sample girder was analyzed. A

comprehensive list of all sample girders used in the parametric study is included in Appendix B.

3.5.3 Parametric Study Results

The parametric study showed that as the magnitude of the prestress force acting on a particular section increased, the tension forces T1 and T2 would also increase in a generally linear fashion up to a certain level of prestress force and would then begin to decrease. A sample of this relationship is shown in Figure 3-15 for the portion of the parametric study which examined normal weight, PCBT-61 girders with ½ in. strand. This figure is representative of the results for all cross sections with normal weight and lightweight concrete and ½ in. strand. The point at which the tension forces began to decrease varied for each section and depended on the number of strands in the girder. In many of the sections with 0.6 in. diameter strands this turn over point was never achieved and the plot increased in a generally linear fashion over the entire range of force analyzed as shown in Figure 3-16.

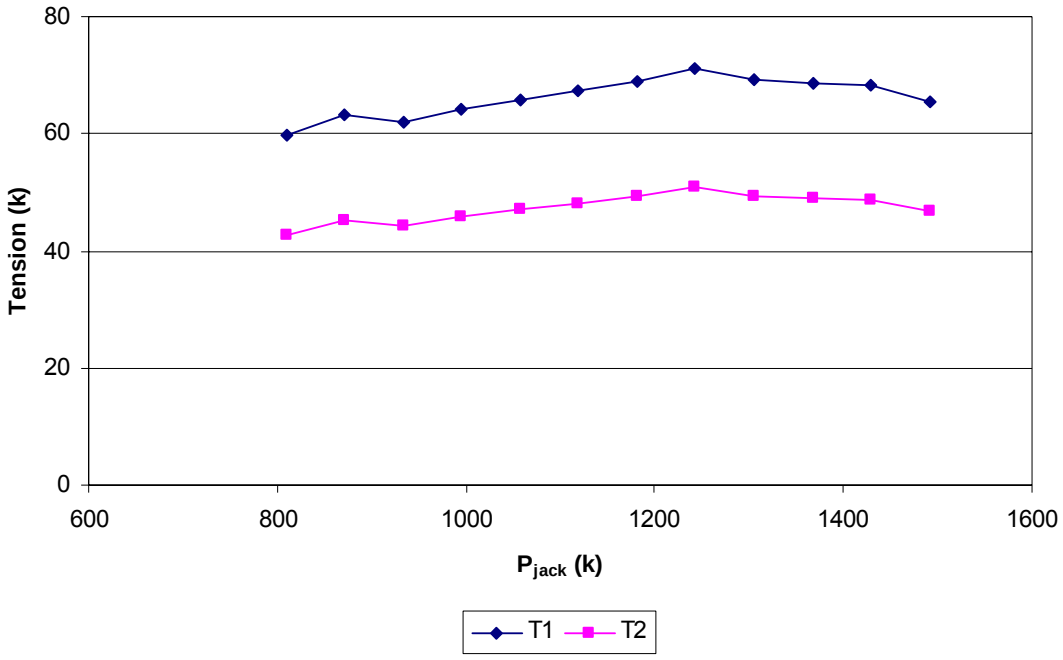

Figure 3-15. Force in T1 and T2 for PCBT-61, NWC, ½ in. diameter strand

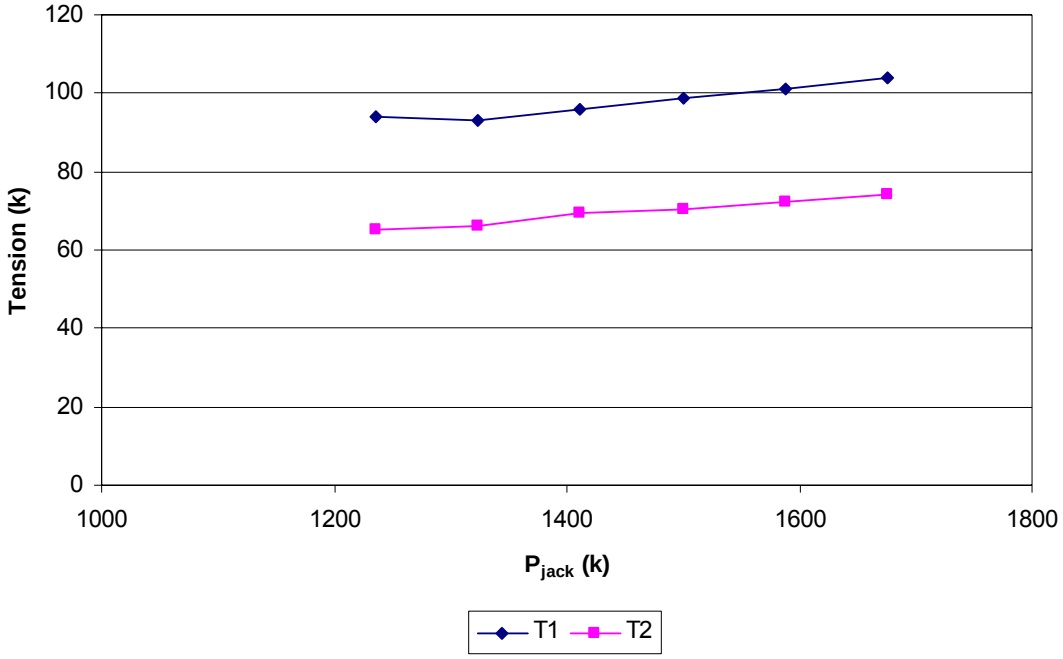

Figure 3-16. Force in T1 and T2 for PCBT-69, NWC, 0.6 in. diameter strands

The relationship between the tension forces and prestress force is intuitive. As the magnitude of the applied prestress force increases, it is reasonable to expect a greater vertical tension force to develop from the diffusion of this force. As the number of strands increases, eventually the bottom flange will become full. When this occurs, then the centroid of the prestress force will be higher in the cross section and the force will not have as great of a vertical distance over which to diffuse. This accounts for the slight decrease in tension force when a very high prestress force was applied such as in Figure 3-15.

The eccentricity of the prestress force is an important factor in the magnitude of the forces in the ties. It was observed that sample girders with the same cross section and same magnitude of prestress force provided by ½ in. strand and 0.6 in. strand would have a significantly higher tension force when the prestress was provided with 0.6 in. strand. Table 3-1 shows the tension forces T1 and T2 for the PCBT-77 with 48 ½ in. diameter strands and 34 0.6 in. diameters strands. The overall prestress force provided by the two strand patterns is almost the same; however, the tension forces from the strut-and-tie models are different. The increase in the tension forces between the ½ in. strand girder and the 0.6 in. strand girder is about 19 percent. This example illustrates that girders with

0.6 in. strand would be more likely to develop anchorage zone cracking when designed under the current AASHTO LRFD provisions which do not include any provisions for the type of strands used or for the eccentricity of the prestress force on the cross section. This trend has also been observed during the site visits. Large girders with 0.6 in. diameter strands in many cases had severe anchorage zone cracks. The two poor case study girders discussed in section 3.2.3 both contained 0.6 in. strands.

Table 3-1. Tension force comparison for PCBT-77 girders with ½ in. strand and 0.6 in. strand

Number of strands	P_{jack} (k)	Eccentricity at *h* from beam end (in)	T1 (k)	T2 (k)
48 ½ in. strands	1,491	22.8	95.1	68.0
34 0.6 in. strands	1,498	25.3	113	81.0

The tension forces computed in the parametric study were also expressed as a percentage of the jacking force. This ratio is currently used in the AASHTO LRFD provisions for pretensioned anchorage zones and is useful for comparison purposes. A comparison of the jacking force and the tension force as a percentage of the jacking force is shown in Figure 3-17 and Figure 3-18. These figures are from the portion of the lightweight concrete parametric study which looked at the PCBT-61 with ½ in. diameter strands and the PCBT-85 with 0.6 in. diameter strands, respectively. These graphs are typical of the relationships observed in the other sections in both the lightweight and normal weight parametric studies.

In general, as the level of prestress force increased, the required bursting resistance decreased relative to the jacking force. However, the total magnitude of the bursting force increased as shown previously. Figure 3-17 shows the bursting resistance required in the region from the beam end to *h*/4 and the region from *h*/4 to 3*h*/4 for a PCBT-61 girder. The current AASHTO LRFD provisions only consider the region from the beam end to *h*/4 as part of the anchorage zone, and these provisions require a minimum of 4 percent resistance. As Figure 3-17 shows, the resistance levels required within *h*/4 ranged from 3 percent to 5 percent of the jacking force. The PCBT-61 is the middle height PCBT girder so it is logical that current AASHTO LRFD requirement of 4 percent should work for most of the PCBT-61 girders. Figure 3-18 shows the required bursting resistance for the PCBT-85 sample girders. For this group of girders the level of

bursting resistance required within *h*/4 ranged from approximately 4.75 percent to 5.5 percent of the jacking force. This suggests the current minimum requirement of 4 percent resistance will be insufficient to control cracks in deep girders which corresponds directly to the field observations already highlighted.

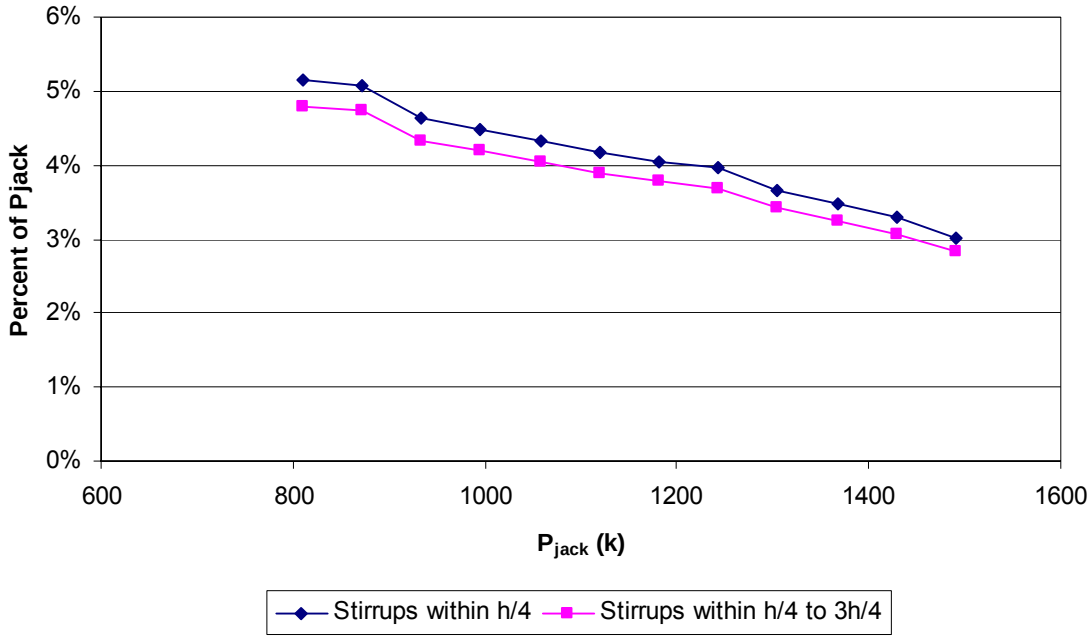

Figure 3-17. Required bursting resistance, PCBT-61, LWC, ½ in. strand

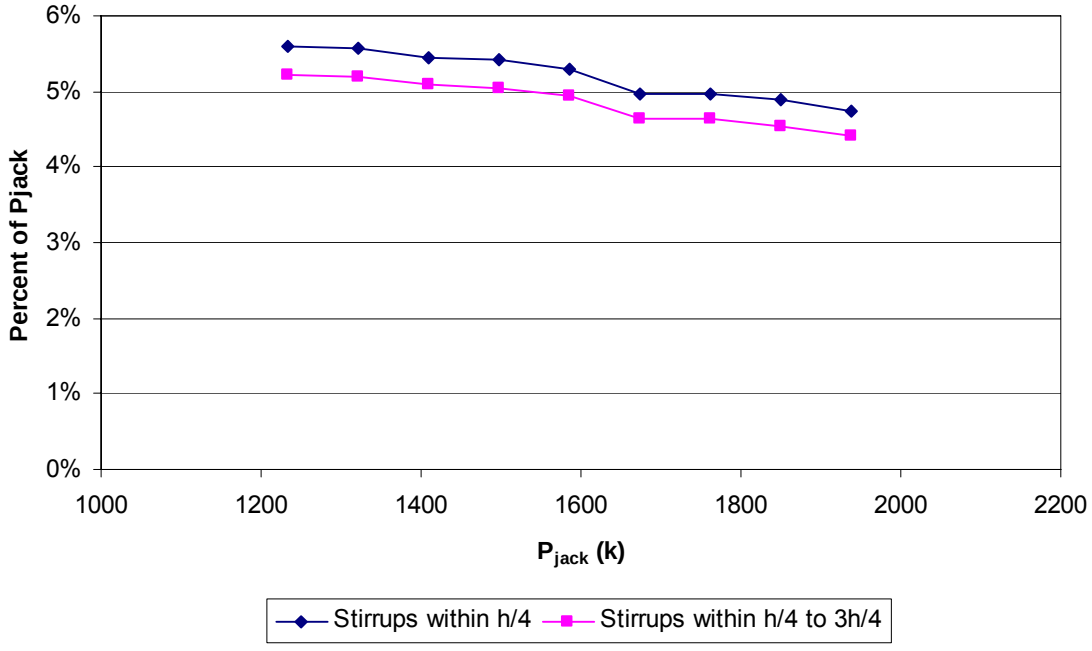

Figure 3-18. Required bursting resistance, PCBT-85, LWC, 0.6 in. strand

The relationship in Figure 3-18 and Figure 3-17 is important when considering the design of girders that are used as drop in segments. These girders typically have a very low level of prestress force and by the trend in Figure 3-18 the required bursting resistance would be a very high percent of $P_{jack.}$ Consider for example the PCBT-93 with 16 0.6 in. diameter strands that is used as a drop in girder discussed in section 3.2.5. The bursting resistance required for this girder within *h*/4 from the end of the beam would be approximately 7.8 percent of P_{jack}. This value seems very high when compared to the current minimum of 4 percent; however, since the level of prestress force is so low for this girder, providing a bursting resistance of 7.8 percent P_{jack} would still result in a reasonable spacing of stirrups.

3.5.4 Development of Design Tables

The results of the parametric study were used to develop anchorage zone design tables for all nine PCBT cross section shapes used by VDOT. Several attempts were first made to develop design equations through linear regression and the graphs in Figure 3-17, Figure 3-18, and from similar graphs for the other cross sections. It was found that the equations from the linear regression were different for each cross section. Based on this it was decided to create design tables for each cross section rather than develop a different design equation for each shape. The design tables provide the area of stirrups required within *h*/4 from the end and between *h*/4 and 3*h*/4. These areas were directly obtained through the results of the sample girders in the parametric study. A sample anchorage zone design table is shown in Table 3-2 for PCBT-61 girders with normal weight concrete. Tables for all PCBT cross sections are included in Appendix C.

As shown in Figure 3-15 the tension forces began to decrease as the prestress force increased beyond a certain level for the sample girders which contained ½ in. diameter strands. In developing the anchorage zone design tables, the tension forces obtained from the strut-and-tie analysis were divided by the appropriate working stress for the given type of concrete to determine the steel required to resist these forces. At high levels of prestress force where the tension forces began to decrease, the required stirrup areas in each region of the anchorage zone also decreased. For the anchorage zone design tables, however, the area of steel was not decreased at the high prestress

levels. Sample girders affected by this decrease in the tension forces were given the highest required area before the force began to decrease. This is shown in Table 3-2. Girders with 40 or more ½ in. strands all have the same required areas of stirrups in the anchorage zone regions.

Table 3-2. PCBT-61, Normal weight concrete, Beam End Design Table

Normal Weight Concrete					Stirrup Stress = 18 ksi		
		End - h/4			h/4-3h/4		
A	B	C	D	E	F	G	H
No. of ½" strands	A_{ps} (in^2)	$A_{req'd}$ (in^2)	Quantity and size	Number and spacing size	$A_{req'd}$ (in^2)	Quantity and size	Number and spacing size
≤ 32	4.9	2.55	7 No. 4	4 spa. @ 3.25"	2.38	6 No. 4	6 spa. @ 5"
≤ 38	5.81	2.74	7 No. 4	4 spa. @ 3.25"	2.56	7 No. 4	7 spa. @ 4.25"
40 or more	6.12	2.83	8 No. 4	4 spa. @ 3.25"	2.64	7 No. 4	7 spa. @ 4.25"
No. of 0.6" strands	A_{ps} (in^2)	$A_{req'd}$ (in^2)	Quantity and size	Number and spacing size	$A_{req'd}$ (in^2)	Quantity and size	Number and spacing size
≤ 26	5.64	3.24	6 No. 5	4 spa. @ 3.25"	3.03	5 No. 5	5 spa. @ 6"
28 or more	6.08	3.43	6 No. 5	4 spa. @ 3.25"	3.2	6 No. 5	6 spa. @ 5"

To use the anchorage zone design table, a designer would select the correct table based on the concrete type and enter the table with the number of fully stressed ½ in. or 0.6 in. diameter strands. The tables assume the jacking force is based on $0.75f_{pu}$ and also includes the force from four courtesy strands. Columns C and F give the required stirrup area from the beam end to *h*/4 and from *h*/4 to 3*h*/4 respectively. Columns D and E give the number and size of the stirrups and the number and size of spaces within a distance of *h*/4 from the beam end. In this region, some number of stirrups will need to be bundled in order to achieve the spacing listed in column E. Columns G and H give the number and size of the stirrups and number and size of spaces between *h*/4 and 3*h*/4. Stirrups will not need to be bundled in this portion of the anchorage zone.

The objective of these anchorage zone design tables was to provide a design aid that would reliably result in anchorage zones with acceptable crack lengths and crack widths as outlined in section 3.3.3. The region between *h*/4 and 3*h*/4 is not typically considered as part of the anchorage zone during design. The stirrups in this area are traditionally controlled by horizontal shear transfer or vertical shear strength. In this design method, the spacing for the stirrups between *h*/4 and 3*h*/4 should be checked against the stirrup spacing for horizontal and vertical shear. The smallest stirrup spacing

requirement shall control; however, in most cases the smallest spacing will result from the anchorage zone reinforcement requirement. Beyond 3*h*/4, stirrups shall be provided at the spacing requirements for horizontal or vertical shear.

The design tables will work for pretensioned girders which contain some number of harped strands. Designers should conduct an analysis with the full strut-and-tie based model for unique situations. This would include cases with no harped strands or harped strands not raised to full height at the end of the girder, debonded strands, 300 ksi strand, and custom sections. The anchorage zone design tables also do not include very lightly prestressed girders which would typically be used as splice girders. For these cases it is recommended that designers should complete the full strut-and-tie analysis to determine the appropriate stirrup requirement. Using the lowest listed value in the table for the section in consideration would result in a very conservative anchorage zone design.

3.5.5 Example Using Design Tables

In section 3.4, a design example was presented using the full strut-and-tie model. This same example will be used to illustrate the design process using the anchorage zone design tables. The results of the comparison are shown in Table 3-3. Recall the sample girder was a PCBT-77 with 34, 0.6 in. strands. Using anchorage zone design Table C-15 from Appendix C, the area of stirrups required in h/4 is 4.25 in^2 and the area of stirrups required between *h*/4 and 3*h*/4 is 3.97 in^2. These stirrup areas can be provided by using 7 No. 5 stirrups in each region of the anchorage zone. This would result in the same anchorage zone detail obtained using the full strut-and-tie model which was shown in Figure 3-14.

Table 3-3. Anchorage zone design example comparison

	As Built		Full Strut-and-Tie Model Results		Design Table Results	
Case Study	Stirrup Area, *h*/4 (in^2)	Stirrup Area, *h*/4 – 3*h*/4 (in^2)	Stirrup Area, *h*/4 (in^2)	Stirrup Area, *h*/4 – 3*h*/4 (in^2)	Stirrup Area, *h*/4 (in^2)	Stirrup Area, *h*/4 – 3*h*/4 (in^2)
PCBT-77 (34) 0.6 in. strand	2.8	2.8	4.53	4.22	4.25	3.97

3.5.6 Alternate Strut-and-Tie Design Model

An alternate strut-and-tie anchorage zone design model is presented in this section which has been calibrated to produce very similar results to the proposed design model. The alternate strut-and-tie model shown in Figure 3-19 was developed to produce required stirrup areas which closely match those from the design tables, and adhere to the fundamental theories used in strut-and-tie modeling. One of the problems with the proposed strut-and-tie based model design approach is that the upper and lower strut-and-tie models are solved independently. Even though there is some overlapping between the ties in the upper and lower models, neither model considers the presence of the other when they are solved. (Dr. Carin L. Roberts-Wollmann, office conversation, January 12, 2007)

The strut-and-tie model shown in Figure 3-19 is a true double-tie, strut-and-tie model of an anchorage zone. From the results of the parametric study and the development of the design tables, it was clear that the required stirrup area within $h/4$ and between $h/4$ and $3h/4$ are always very similar. In many cases, the number of stirrups in the two anchorage zone regions will be the same. From this observation, the angles in the ties in the model in Figure 3-19 are set so that the forces T1 and T2 are equal. The location of the compression strut is placed at a distance of $3h/4$ from the beam end as opposed to a distance h. This calibration is necessary to ensure this alternate strut-and-tie model provides the same results as the proposed model.

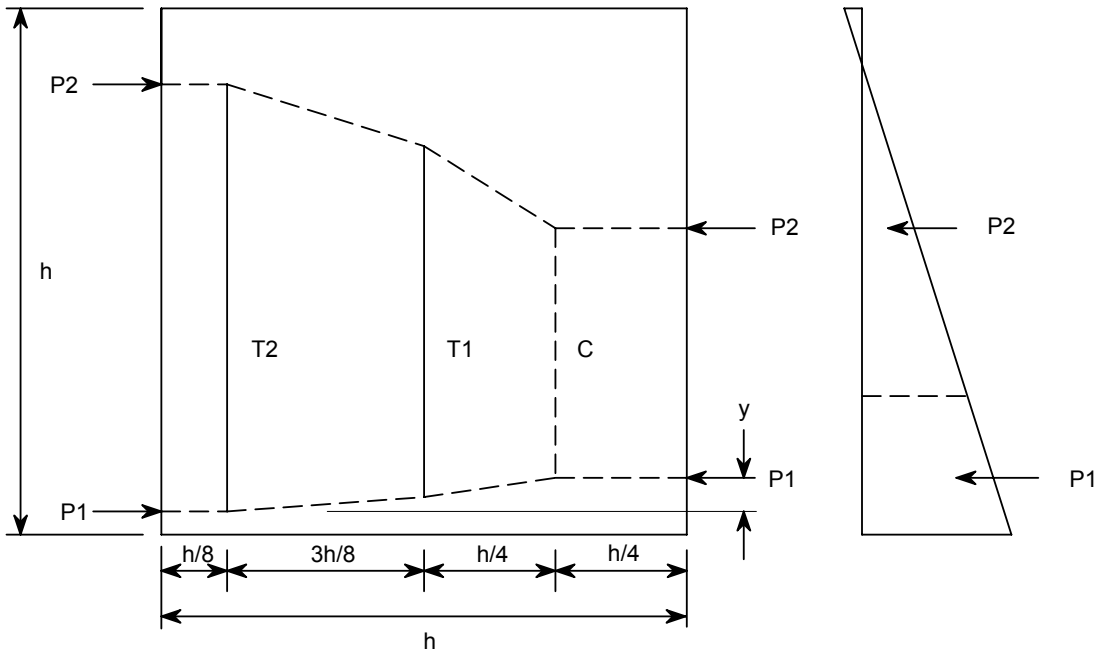

Figure 3-19. Alternate strut-and-tie model

Solving a double-tie strut-and-tie model is more challenging than a model with a single tie. With the assumption that T1 and T2 will be equal, the model was solved symbolically which resulted in Equation 3-2. This derivation is presented in Appendix D.

$$T1 = T2 = \frac{8P_1 y}{7h} \qquad (3\text{-}2)$$

Where:

P_1 = force in straight strand group (kip)

y = difference in height between resultant force and applied prestress force (in.)

h = girder height (in.)

The process of using this alternate strut-and-tie model is the same as the proposed model. Transformed section properties are computed, the forces in the straight strand group is computed in the same manner, and the integration of the stress over the area of the concrete is the same. Once the location of the resultant force is determined, Equation 3-2 is used to determine the tension forces. The same recommendations for stirrup working stress apply and the appropriate area of stirrups can be calculated.

To demonstrate the use of this alternate method, the PCBT-77 example from section 3.4.2 is used. Recalling the value for the force in the straight strand group and the difference in resultant force height and applied force height from Figure 3-13 and using Equation 3-2, the forces T1 and T2 are 81.6 kips. The reinforcement for T1 is evenly distributed between $h/4$ and $3h/4$ which results in an area of reinforcement of 4.53 in^2. The reinforcement for T2 is placed between the end and $h/4$ and this area of reinforcement is also 4.53 in^2. The results from the proposed model for this example required a stirrup area of 4.53 in^2 within $h/4$ and 4.22 in^2 between $h/4$ and $3h/4$.

3.5.7 Parametric Study Results Compared to Other Design Methods

In Chapter 2 several anchorage zone design methods were discussed. Three of these design methods were compared to the anchorage zone design tables developed from the parametric study. These methods included the design procedures developed by Marshall and Mattock (1962), Castrodale, et al. (2002), and Tuan, et al. (2004). Three sample girders were selected to compare these anchorage zone design methods. The size, prestress force, and concrete type of the sample girders are shown in Table 3-4.

Table 3-4. Sample girders used in design method comparison

Size	Number of strands	Harped Strands	Concrete Type
PCBT-45	34 ½ in.	6	Normal weight
PCBT-77	34 0.6 in.	6	Normal weight
PCBT-93	46 ½ in.	8	Light weight

The anchorage zone design methods used in these comparisons recommended different regions over which to distribute the anchorage zone stirrups. The methods presented in Marshall and Mattock and Castrodale, et al. recommended distributing the anchorage zone stirrups over a length of $h/5$ from the end of the beam. The method presented in Tuan, et al. recommended distributing half of the reinforcement over a region from the beam end to h/8 and the remainder over a second region from $h/8$ to $h/2$. To account for these differences, each of the four design methods was performed for the sample girders listed in Table 3-4. The required area of stirrups was determined for each model and was divided over the length which the particular model recommended distributing the reinforcement. This resulted in a required stirrup area per linear inch.

The results of the comparisons are shown graphically in Figure 3-20, Figure 3-21, and Figure 3-22.

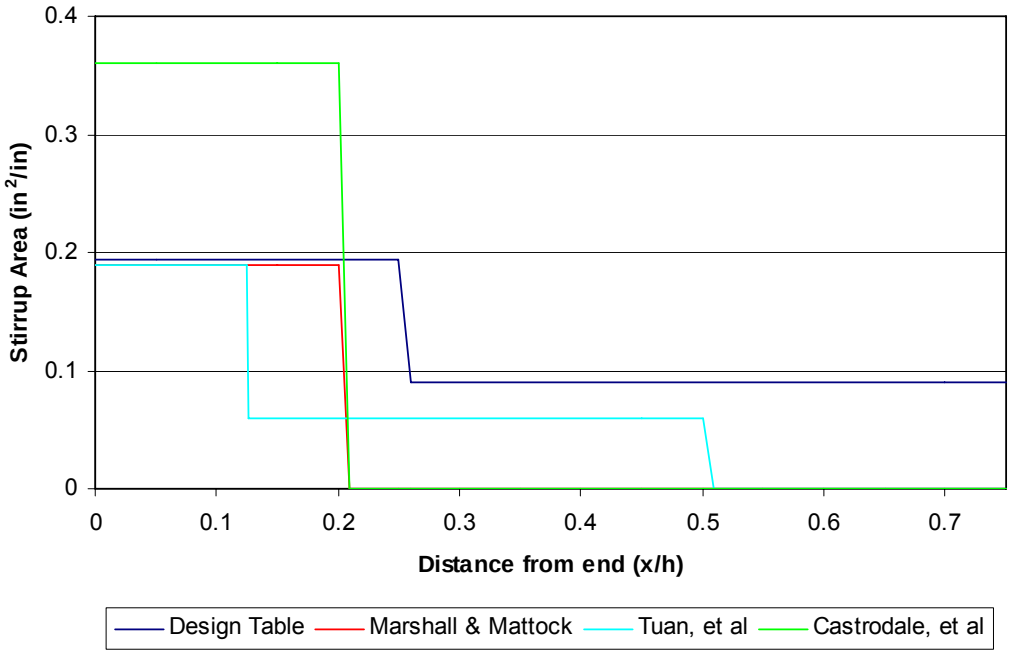

Figure 3-20. Design Method Comparison, PCBT-45, NWC, 34 ½ in. strands

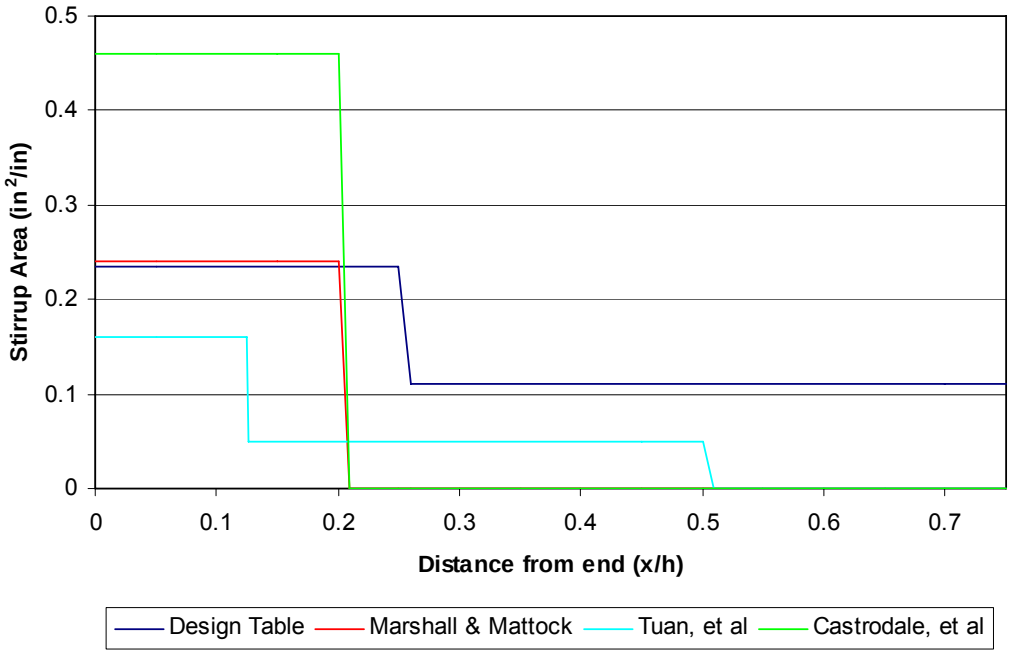

Figure 3-21. Design Method Comparison, PCBT-77, NWC, 34 0.6 in. strands

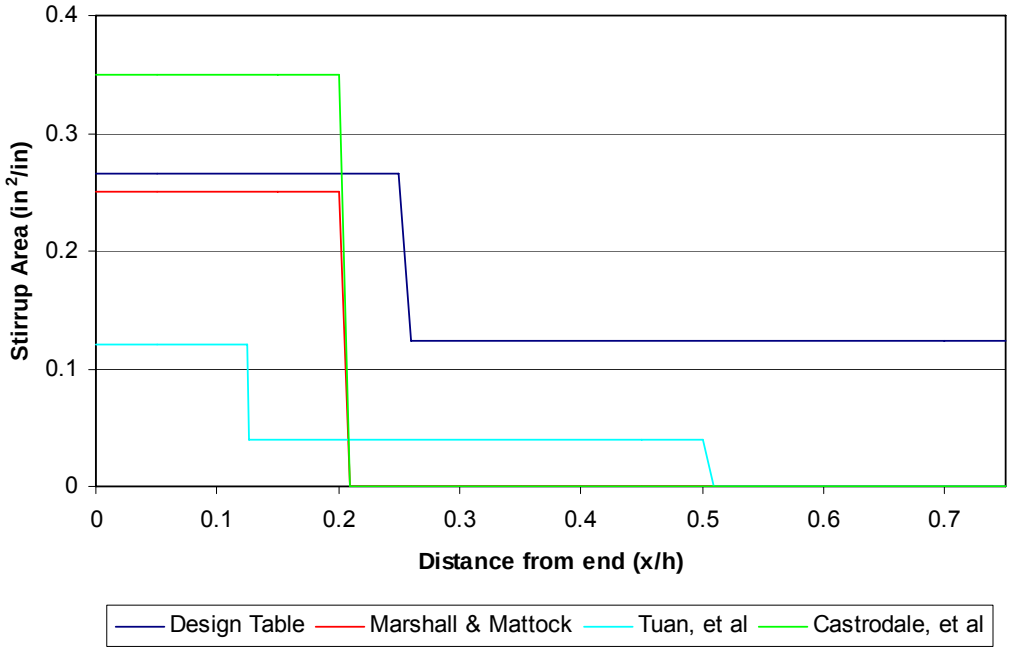

Figure 3-22. Design method comparison, PCBT-93, LWC, 46 ½ in. strands

The comparison of the four design methods for the sample PCBT-45 girder, given in Figure 3-20, showed the required stirrup area per linear inch within *h*/8 from the end of the girder obtained from the parametric study was very similar to the required stirrup area per linear inch obtained when using the Marshall and Mattock and the Tuan, et al. methods. The Marshall and Mattock method includes the ratio of the girder height to the transfer length in the equation for the stirrup area. For the purpose of this comparison, the transfer length was assumed to be 60 strand diameters as specified in the AASHTO LRFD code. The strut-and-tie model developed by Castrodale, et al. produced the most conservative results of all four design methods. This occurred because of the close placement of the tie to the vertical strut in this strut-and-tie model. Figure 3-20 shows the new anchorage zone design model is not significantly different from these previously developed models when applied to a small girder. Typically small girders such as the PCBT-45 have minimal anchorage cracking which suggests good calibration of the proposed model.

The comparison between the design methods when applied to a PCBT-77 girder and a PCBT-93 girder with lightweight concrete, display a different trend. As shown in Figure 3-21 and Figure 3-22, the results from the Castrodale, et al. strut-and-tie model

again resulted in the highest concentration of stirrup area for reasons previously discussed. The results from the proposed model and the Marshall and Mattock method are similar for the PCBT-77 and PCBT-93; however, for both of these sample girders, the Marshall and Mattock method would produce conservative results according to the recommendations in their 1962 study. In this study Marshall and Mattock stated that their design equation would produce conservative results when the ratio of the girder height to the transfer length exceeded 2. Assuming a 60 strand diameter transfer length, this ratio would equal 2.1 for the beam in Figure 3-21 and 3.1 for the beam in Figure 3-22. The results from the proposed model were significantly higher than the results obtained from the Tuan, et al. method for both sample girders.

The Castrodale, et al. strut-and-tie model and the design table method result in a similar stirrup area required near the beam end for the lightweight PCBT-93 girder. The total stirrup area required within $h/5$ from the Castrodale, et al. model was 6.5 in^2, and the total stirrup area required within $h/4$ from the design table was 6.16 in^2. The Castrodale, et al. model results tend to be very conservative for most girders; however, in this case with a very deep girder made with lightweight concrete the results are relatively close to the design table method. It should be noted, that the Castrodale, et al. model places all of the anchorage zone reinforcement within $h/5$ and from field observations, a dense region of stirrups at the very end of the girder will not control the formation of diagonal web cracks.

Although the results from the proposed model for the comparison with the PCBT-77 sample girder and PCBT-93 sample girder showed a high required stirrup area in the anchorage zone, it is believed this level of reinforcement is necessary to control anchorage zone cracking. As the case studies in section 3.2 illustrate, large girders with high levels of prestress force tend to develop numerous anchorage zone cracks. These cracks tend to be very long and may also be very wide and require additional repair work. The cost of providing several additional stirrups at each end of the girder is almost negligible in comparison to the overall cost of a large girder and is significantly less than the cost of repairing a damaged anchorage zone with epoxy injection. Also, lifetime inspection is greatly complicated when damage is noted and must be monitored.

A main concern with providing additional stirrups in the anchorage zone is creating too much congestion which would lead to poor consolidation of the concrete. This concern can be overcome by using larger diameter stirrups, such as No. 5 bars, and by bundling some stirrups between the end and *h*/4. The stirrups between *h*/4 and 3*h*/4 should typically not need to be bundled to achieve a reasonable spacing. Field observations indicate that heavy anchorage zone reinforcement has a negligible influence on the quality of casting. Bundled No. 5 bars spaced at 3-½ in. allow for plenty of clearance for internal vibration.

3.5.8 Parametric Study Results Compared to Other Bridge Design Codes

Design provisions from AASHTO LRFD, the Australian Bridge Design Code, and the Canadian Highway Bridge Design Code were presented in section 2.3. These design codes were applied to the sample girders from the portions of the parametric study that analyzed PCBT-45 girders with ½ in. strand and normal weight concrete, PCBT-77 girders with normal weight concrete and 0.6 in. strand, and PCBT-93 girders with lightweight concrete and ½ in. strand. The results were compared to the results from the proposed design model. All three of these design codes require the anchorage zone reinforcement to be placed within *h*/4 from the end of the girder and do not consider the region between *h*/4 and 3*h*/4 as part of the anchorage zone. For this comparison only the stirrup area required within *h*/4 obtained from the proposed model was used for the following graphs. These three comparisons are shown in Figure 3-23, Figure 3-24 and Figure 3-25.

Figure 3-23 illustrates the comparison between the three design code provisions and the proposed model for the sample PCBT-45 girders with ½ in. strand and normal weight concrete from the parametric study. Typical PCBT-45 girders cast in Virginia would have a level of prestress which would fall in the middle to the upper range of this figure. In this region there is very little difference in the area of stirrups required within *h*/4 between the three design codes and the proposed model. The area of steel required by the proposed model between *h*/4 and 3*h*/4 is slightly less than the area required within *h*/4. The AASHTO LRFD and Australian Bridge Design Code have almost identical provisions, except for a different stirrup working stress. The Australian Code allows for a

working stress of 150 MPa or 21.8 ksi. This figure illustrates that the proposed design method results in stirrup areas very similar to girders designed under current code provisions for smaller cross sections.

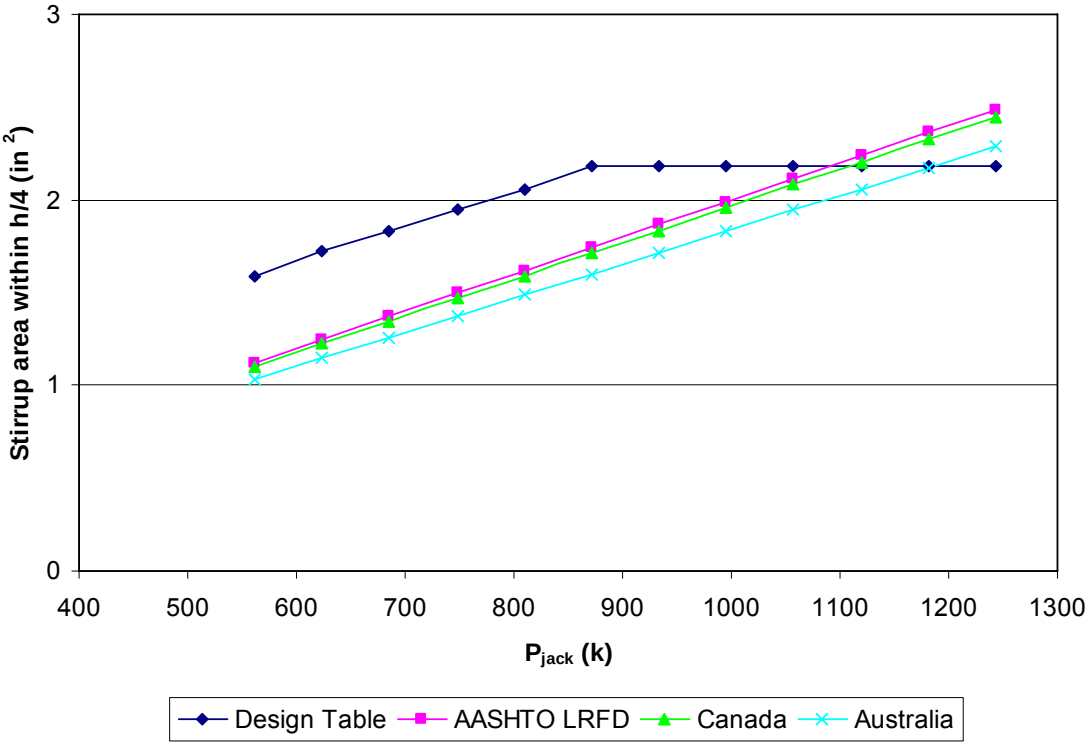

Figure 3-23. Design code comparison, PCBT-45, NWC, ½ in. strand

The comparison between the three design codes and the proposed model is shown for the PCBT-77 girders with normal weight concrete and 0.6 in. strand in Figure 3-24. As this figure shows there is a substantial difference between the area of reinforcement required by the proposed model and the design codes for this group of sample girders. All three design codes result in very similar anchorage zone reinforcement requirement; however, the proposed design model typically required between 1.0 to 1.5 in^2 more reinforcement within h/4 than required by the current design codes. In design this would result in the addition of 2 or 3 stirrups if No. 5 bars are used in the anchorage zone.

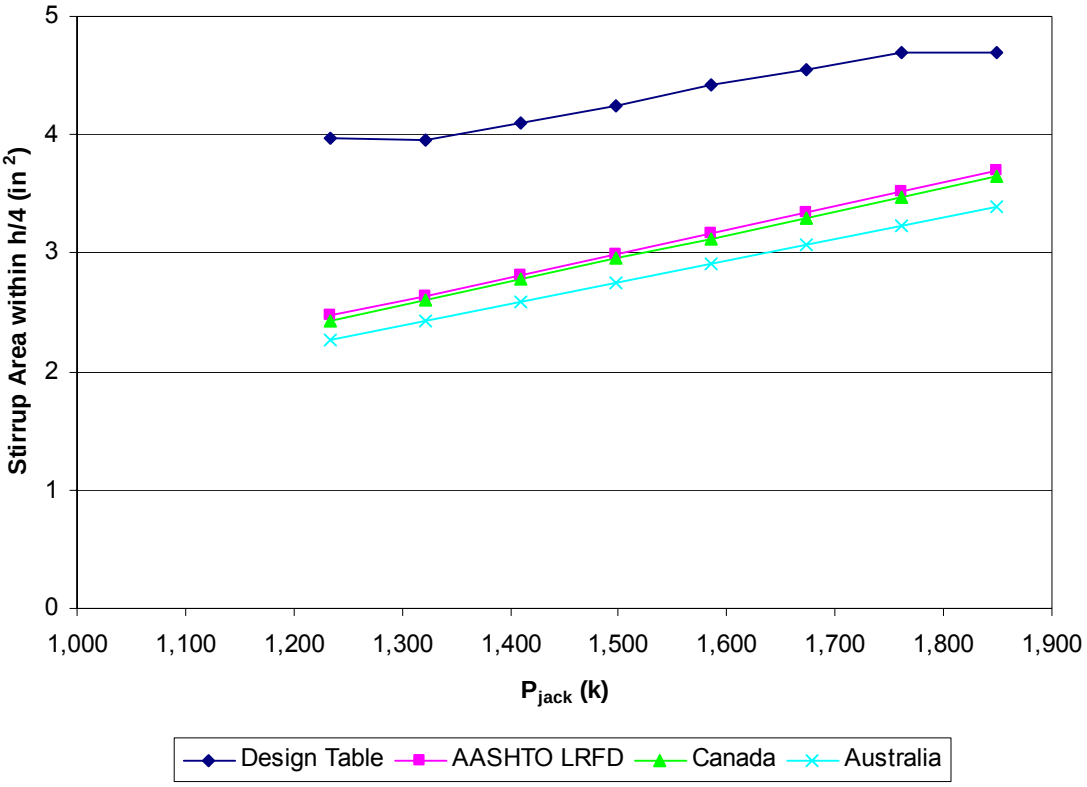

Figure 3-24. Design code comparison, PCBT-77, NWC, 0.6 in. strand

The final design code comparison included the group of sample PCBT-93 girders with lightweight concrete and ½ in. strands. This comparison is shown in Figure 3-25. While there is little difference among the three design codes, the stirrup requirement obtained with the proposed model was significantly higher. In some cases the difference was almost a 140 percent increase in the required stirrup area from the design codes to the proposed value. This large increase is caused by several factors. The working stress selected for the lightweight parametric study was 12 ksi. The value for the working stirrup stress for the other design codes was based on the maximum stress allowed by the respective code. A designer could select a lower working stress for the stirrups; however, none of the codes reviewed for this study provide recommendations on reducing the working stress based on concrete type or environmental conditions. The proposed model recommends a lower working stress for girders with lightweight concrete because the splitting tensile strength at transfer is generally lower than that for a normal weight concrete member. This series of girders also represents the largest and most heavily prestressed girders analyzed in the parametric studies. As the case study girders showed

in section 3.2, the large, heavily prestressed girders typically displayed the most severe anchorage zone cracking. It is reasonable to expect that a significantly greater area of reinforcement would be required for these girders in comparison to current anchorage zone designs.

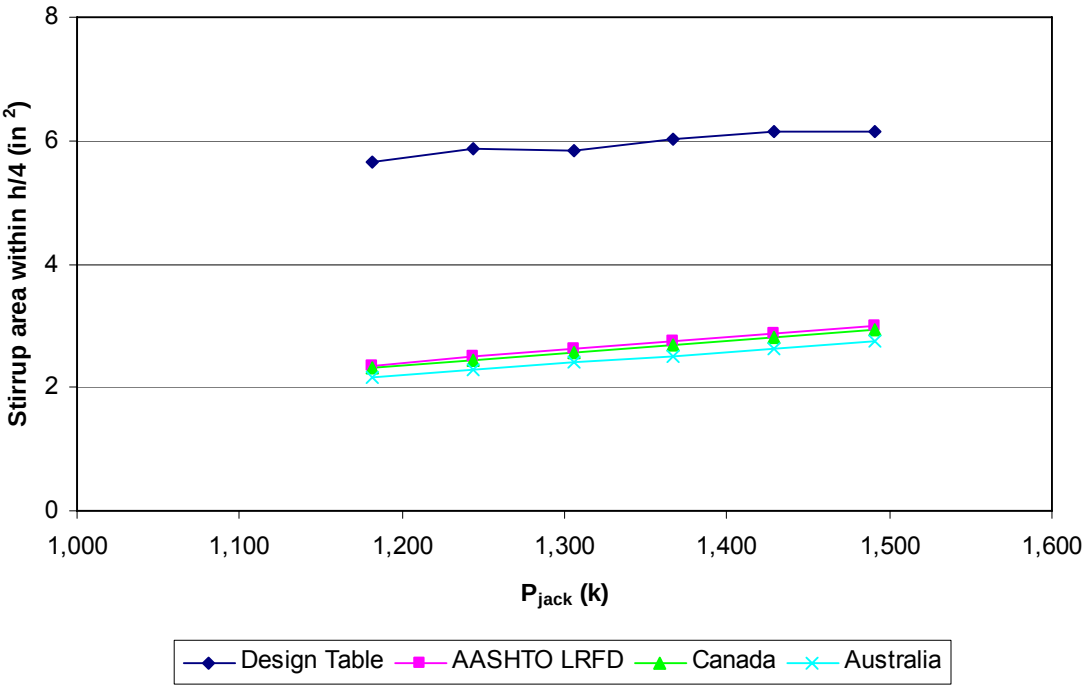

Figure 3-25. Design code comparison, PCBT-93, LWC, ½ in. strand

3.5.9 Parametric Study Results Compared to Case Study Girders

The results from the parametric study were compared to the case study girders presented in section 3.2. A comparison was made between the actual area of stirrups placed within $h/4$ in each case study girder and the stirrup area required by the appropriate design table for a girder with the same number of strands. This comparison is shown in Table 3-5. A second comparison was made between the actual area of stirrups within $h/4$ and $3h/4$ in the case study girders and the area required in this region according to the appropriate design tables. This comparison is shown in Table 3-6.

Table 3-5. Comparison of stirrup area within *h*/4 for case study girders and design tables

Case Study Girder	Rating of cracking within *h*/4	Actual Stirrup Area (in^2)	Design Table Required Stirrup Area (in^2)	Required/ Actual
PCBT-53	Acceptable	3.1	2.44	0.77
PCBT-61	Acceptable	2.8	2.83	1.01
PCBT-77 (34 0.6 in. strands)	Unacceptable	2.8	3.92	1.40
PCBT-77 (30 0.6 in. strands)	Unacceptable	2.0	3.69	1.85
PCBT-93	Unacceptable	3.47	6.10	1.76

Table 3-6. Comparison of stirrup area between *h*/4 and 3*h*/4 for case study girders and design tables

Case Study Girder	Rating of cracking within *h*/4 - 3*h*/4	Actual Stirrup Area (in^2)	Design Table Required Stirrup Area (in^2)	Required/ Actual
PCBT-53	Unacceptable	1.6	2.28	1.43
PCBT-61	Acceptable	3.2	2.64	0.82
PCBT-77 (34 0.6 in. strands)	Unacceptable	2.8	3.97	1.42
PCBT-77 (30 0.6 in. strands)	Unacceptable	2.4	3.70	1.54
PCBT-93	Unacceptable	Unknown	5.69	N/A

Two of the case study girders examined had an acceptable level of cracks within a length of *h*/4 from the end of the beam. The ratio of the required stirrup area from the design table to the actual stirrup area for the PCBT-53 and PCBT-61 case study girders was ≤ 1.0 which would suggest that these girders had adequate vertical resistance in this region of the anchorage zone. It is important to note that if these girders were redesigned using the proposed design tables, the actual area of stirrup provided may be slightly higher than the value in the fourth column of Table 3-5 based on the size and number of bars selected. The other three case study girders had unacceptable cracking within *h*/4, and as Table 3-5 shows, the ratio of the required stirrup area from the design table and the actual stirrup area provided was ≥ 1.0 for these girders. This suggests these girders did not have sufficient vertical resistance in *h*/4 to properly control the lengths of the cracks.

All of the case study girders experienced some diagonal cracking. The PCBT-61 case study girder was the only beam in which the diagonal crack terminated within an acceptable length of $h/2$. Table 3-6 shows the ratio of the required stirrup area to the actual stirrup area was 0.82 for this girder, which would indicate this girder was adequately designed. The remainder of the case study girders had cracking which extended well beyond $h/2$ and the areas of reinforcement required by the design tables were all significantly higher than the areas provided. Due to the extensive cracking which may extend out to 75 percent of the height of the girder in some cases, the results in Table 3-6 indicate the length of the region affected by the diffusion of prestress force is greater than $h/4$. To control the propagation of the diagonal web cracking seen in the VDOT PCBT girders, a dense region of stirrups is needed between $h/4$ and $3h/4$. The proposed design process was specifically calibrated to ensure adequate reinforcement is provided in this region to control the propagation of these diagonal cracks.

A comparison was also conducted for the "drop-in" girder shown in section 3.2.5. The area of reinforcement provided in this girder within $h/4$ was 1.24 in^2. The full strut-and-tie model analysis was performed on this girder. The area of reinforcement required within $h/4$ obtained from the model was 4.34 in^2. The area of reinforcement provided in the girder from $h/4$ to $3h/4$ was 2.48 in^2 and the corresponding required area obtained from the strut-and-tie model was 4.05 in^2. The stirrup requirements from the proposed model are much greater than the area provided; however, cracking in the end region of this girder could adversely affect the structural performance of the member. Providing the additional area of reinforcement would not significantly increase the cost of the girder or add significant congestion to the end region and is necessary to limit the formation of these cracks.

3.6 Development of New Standard Details for VDOT

3.6.1 Overview of New Details

Standard details were developed for VDOT which incorporate the aspects of the proposed design model. The standard details were developed to be used in conjunction with the design tables given in Appendix C. To include elements of the design model, the end of the girder was divided into two regions. One region of the anchorage zone

extends from the beam end to $h/4$ and the other extends from $h/4$ to $3h/4$. The number and size of stirrups and spacing size for the reinforcement in these two regions are obtained from the correct anchorage zone design table for the cross section, concrete type, and strand type.

The new standard details include three different types of main stirrups. The main stirrups used in the anchorage zone regions have a 90° standard hook on the bottom as shown in Figure 3-26 (a) and (b). The hook is included in the detail to provide improved anchorage for these stirrups. Using a standard hook on the stirrups will ensure they are fully developed when they enter the web. The stirrups placed beyond $3h/4$ are the standard 180° bend, double leg stirrup currently used by VDOT and illustrated in Figure 3-26 (c). There are two different lengths of stirrups recommended for use within the anchorage zone. One type of stirrup in the anchorage zone is intended to extend out of the top flange of the girder and to at least mid-depth of the deck slab to provide horizontal shear transfer and ensure composite action between the girder and the deck. This type of stirrup is shown in Figure 3-26 (a). The length of this stirrup depends on the height of the girder and the depth of the bridge deck. The second type of stirrup used in the anchorage zone is contained within the cross section of the girder which is shown in Figure 3-26 (b).

The use of two different stirrup lengths in the anchorage zone is intended to facilitate future deck removal or replacement. Typically the spacing for the anchorage zone reinforcement will be small and much closer than that required for horizontal shear transfer. When detailing the anchorage zone reinforcement, a stirrup will project out of the top of the girder only if it is required for horizontal shear transfer. Stirrups which are required for anchorage zone reinforcement but not needed to provide horizontal shear transfer should be contained within the girder cross section.

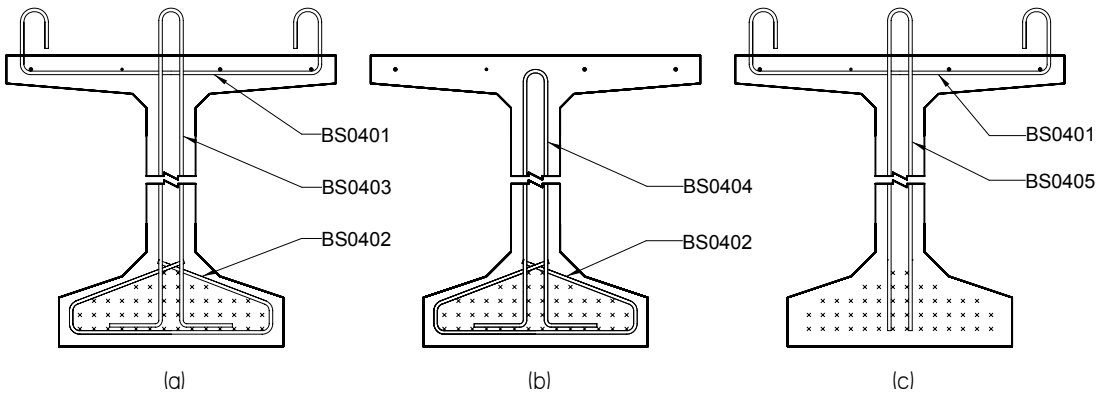

Figure 3-26. Proposed stirrup types

Another change to the reinforcement detailing pertained to the confinement reinforcement. The current VDOT standard detail uses confinement reinforcement which is open at the top. The new confinement reinforcement detail is crossed at the top as illustrated in Figure 3-26 (a) and (b). This detail is added to help control the cracks which frequently develop at the second fillet between the bottom flange and web. The current VDOT standard detail includes two No. 5 longitudinal bars in the bottom flange which are recommended for removal and are not shown in this detail. These bars are unnecessary and will absorb prestress force which is intended to enter the concrete. The cross section views shown in Figure 3-26 all include four courtesy strands in the top flange. These strands should be stressed to 1 kip each and will assist the fabricators in tying the reinforcement cage.

An elevation view of the standard detail of the anchorage zone is shown in Figure 3-27 and Figure 3-28. The beam end shown in Figure 3-27 is the typical detail which would be used for girders in simple spans or girder ends at expansion joints. The beam end shown in Figure 3-28 is the typical detail for girder ends which are enclosed in cast-in-place diaphragms in spans made continuous for live load. Both beam end elevations have two regions called out which correspond to the two regions of the design model. It is recommended that the first stirrup at the end of the beam always consist of a pair of bundled stirrups.

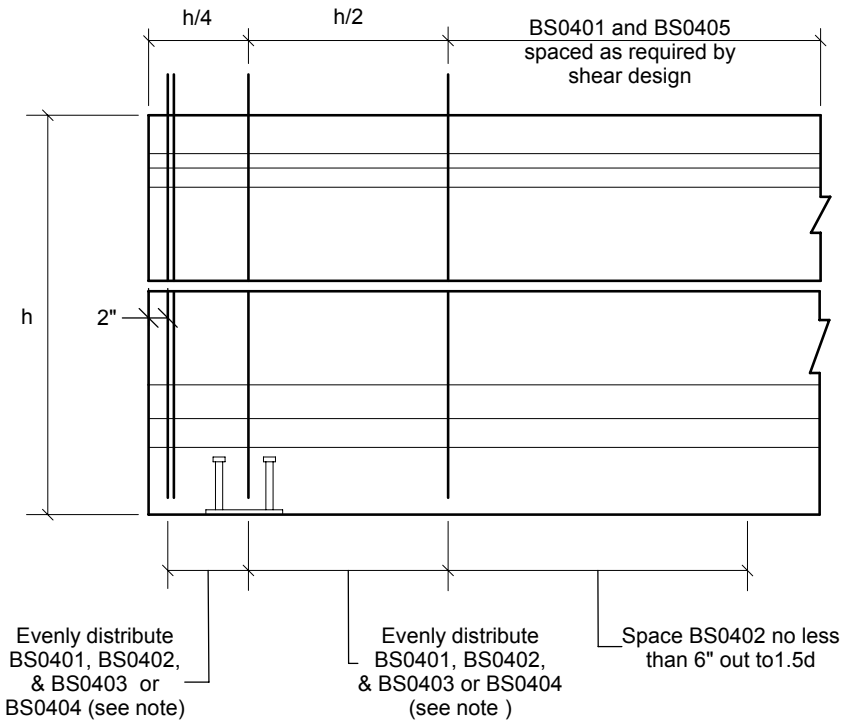

Note: BS0403 shall extend out of the top flange of the girder and is used when stirrup is required for both anchorage zone reinforcement and horizontal shear transfer. BS0404 is contained within the cross section and is used when stirrup is needed for anchorage zone reinforcement only.

Figure 3-27. Anchorage zone elevation – simple span beam end

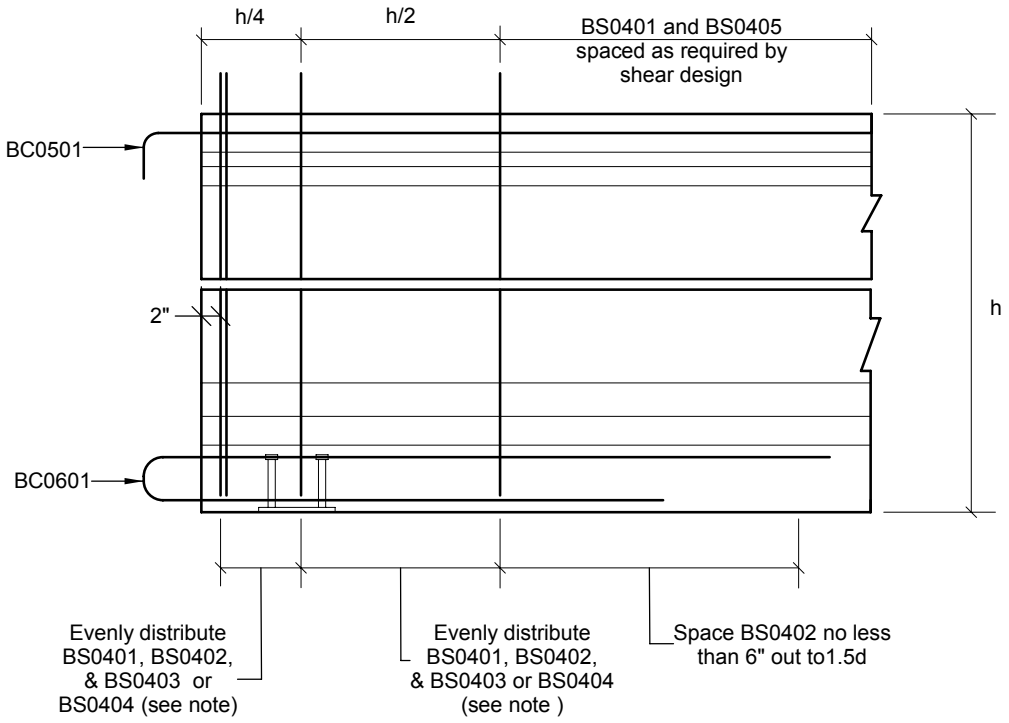

Figure 3-28. Anchorage zone elevation – end diaphragm

3.6.2 Comparison of New Details to Other State Standard Details

Several comparisons were made between the anchorage zone reinforcement details obtained using the proposed design tables, and the anchorage zone standard details used by other states. For this comparison, standard details for bulb-tee girders from Washington, Florida, North Carolina, and Oklahoma were obtained from the respective state DOT web pages. Each of these states provide standard anchorage zone details for bulb-tee girders commonly used by their DOT. The standard anchorage zone details did not vary depending upon prestress force magnitude or materials as the proposed plan for Virginia would. The state standard details used for comparison were rather robust and appeared to be developed to apply to any level of prestress force. Additionally, the bulb-tee girders commonly used by these states did not directly correspond in size to the girders used by Virginia. To make this comparison, the closest sized PCBT girder used by Virginia was selected. Four of these comparisons are shown in the following figures.

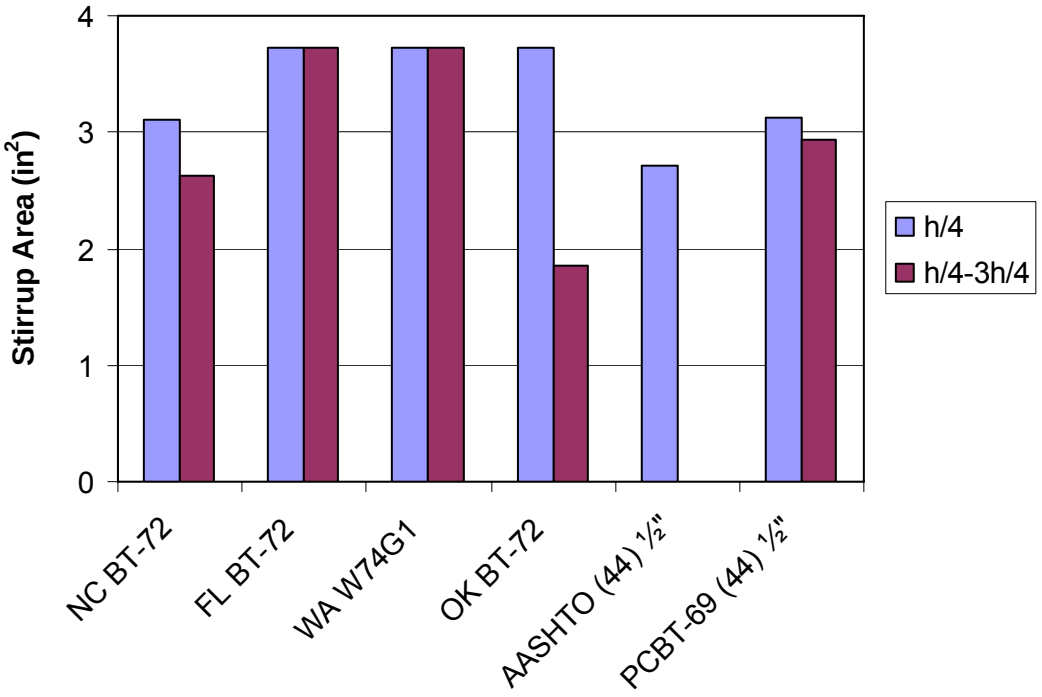

Figure 3-29. Standard detail comparison – PCBT-69, NWC, 44 ½ in. strands

Figure 3-29 shows a comparison between the standard anchorage detail for the 72 in. bulb-tee girder used by North Carolina, Florida, and Oklahoma, a 74 in. bulb-tee girder used by Washington, and the required stirrup area for a PCBT-69 with 44, ½ in. strands designed with the proposed anchorage zone tables. This figure shows the required stirrup area within *h*/4 using the proposed design tables for this sample girder is slightly less than the area of stirrups within *h*/4 used in Florida, Washington, and Oklahoma. The required stirrup area for this sample girder within *h*/4 is the same as that currently used in the North Carolina BT-72. All states in this comparison would place more stirrups within *h*/4 than is required by current AASHTO LRFD provisions. Figure 3-29 also shows that North Carolina, Washington, and Florida currently place a large area of stirrups between *h*/4 and 3*h*/4. The required stirrup area for the PCBT-69 from *h*/4 to 3*h*/4 using the anchorage zone design tables is similar to what these states already use in their standard details. Also note that Oklahoma does not place a very large area of stirrups in this region according to their standard detail.

Figure 3-30. Standard detail comparison – PCBT-69, NWC, 32 0.6 in. strands

The comparison in Figure 3-30 shows the same girders as the previous figure; however, this comparison uses a PCBT-69 with 32, 0.6 in. strands to provide a similar level of prestress as 44, ½ in. strands. Using 0.6 in. strand as opposed to ½ in. strand creates a much larger eccentricity for the prestress force. As a result of the larger eccentricity, the required stirrup area for this girder is higher and slightly exceeds the area of reinforcement used by Florida and Washington. This figure illustrates how the proposed design tables provide flexibility to customize the design of the anchorage zone based on the materials used.

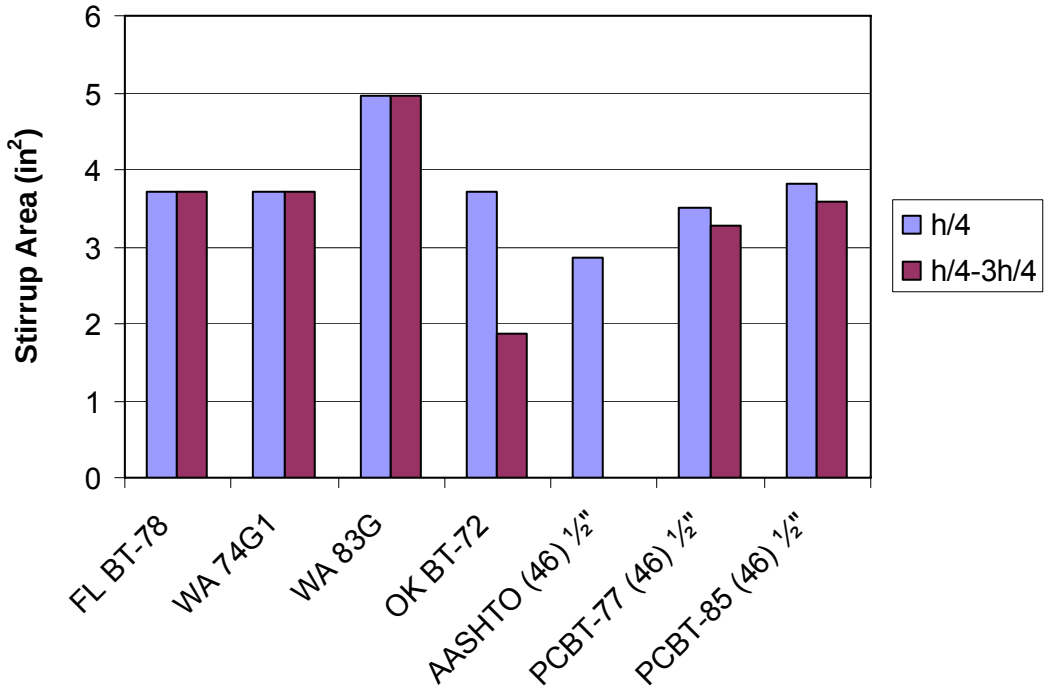

Figure 3-31. Standard detail comparison – PCBT-77 and PCBT-85, NWC, 46 ½ in. strands

Figure 3-31 is a comparison of several of the larger girders used by Florida, Washington, Oklahoma, and the Virginia PCBT-77 and PCBT-85. This comparison shows when these girders are used with ½ in. strands the area of reinforcement required by the design tables is similar to the Florida BT-78 and Washington 74G1. Once again, all states designs exceeded the AASHTO LRFD minimum stirrup requirement. Figure 3-32 compares the same girders as Figure 3-31 but the Virginia PCBT-77 and PCBT-85 have 0.6 in. strands in this example. This figure shows that the required stirrup area for the PCBT-77 and PCBT-85, when 0.6 in strands are used, is slightly greater than the areas used in the BT-78 and 74G1, but still less than the stirrup area used in the Washington 83G.

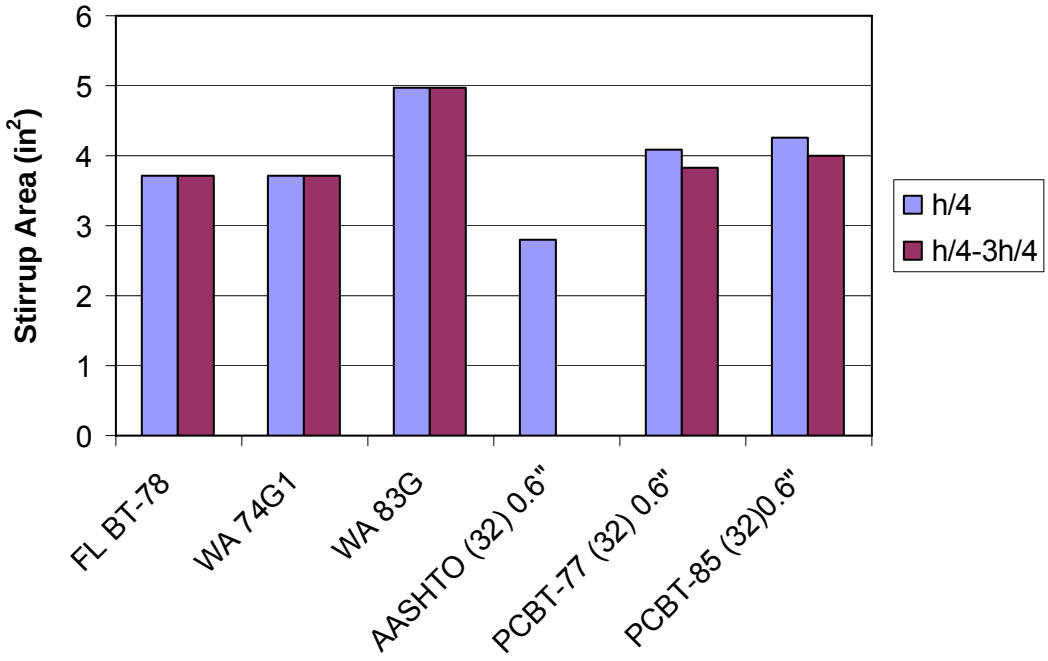

Figure 3-32. Standard detail comparison – PCBT-77 and PCBT-85, NWC, 32 0.6 in. strands

In general the proposed anchorage zone design tables require an area of stirrups similar to what other states currently use. For the smaller girders used in Virginia, such as the PCBT-29, 37, 45, 53, and 61, the area of stirrups required in *h*/4 by the design tables is a slight increase from what is currently used in Virginia. The area of stirrups required from *h*/4 to 3*h*/4 for these girders is necessary to control diagonal cracks in the girder and will typically be slightly more than is currently used in this region to ensure horizontal shear transfer. The larger girders used in Virginia, such as the PCBT-69, 77, 85, and 93 will contain significantly more stirrups within *h*/4 and within *h*/4 and 3*h*/4 in comparison to current designs in Virginia. In particular, large girders with 0.6 in. strand or large girders with lightweight concrete have the largest increase in the area of stirrups compared to current designs used in Virginia.

3.7 Conclusions

This chapter has shown there are a wide variety of anchorage details used in Virginia and a wide variety in the performance of these anchorage zones. The anchorage zone design tables developed for this research study have been calibrated to actual field performance and are intended to ensure anchorage zones have acceptable crack lengths

and widths. It is not likely that details developed with the anchorage zone design tables will completely eliminate anchorage zone cracking, but they will offer a significant improvement over current design practices in Virginia. The anchorage zone constitutes a relatively small portion of the overall design. The design tables developed for this research provide a quick means to complete this aspect of the design and ensure reliable performance. Using the full anchorage zone strut-and-tie model is recommended for girders not covered by the design tables.

Chapter 4. Experimental Testing and Results

4.1 Overview

An experimental 65 ft PCBT-53 bridge girder was fabricated in October 2006 to verify the new anchorage zone design model. As part of an on-going research project conducted by the Innovative Bridge Research and Construction Program, the girder was cast with lightweight self-consolidating concrete (SCC) and then tested at Virginia Tech. Experimental anchorage zone details were developed for each end of the beam to compare cracking at transfer. This girder was later used in a test to quantify the shear strength of lightweight SCC. For this test a 7 ft. wide, 9 in. deep deck was added to the top of the girder.

The anchorage zone details at each end of the beam were designed using the proposed strut-and-tie anchorage zone model. At one end of the beam a stirrup working stress of 12 ksi was selected, which corresponded to the recommendations of the model discussed in section 3.3.2 for girders with lightweight concrete. This end will be referred to as the 12 ksi anchorage zone for the remainder of the chapter. At the other end, a working stress of 18 ksi was selected in the design of the stirrups. This end will be referred to as the 18 ksi anchorage zone throughout this chapter. The design process, testing, and results of the testing are presented in the following paragraphs.

4.2 Design of Experimental Anchorage Zone Details

The PCBT-53 test girder was pretensioned with 32 ½ in. strands. Six of the strands were harped at the end of the girder. The harping points for the strands were located 30 in. from the center line of the girder. The release strength of the concrete used in the design of the anchorage zones was 5,500 psi and the unit weight was assumed to be 120 lb/ft^3. In the design of the anchorage zone details the force from four courtesy strands located in the top flange was considered. These strands were each stressed to 4 kips. In Virginia, the courtesy strands are typically only tensioned with 1 kip of force, but in order to reduce the tensile stresses in the top flange of the girder at transfer a higher force was used for this experiment. A cross section view of the test girder is shown in Figure 4-1.

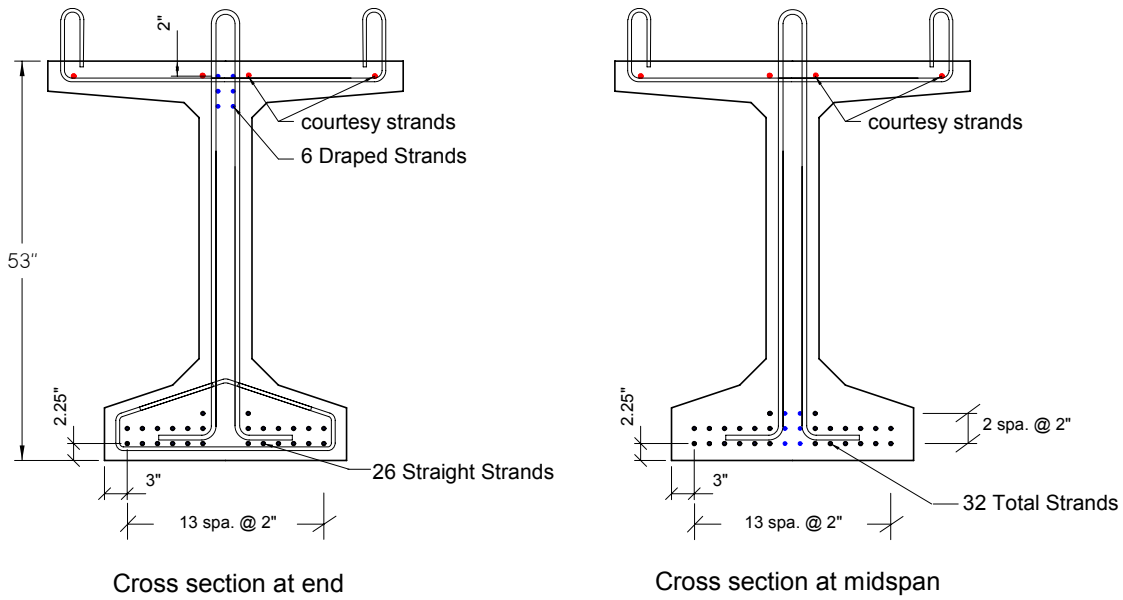

Figure 4-1. Cross sections of test girder

There were two small variations between the stirrup detail shown in Figure 4-1 and the proposed standard details discussed in section 3.6.1. In the test girder, stirrups with standard hooks on the bottom were used over the entire length of the member. The proposed standard detail from section 3.6.1 recommends using the 180° bend, double leg stirrups currently used by VDOT beyond 3*h*/4 from the beam end. Using stirrups with hooks on the bottom adds to the girder fabrication time and the additional anchorage they provide is not necessary over the entire length. The stirrups with hooks were used over the whole length in this test due to the high shear forces anticipated in subsequent tests with the girder. The confinement reinforcement used in this member was made up from two pieces spliced together which is visible in the end cross section view of Figure 4-1. After construction of this test girder, the confinement detail shown in Figure 3-26 was selected as a better alternative.

The calculations for solving the strut-and-tie models for the anchorage zones at each end of the beam are presented in Appendix E. The steps for solving the strut-and-tie models were the same as those discussed in the full design example presented in section 3.4.2. The only difference in the design of the two anchorage zones for this girder was the selected working stress for the stirrups. No. 5 stirrups were selected for the

anchorage zone reinforcement at both ends to ensure the spacing between bars was sufficient to achieve good consolidation at the end of the girder. The reinforcement details for the two anchorage zones are shown in Figure 4-2.

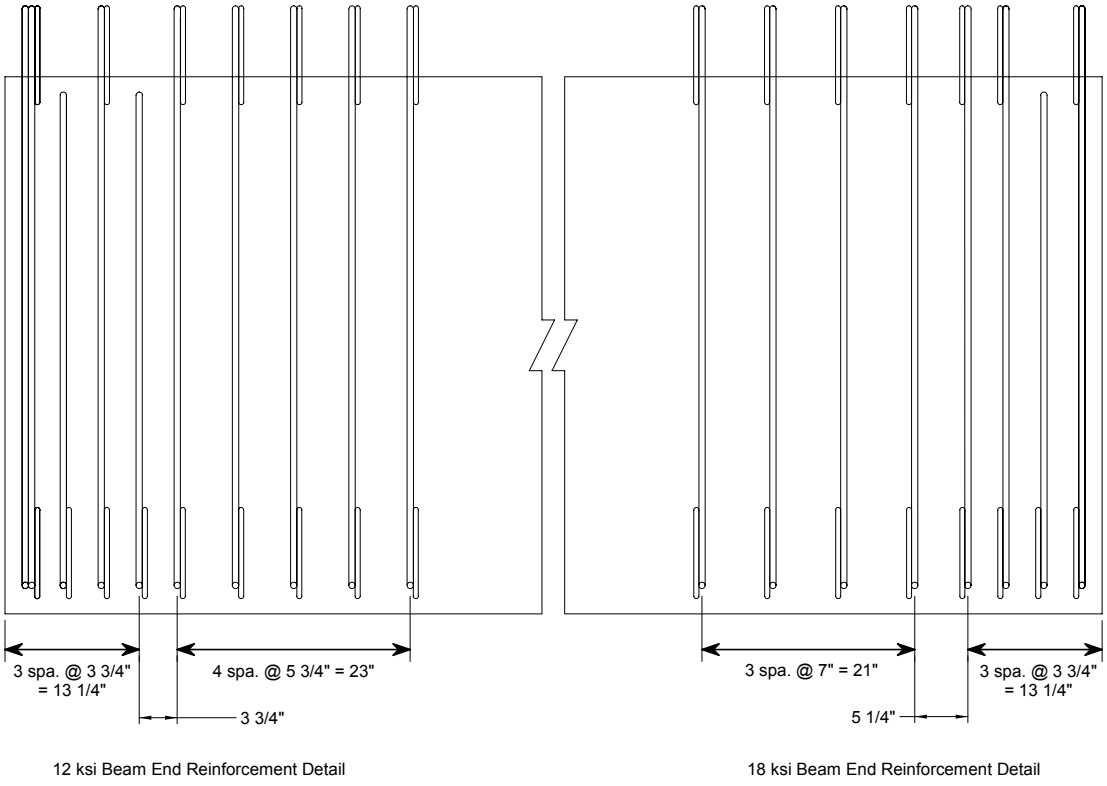

Figure 4-2. Reinforcement details for experimental PCBT-53 girder

As the calculations in Appendix D show, the force in the tie from the lower strut-and-tie model was approximately 4 percent of the total jacking force. This shows how the proposed strut-and-tie model is calibrated so that for shallow beams, such as the PCBT-53, the force in the lower strut-and-tie model is usually very close to the current AASHTO LRFD requirement of 4 percent. There are two key differences between the design of the experimental anchorage zone details for this girder and details designed using current AASHTO LFRD practice. The first difference is the average working stress for the stirrups. This test beam example illustrates the importance of the recommendations for the working stress which are based on concrete type and environmental conditions. The second difference is the extension of the anchorage zone reinforcement out to $3h/4$. Under current design practices, this girder would have a dense region of stirrups between the end and $h/4$ and then stirrups would be spaced as

required for horizontal or vertical shear. As field observations have shown, a dense region of reinforcement in *h*/4 may not be sufficient to control the formation of diagonal cracks in the upper web region.

The difference in the stirrup area between the two anchorage zones is rather small. Table 4-1 provides a summary of the required stirrup area and number of stirrups used in each anchorage zone. This table shows that the 12 ksi anchorage zone contained only two more stirrups than the 18 ksi anchorage zone. It is also important to note that both anchorage zones exceed the minimum stirrup requirement from AASHTO LRFD within the distance between the beam end and *h*/4. The 18 ksi anchorage zone contained one more stirrup between the beam end and *h*/4 compared to what AASHTO LRFD design practice would require in this region.

Table 4-1. Summary of anchorage zone details

Anchorage Zone	Required Stirrup Area (in^2) end – h/4	Qty of No. 5 bars	Required Stirrup Area (in^2) h/4-3h/4	Qty of No. 5 bars
12 ksi	3.36	5	3.14	5
18 ksi	2.24	4	2.09	4

The stirrups used in the test girder included a standard hook on the bottom as illustrated in Figure 4-2. In both ends of the beam, short stirrups were used in locations where reinforcement was needed in the anchorage zone, but was not needed for horizontal shear transfer between the girder and the composite deck. The minimum stirrup spacing required for horizontal shear transfer at the end of the girder was 7 in. In the 18 ksi anchorage zone, the spacing of the stirrups between *h*/4 and 3*h*/4 exceeded this spacing limit for horizontal shear transfer, and as a result the smaller spacing limit controlled. It is not typical that the spacing requirement for horizontal shear transfer will control in this region; however, in this particular case the spacing requirement for horizontal shear transfer did control due to the high shear forces expected when the girder was later tested to failure for a subsequent research project.

4.3 Testing Procedure

4.3.1 Instrumentation

The stirrups in both anchorage zones of the girder were instrumented with electrical resistance gages to measure strains and provide insight on the bursting forces acting in the anchorage zones. Each anchorage zone consisted of four groups of strain gages. Two groups of gages were placed in the upper portion of the web close to the location where the diagonal cracks previously discussed typically develop. The third group of gages was placed lower in the web at the height of maximum moment from the Gergely and Sozen model. The fourth group of strain gages was placed at the intersection between the bottom flange and web where longitudinal cracks frequently develop. A diagram for the location of strain gages at each end of the girder is shown in Figure 4-3 and Figure 4-4.

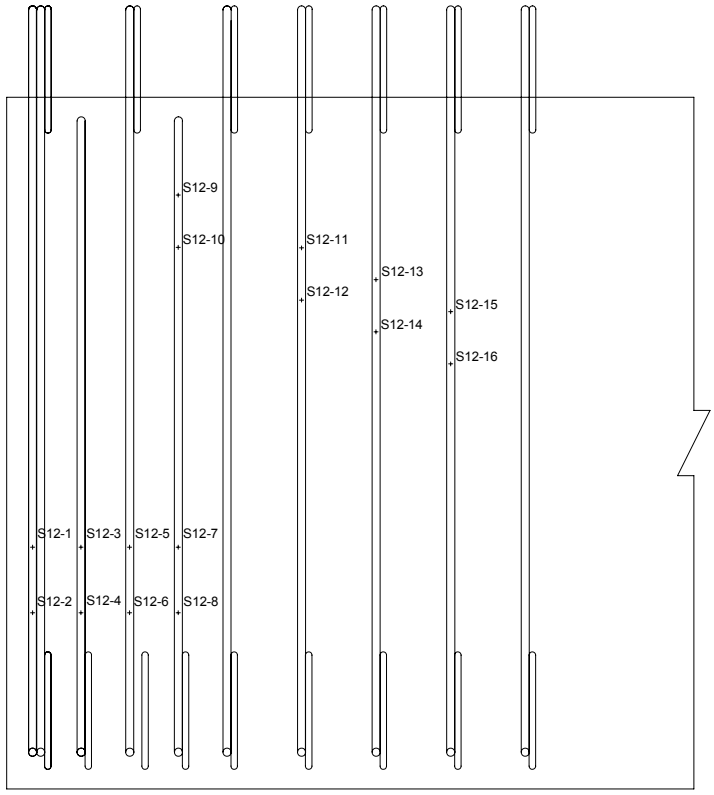

Figure 4-3. Strain gage layout at 12 ksi anchorage zone

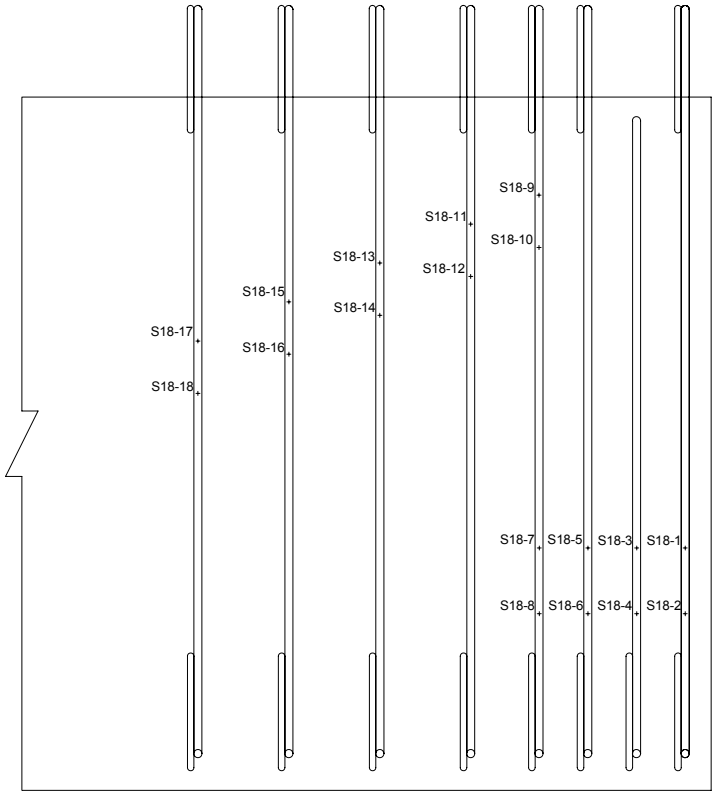

Figure 4-4. Strain gage layout – 18 ksi anchorage zone

The strain gages were numbered sequentially, and they were each given a prefix of either S12 or S18. The "S" in the prefix denotes that the instrument was used to measure strain. (Additional instruments were placed in the girder for the shear tests conducted at a later date) The "12" or "18" in the prefix refers to either the 12 ksi anchorage zone or the 18 ksi anchorage zone of the girder. The CEA-06-125UN-350-P2 strain gages were purchased from Vishay Micro-Measurements. These gages included pre-attached 10 ft. lead wires which greatly reduced the application time. The gages were mounted to the stirrups using Vishay Micro-Measurements M-Bond 200 and protected with the M-Coat F protective coating system.

The stirrups were instrumented in the Virginia Tech Structures Laboratory a few weeks prior to casting the beam. Bayshore Concrete Products Corp. (Bayshore) provided uncoated, grade 60 stirrups which were bent to the correct shape. Before each gage was applied, a section of the stirrup was grinded and sanded smooth at the gage location. The strain gages were then applied to the stirrups and protected in accordance with the manufacturer's recommendations. A total of 36 strain gages were applied to the stirrups

at the laboratory. These stirrups were brought to Bayshore on October 23, 2006, and installed in the appropriate locations within the girder. After installing the stirrups, the lead wires from the strain gages were spliced with longer wires and attached to the data acquisition system located at midspan of the girder.

A CP23X Micrologger made by Campbell Scientific Inc. (Campbell) was used to collect data from the strain gages during transfer and to collect long-term data from the thermocouples and vibrating wire gages installed in the girder for subsequent tests. This system operates on a user-provided program which specifies which channels to read and the frequency of the readings. The Campbell program was prepared and tested at the Structures Laboratory a few weeks prior to casting to ensure it was working properly. The Campbell was initially programmed to take readings from all instruments at 1 minute intervals from the morning the girder was cast until shortly after transfer when the girder was lifted from the casting bed. After the girder was lifted, the Campbell was reprogrammed and the frequency of readings was adjusted to a 90 minute interval. The Campbell was placed in an environmentally resistant box at the precast yard and the lead wires from the instrumentation were passed through two access holes in the box. Throughout all of the testing the Campbell was powered by a solar panel.

The strain gages (and other instruments) were connected to the Campbell in the field on October 23, 2006. After the system was installed, each strain gage was tested with a voltmeter to ensure it had the correct resistance of 350 Ohms. During this test it was discovered that six of the strain gages were not working correctly. Four of these six strain gages were severely damaged during the process of placing the stirrups in position within the girder. Efforts were made to troubleshoot the other two gages which were not functioning correctly but the gages could not be fixed before fabrication began. Photographs of the strain gages installed in their final positions in the girder are shown in Figure 4-5 and Figure 4-6.

The original instrumentation plan also called for twelve strain gages to be applied in the field on the prestress strand. These gages were to be placed on strands at $h/4$, $h/2$, and $3h/4$ at each end to help quantify the length of the general zone. Placing these gages in a field environment proved challenging and was not successful. It is believed that due to the low temperatures in the field on October 23, there was not enough heat for the

adhesive to properly bond the gage to the prestressing strand. As a result, this plan was abandoned at the precast yard. Three gages were successfully mounted to the strand and are visible in Figure 4-5 and Figure 4-6. Readings collected from these gages were not used in the following analysis.

Figure 4-5. Strain gages installed at the 12 ksi anchorage zone

Figure 4-6. Strain gages installed at the 18 ksi anchorage zone

4.3.2 Fabrication of Test PCBT-53

Concrete was poured for the test girder during the afternoon of October 24, 2006. This was one of the first attempts by Bayshore to construct a beam with high performance lightweight SCC and the process of getting the mix correct took several hours. A total of three ready-mix trucks were rejected before the mix was finally accepted. Prior to placing concrete in the formwork, workers from Bayshore performed a slump test and measured the concrete unit weight and percent air content. Figure 4-7 shows the slump test being performed on a trial batch of concrete.

Figure 4-7. Slump test on batch of LWSCC concrete

The concrete pour took approximately one hour to complete. The SCC required a minimal amount of external vibration on the formwork. Workers provided some internal vibration with pencil vibrators from the walkway on top of the girder. The beam was covered with blankets after the concrete was placed and steam cured overnight. Figure 4-8 shows the girder steam curing on the morning of October 25. At 8:40 a.m. on October 25, a modulus of elasticity test, a compression test, and a split cylinder test were performed on concrete samples. The results of these tests are given in Table 4-2. This first test showed the concrete had already exceeded the design release strength of 5,500 psi and at this time the decision was made to turn off the steam and remove the formwork. These same tests were performed a second time three hours later during transfer and the results from this set of material tests are also listed in Table 4-2.

Table 4-2. Concrete material properties on October 25, 2006

Test Time	$f`_{ci}$ (psi)	E_{ci} (ksi)	f_{ct} (psi)
8:40 a.m.	7,752	3,550	558
11:30 a.m.	8,917	3,640	626

Figure 4-8. Girder steam curing on October 25, 2006

After the forms were removed, the strands were flame cut with an acetylene torch. The strands were cut at both ends of the girder simultaneously. The top row of courtesy strands was cut first, followed by the harped strands, and straight strands. The process of cutting all strands took almost three hours. The test beam was located at one end of a casting bed which was over 200 ft long. There were no other girders being fabricated in the same casting bed. When strands were cut at the long free end they would become very tangled, and workers would remove the tangled strands periodically, causing the transfer process to proceed very slowly. After all the strands were cut the girder was lifted and then returned to the same position in the casting bed until it was transported to the Virginia Tech Structures Laboratory on December 13, 2006.

4.3.3 Test Procedures

Anchorage zone cracking develops almost immediately after transfer and cracks often open and propagate further while the girder is lifted. The boundary conditions on the anchorage zone are the most severe during the lifting process. Combine these boundary conditions with early age concrete, and the girder is very likely to crack during

this process. When the girder is being lifted, the self-weight of the girder is acting on the lifting devices which are often located several feet inward from the end of the girder. For this test, a special lifting device was designed which did not require additional steel placed in the web of the girder. This lifting device was developed and used to prevent interference with the shear tests which were later performed on the girder. A photograph of the girder being lifted from the casting bed is shown in Figure 4-9.

Figure 4-9. Test girder lifted from casting bed on October 25, 2006

The testing procedure for the anchorage zone model consisted of a visual inspection of the cracking in the ends during transfer and after the girder was lifted from the casting bed. The anchorage zones were also visually inspected 50 days after transfer when the girder arrived at the Structures Laboratory and once again after the 7 ft wide deck was poured on the girder. The cracks in the two anchorage zones were marked on the girder and measured with a crack comparator card.

An important component in this test was the initial lift from the casting bed. During this first movement, the girder is most vulnerable because the prestress force is the highest, since long term prestress losses have not started, and the concrete is relatively weak. Bayshore had planned to leave the girder in the casting bed until it was transported

to Virginia Tech, but since lifting the girder was necessary to verify the anchorage zone model, they agreed to lift the girder briefly. The readings from the strain gages were monitored throughout casting, transfer, and the first lift of the girder. After the girder was lifted, the data acquisition system was adjusted to take readings every 90 minutes and the strain gage readings were recorded throughout the life of the gages.

4.4 Results and Discussion

4.4.1 General

The difference in performance between the two anchorage zones was visibly noticeable. There was significantly more cracking in the anchorage zone designed with a stirrup working stress of 18 ksi which was expected. The readings from the strain gages also showed higher strains in the stirrups at the 18 ksi anchorage zone. The strain gage data showed a region of high strains where diagonal cracks typically develop. The following sections present and discuss these results.

4.4.2 Anchorage Zone Crack Pattern at Transfer

4.4.2.1 12 ksi Anchorage Zone

The photographs in Figure 4-10 show both faces of the 12 ksi anchorage zone and the level of cracking which developed after transfer. The photographs were taken after the girder was lifted from the casting bed and set back down. This anchorage zone performed very well and the level of cracking would be considered acceptable in accordance with the criteria outlined in section 3.3.3. The cracks were very fine and the largest crack width measured was 0.003 in. This crack width is well below an acceptable width for almost any environmental conditions to which the girder could be exposed. As Figure 4-10 shows, a horizontal crack developed at the bottom flange-to-web interface. This crack extended longitudinally for approximately 9 in., which is about 17 percent of the girder height. This crack length is within the crack length limits discussed in section 3.3.3. The cracks at this end developed as the girder was lifted from the casting bed. No cracks were observed to develop in this anchorage zone during the three hour process of cutting the strands.

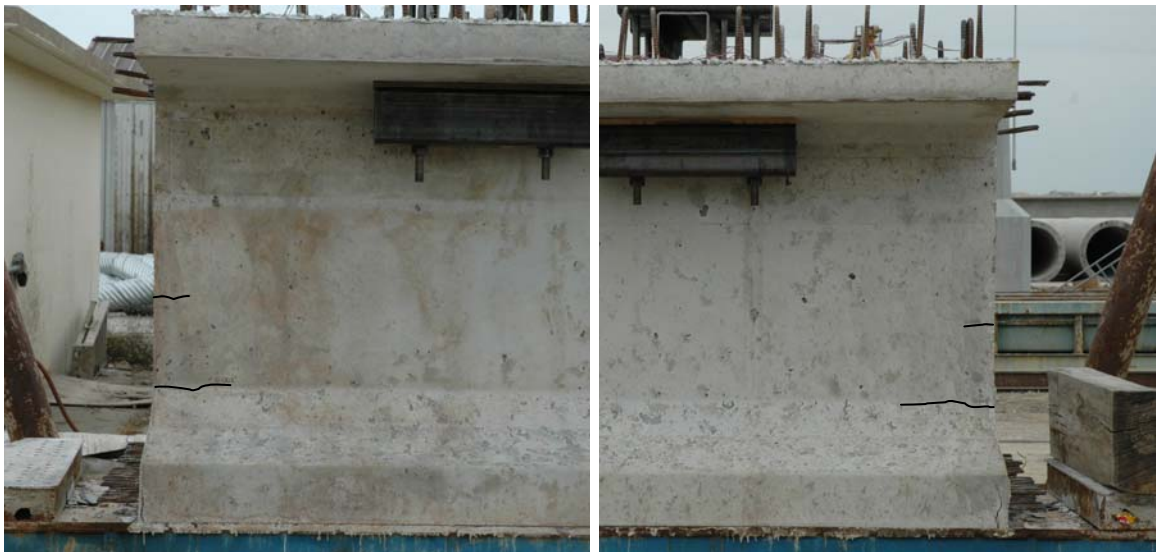

Figure 4-10. Crack pattern in the 12 ksi anchorage zone after lifting

4.4.2.2 18 ksi Anchorage Zone

The anchorage zone designed with a stirrup working stress of 18 ksi did not meet the acceptable crack levels discussed in section 3.3.3. Photographs of both faces of this anchorage zone are shown in Figure 4-11. These photographs were also taken after the girder was first lifted from the casting bed. As Figure 4-11 illustrates, the cracking in this anchorage zone was much more pronounced. The largest crack width measured on this end was 0.005 in. This size crack width would be acceptable for any exposure condition. The lengths of the cracks which developed in this end of the girder did not meet the limits given in section 3.3.3. A diagonal crack opened near the top flange, several inches in from the end of the girder. The crack extended longitudinally 37 in., or 70 percent of the girder height. The acceptable crack length of a diagonal crack is 50 percent of the girder height. Several smaller horizontal cracks also developed lower in the web. The longest of these cracks extended longitudinally 15 in., or 28 percent of the girder height. This also exceeds the limitations on crack lengths discussed in section 3.3.3. In this anchorage zone all cracks also developed during the lifting process.

Figure 4-11. Crack pattern in the 18 ksi anchorage zone after lifting

4.4.2.3 Material Properties at Transfer

A set of compression, split cylinder, and modulus of elasticity tests were performed on cylinders at 11:30 a.m. as workers were beginning to cut the strands on October 25, 2006. The results from these tests were provided in Table 4-2. The average compressive strength of the concrete at this time was 8,900 psi, which was significantly higher than the 5,500 psi used in the anchorage zone design. However, the higher compressive strength has little influence on the performance of the anchorage zones.

More important to the performance of the anchorage zones was the tensile strength of the concrete. The splitting tensile strength measured during transfer was 626 psi. The theoretical modulus of rupture of the concrete for the design release strength using the AASHTO LRFD material properties for sand lightweight concrete was 469 psi. This suggests that cracking could have been more extensive at both ends of the girder if the strands were cut earlier in the day. The theoretical modulus of rupture of the concrete for the measured compressive strength was 597 psi. This indicates that the mix of lightweight concrete used in this girder had a relatively high tensile strength. The theoretical modulus of rupture for normal weight concrete with the same release strength was 717 psi which was approximately 14.5 percent greater than the measured splitting tensile strength of the concrete in the girder. These values would suggest that the tensile

strength of the concrete in the girder was slightly lower than the tensile strength of normal weight concrete with the same compressive strength.

From the visual inspection after transfer, the 12 ksi anchorage zone outperformed the 18 ksi anchorage zone. The cracks at this end of the girder met the design goals for acceptable crack widths and crack lengths from section 3.3.3. The cracks in the 18 ksi anchorage zone were acceptable in width, but the length of the cracks exceeded the goals set in section 3.3.3.

4.4.3 Strain Gage Readings at Transfer

The electrical resistance gages mounted on the stirrups measured strain throughout transfer. Table 4-3 provides a comprehensive summary of the status of each gage at the time of transfer. Four of the gages were destroyed before the pour, (two are listed in Table 4-3 and two were removed from the numbering sequence and are not listed) and several stopped working during the pour or during transfer. Some of the gages provided very erratic results which were not used in the subsequent analysis.

Table 4-3. Status of strain gages at transfer

Gage Number	Gage Status	Gage Number	Gage Status
S12-1	Working	S18-1	Stopped during pour
S12-2	Erratic Results	S18-2	Working
S12-3	Working	S18-3	Erratic Results
S12-4	Working	S18-4	Working
S12-5	Working	S18-5	Stopped during pour
S12-6	Not Working	S18-6	Working
S12-7	Erratic Results	S18-7	Working
S12-8	Erratic Results	S18-8	Working
S12-9	Working	S18-9	Working
S12-10	Erratic Results	S18-10	Damaged during placement
S12-11	Working	S18-11	Working
S12-12	Working	S18-12	Working
S12-13	Stopped during transfer	S18-13	Working
S12-14	Working	S18-14	Stopped during transfer
S12-15	Working	S18-15	Stopped during transfer
S12-16	Working	S18-16	Not working
		S18-17	Damaged during placement
		S18-18	Working

The readings recorded by the strain gages were adjusted to determine the actual strain values. The values recorded by the Campbell data acquisition system were voltages. To convert the voltage into a strain, Equation 4-1 was used.

$$\Delta\varepsilon = \frac{4000 \times zerovoltage}{GF\left[1 - 2\left(\frac{zerovoltage}{1000}\right)\right]} \tag{4-1}$$

Where:

$\Delta\varepsilon$ = change in strain measured in microstrain

Zero voltage = reading – initial reading

GF = gage factor (2.1 for this type gage)

To determine the initial reading used in computing the zero voltage, the data recorded between 7:00 a.m. and 9:00 a.m. on October 25 were averaged. During this time frame the steam blankets and forms were removed from the girder.

Figure 4-12 through Figure 4-15 show the strains recorded on the morning and early afternoon of October 25, 2006. The elapsed time in these figures started at 9:00 a.m. and went to 2:00 p.m. Several of the key events during transfer are noted in each figure.

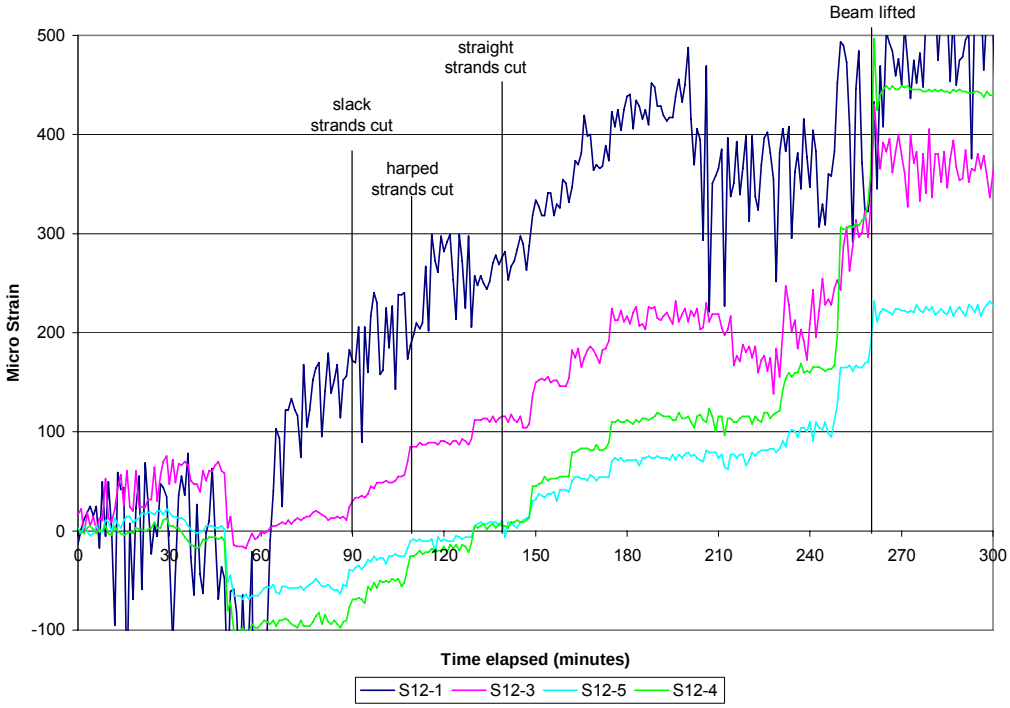

Figure 4-12. 12 ksi anchorage zone – gages in lower portion of web

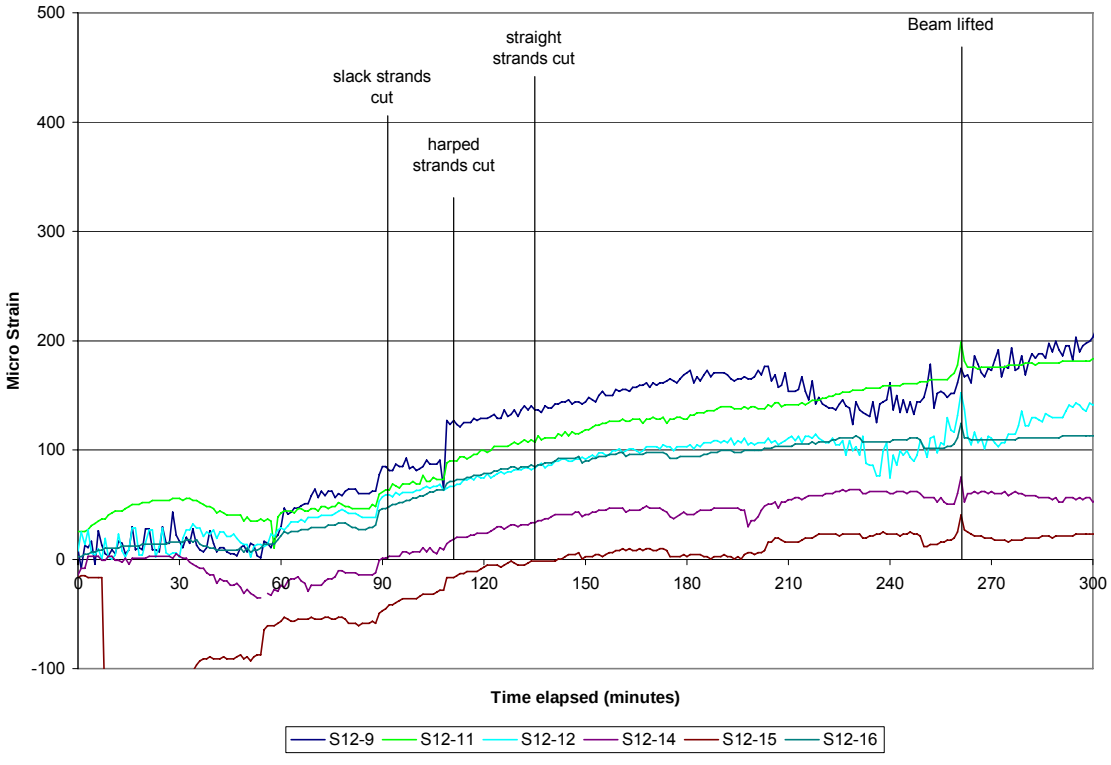

Figure 4-13. 12 ksi anchorage zone – gages in upper portion of web

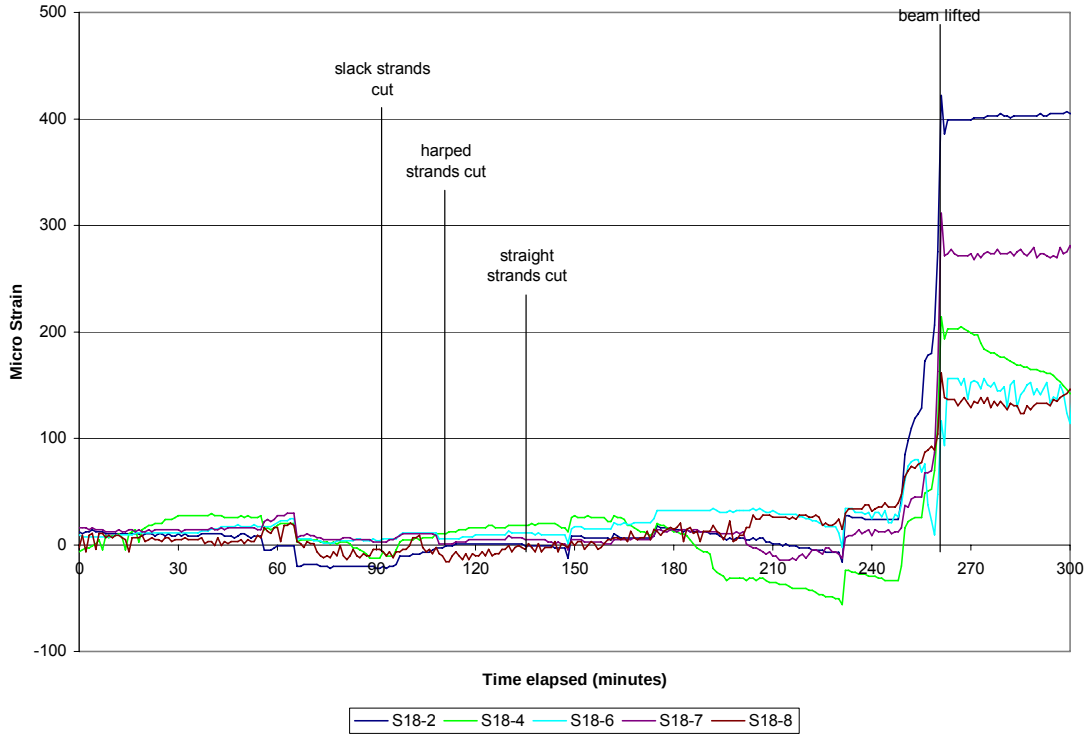

Figure 4-14. 18 ksi anchorage zone – gages in lower portion of web

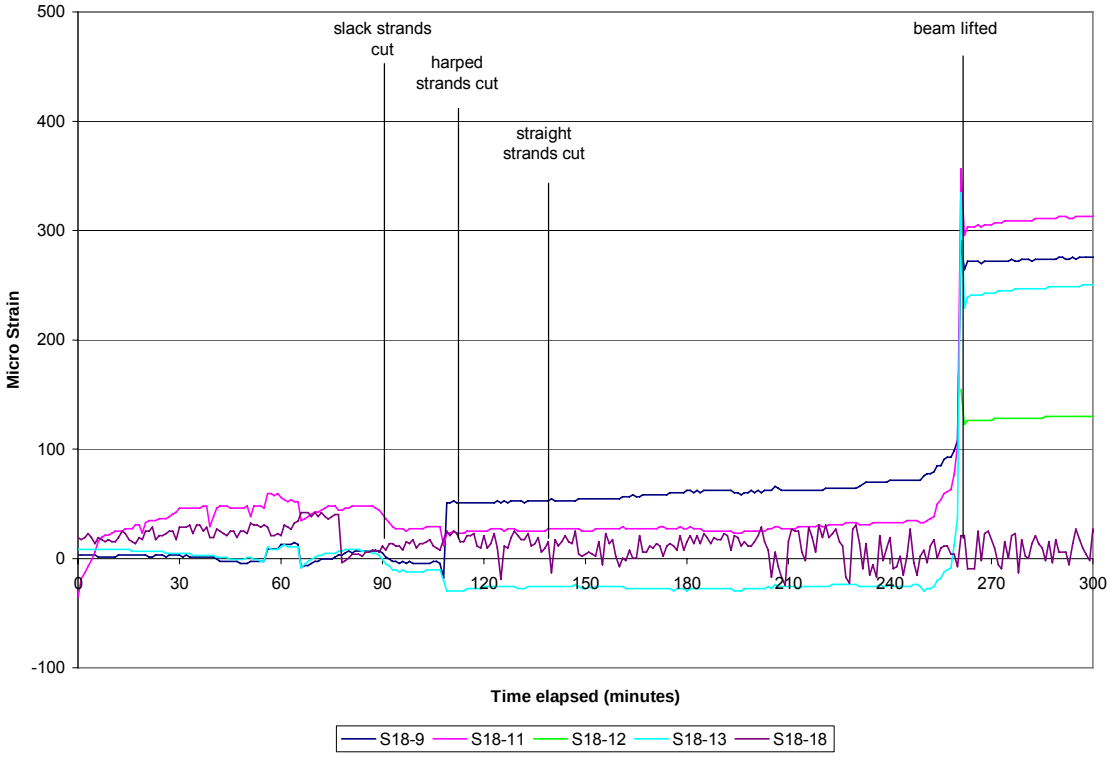

Figure 4-15. 18 ksi anchorage zone – gages in upper portion of the web

4.4.3.1 12 ksi Anchorage Zone

The gages in the 12 ksi anchorage zone located in both the lower portion and the upper portion of the web displayed a steady increase in strain over the time period in which the strands were cut. The gages in the lower portion of the web were closest to the end of the girder and displayed the highest level of strain, as shown in Figure 4-12. These gages were located very closely to the small horizontal cracks in this end of the girder shown in Figure 4-10. The gages in the upper portion of the web did not measure strain readings as high as those lower in the web. The strain values measured in the upper portion of the anchorage zone were all below 200 microstrain as illustrated by Figure 4-13. This region was also free of cracks.

There was a slight increase in the strain readings for the gages in the lower and upper portions of the web after the girder was lifted from the casting bed during the 265th minute. After the girder was placed back in the casting bed, the strain readings returned back to the level prior to the lift and remained relatively constant for the remainder of the time period shown. It was at this point after the girder was lifted that the cracks located near the bottom flange-to-web interface were first visible.

The high strain readings in the stirrups located closest to the end of the girder were similar to the trend observed in previous experimental research conducted by Marshall and Mattock (1962) and Tuan, et al. (2004). The stirrups located farther from the end of the girder experienced smaller strain levels which was also observed by this previous experimental anchorage zone research. The increase in strain observed when the girder was lifted helps to confirm one of the key assumptions in developing the model. The boundary conditions for the anchorage zone design model represent the condition when the girder is lifted. With these boundary conditions, the girder is very vulnerable to crack development. The increase in strain when the girder was lifted supports this assumption.

The readings from the strain gages were translated into a stress by calculating the product of the strain and an assumed modulus of elasticity for the stirrups of 29,000 ksi. For this analysis, individual strain readings taken during a ten minute period were averaged. These readings were taken immediately after the girder was lifted. This average strain was then converted to a stress. Figure 4-16 shows the distribution of the

stress in the stirrups over the length of the anchorage zone. The maximum stirrup stress in the anchorage zone ranged from 13.8 ksi to 0.68 ksi. The stress values calculated from the measured strains were almost all less than the assumed average working stress of 12 ksi used in this design. Only the first stirrup experienced a stress higher than 12 ksi. The low stress values suggest the actual total bursting force in the anchorage zone is less than the bursting force predicted with the design model.

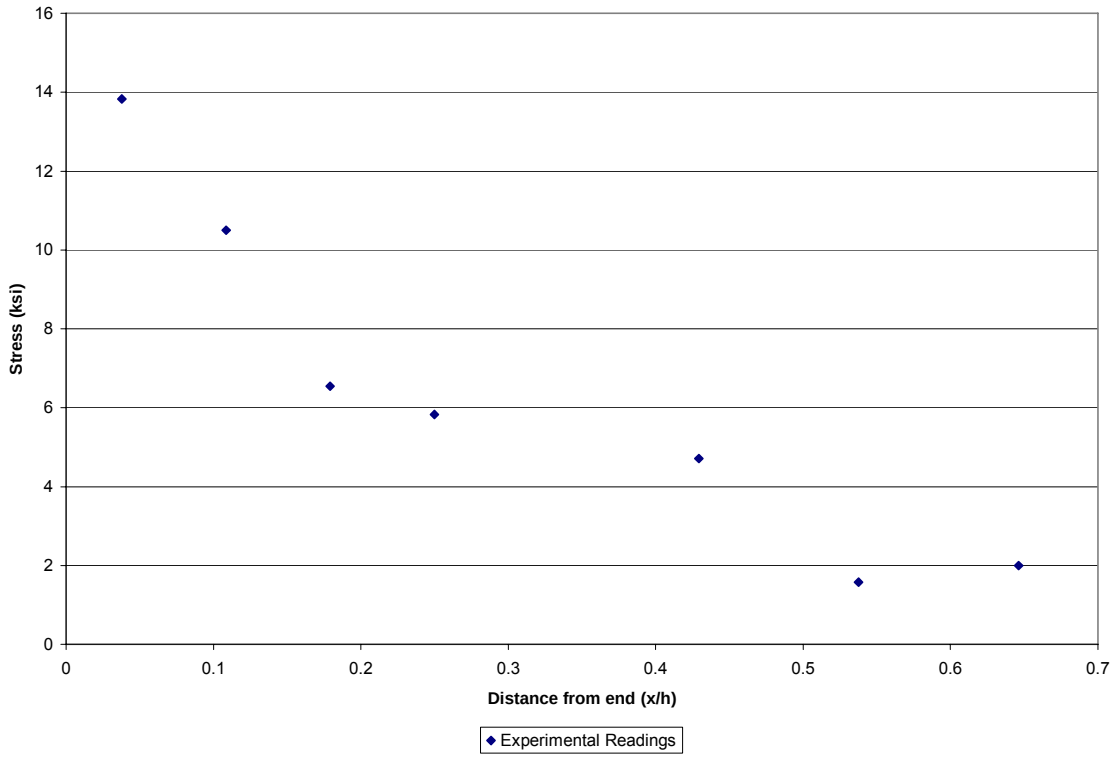

Figure 4-16. Distribution of tensile stress over the anchorage zone after lifting – 12 ksi end

4.4.3.2 18 ksi Anchorage Zone

The strains measured in the stirrups in the 18 ksi anchorage zone displayed a different trend. Figure 4-14 and Figure 4-15 show that the strain was very small and changed very little while the strands were cut. There was a very large and sudden increase in the strain in the stirrups when the girder was lifted. After the girder was placed back on the casting bed, the strain decreased slightly and then remained constant. The strain that remained after the girder was lifted was relatively high. The strain in the gages located in the lower portion of the web ranged from 150 to 400 microstrain, with the gage located closest to the end experiencing the highest strain. The gages located in

the upper portion of the web measured strains which varied from 0 to 300 microstrain. The gage located farthest from the end recorded the lowest strain reading. The cracks in this anchorage zone all developed at the time the girder was lifted. This sudden increase in the strain when the girder was lifted serves to confirm the assumption for the design model discussed previously.

The large strains measured by the gages in the upper portion of the web in the 18 ksi anchorage zone show that large tensile forces can exist in this region. The gages in this area of the anchorage zone were located between $h/4$ and $3h/4$. The three gages which measured the highest strains in this group were S18-9, S18-11, and S18-13, which were located at $0.25h$, $0.35h$, and $0.48h$ respectively. These readings support the field observations which demonstrated that the region between $h/4$ and $3h/4$ was highly affected by the diffusion of the prestress force into the girder. These readings also support including this region of the girder as part of the anchorage zone design.

The strain readings from the gages in this anchorage zone were also translated into stresses. The distribution of the stresses in the anchorage zone is shown in Figure 4-17. The stresses in these stirrups ranged from 11.8 ksi to 0.38 ksi. The stress values did not decrease smoothly as the distance from the end increased as illustrated in Figure 4-16. In this anchorage zone, the stresses decreased within $h/4$ but then increased at the distance where the diagonal cracks developed. The stresses in this anchorage zone were all below the average working stress assumed in the design phase, which indicates the actual bursting force was lower than that predicted by the design model. This is expected, since strut-and-tie models tend to produce conservative results.

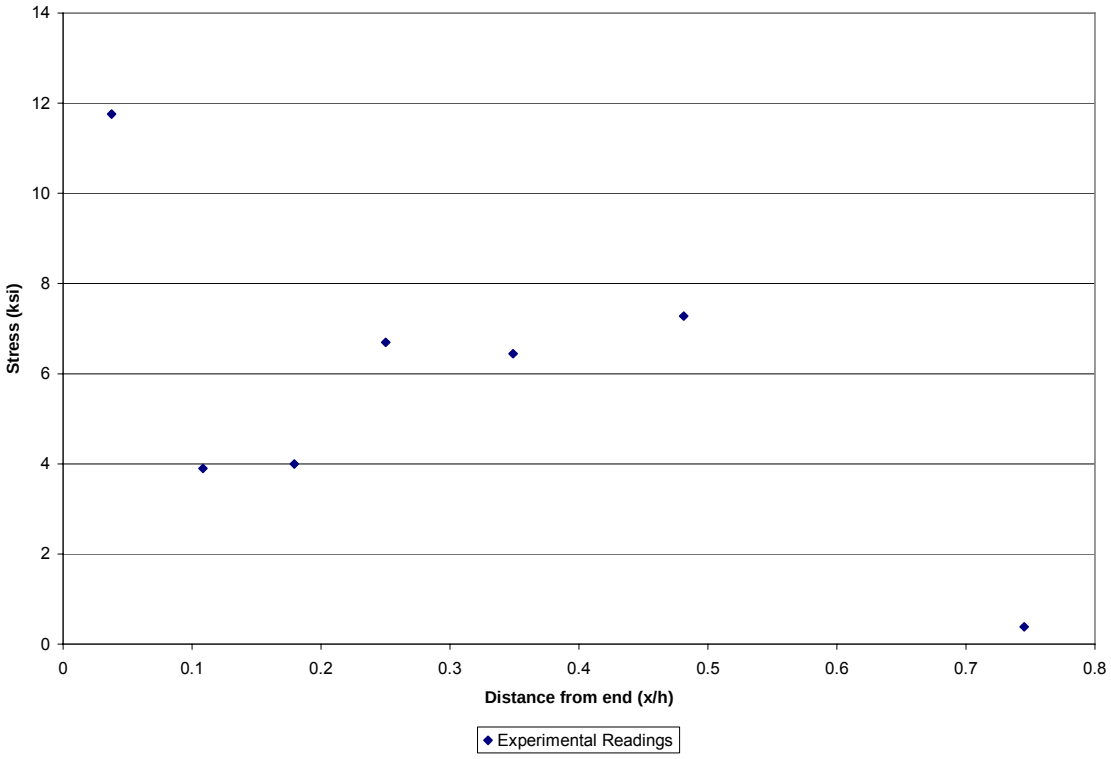

Figure 4-17. Distribution of tensile stress over the anchorage zone after lifting – 18 ksi end

4.4.4 Crack Condition when Placed on Supports

The girder arrived at the Virginia Tech Structures Laboratory on December 13, 2006. It was 50 days old when it arrived. The girder was placed on supports so a composite lightweight concrete deck could be added. The cracks were surveyed after the girder was moved to its final position to determine if any of the anchorage zone cracks had healed after the initial lift from the casting bed. During this visual inspection it was observed that the crack lengths and crack widths had not changed since the initial inspection after transfer on October 25, 2006.

4.4.5 Crack Condition after Deck Placement

A 7 ft wide, 9 in. deep composite deck was added to the girder on day 77. After the deck was moist cured for 7 days the formwork was removed. At this point, a third visual inspection was made of the crack lengths and crack widths. During this inspection the crack lengths and crack widths did not change significantly. Several researchers have

suggested the addition of self weight from the deck will close the cracks in the anchorage zone, but this did not occur in this case.

4.5 Conclusions from Experimental Test

The goal of this test was to verify the design model for use in the VDOT PCBT girders. The girder was instrumented in order to confirm some of the assumptions and calibrations for the proposed anchorage zone model. Based on the visual comparison of the two anchorage zones and the data recorded by the embedded strain gages, the new anchorage zone design approach was successful.

The working stress recommendations outlined in section 3.3.2 provide flexibility to customize the anchorage zone design based on material properties of the concrete and environmental conditions. In this test, one anchorage zone was designed with a 12 ksi working stress which matched the recommended working stress for lightweight concrete members. This anchorage zone had an acceptable level of cracking. The other anchorage zone used an 18 ksi working stress and the stirrup detail at this end exceeded the minimum anchorage zone reinforcement required by AASHTO LRFD. The cracking at this end of the girder, however, was not within the acceptable limits for this model.

The data recorded by the strain gages confirmed several assumptions of the design model. First, the region affected by the diffusion of the prestress force extends beyond $h/4$, which is the length that has traditionally been considered in the anchorage zone design for pretensioned members. These results showed that a significant tension force was present between $h/4$ and $3h/4$ in the 18 ksi anchorage zone. The strain gage data also confirmed the assumption to neglect the reaction and self weight in the strut-and-tie models. The act of lifting the girder shortly after transfer increased the strain in the stirrups. This strain increase was very sudden and large in the 18 ksi anchorage zone and this end of the girder experienced a large level of cracking. The increase in strain the 12 ksi anchorage zone was present but was less dramatic.

Chapter 5. Conclusions and Recommendations

5.1 Summary

Field observations of PCBT girders have shown that many of the girders used in Virginia develop cracks in the anchorage zone. The lengths and widths of the anchorage zone cracks vary from acceptable to poor and in need of repair. The field surveys have shown that the current AASHTO LRFD minimum anchorage zone reinforcement requirement is usually adequate for shallow girders. Deep girders, heavily prestressed girders, and girders cast with lightweight concrete, however, typically develop numerous cracks in the anchorage zone when designed to meet AASHTO LRFD minimum standards. The cracks in the anchorage zone are primarily a serviceability concern, although in a few cases these cracks may also be a structural concern. The cracks in the anchorage zone are also a concern from an ownership and inspection standpoint. Heavily cracked anchorage zones will need to be monitored closely over the service life of the structure and can be a burden for the owner.

Several experimental and analytical studies have been conducted to determine a design approach for anchorage zones in pretensioned girders. Davis, et al. (2005) proposed a new procedure which was based on two strut-and-tie models of the anchorage zone. The geometries of the strut-and-tie models were calibrated based on field observations of numerous PCBT girders. The proposed design approach also allowed for customization of the anchorage zone design based on environmental conditions and material considerations. The goal of this model was to reliably produce anchorage zones with a minimal level of cracking. This new anchorage zone design model served as the basis for this thesis.

This research had three objectives. The first objective was to develop design aids for the anchorage zones of the VDOT PCBT girders. To achieve this objective a parametric study was conducted using the anchorage zone design model proposed by Davis, et al. The results of this parametric study were consolidated into anchorage zone design tables which cover all nine PCBT cross sections used by VDOT. Design tables were created for girders with lightweight and normal weight concrete. The second

objective was to conduct a full scale experimental test of the proposed anchorage zone design model. This test was used to verify this design approach for application by VDOT. A 65 ft long PCBT-53 girder with experimental anchorage zone reinforcement details was constructed from lightweight SCC to support this test. The final objective was to develop new anchorage zone standard details for VDOT which incorporate the elements of this design model and are compatible with the anchorage zone design aids.

5.2 Conclusions

The following conclusions are made based on the analytical and experimental portions of this research.

- For typical PCBT girders 61 in. or less in height, stressed with ½ in. strand, and cast with normal weight concrete, the area of reinforcement required within $h/4$ will slightly increase from current practice in Virginia. In many cases the slight increase in the required reinforcement area will not result in the addition of more stirrups.
- For typical PCBT girders taller than 61 in., stressed with ½ in. strand, and cast with normal weight concrete, the area of reinforcement required within $h/4$ will increase from current practice by one to three stirrups depending on the size of the stirrups selected for the anchorage zone reinforcement.
- All PCBT girders cast with lightweight concrete, girders subjected to harsh environmental conditions, or girders stressed with 0.6 in. strand will require significantly more stirrups within $h/4$ compared to current practice in Virginia. To ensure good consolidation of the concrete and to reduce anchorage zone congestion, bundled stirrups will typically be needed in the anchorage zone for girders in these categories.
- For all girders, the area of reinforcement required between $h/4$ and $3h/4$ is always slightly less than that required within $h/4$. As a general rule, the same number of stirrups placed within $h/4$ should be placed between $h/4$ and $3h/4$ to properly control the development of diagonal cracks in the upper portion of the web.

- The anchorage zone details developed with these design aids are very similar to the standard details for similar sized girders used by the North Carolina, Florida, and Washington Departments of Transportation.
- The full-size, experimental lightweight PCBT-53 girder showed the anchorage zone detail designed in accordance with the recommendations of the proposed model had a very small amount of cracking. The anchorage zone detail designed with a working stress of 18 ksi had a large amount of cracking which would not be considered acceptable by the standards of this model.
- Readings from the instrumentation during the full scale test served to verify several of the assumptions used in creating the model.
- There was a significant tensile force between $h/4$ and $3h/4$ which suggested the region affected by the diffusion of the prestress force is longer than $h/4$ This region located beyond $h/4$ should be considered in the design of the anchorage zone reinforcement.
- Lifting the girder places the self weight dead load on the lifting provision. Removing this reaction from the anchorage zone causes an increase in the tension in the stirrups and can lead to crack development or crack propagation.

5.3 Recommendations

Based upon the extent of cracking observed in the girders of many anchorage zones manufactured for VDOT, the anchorage zone design tables and new standard details should be implemented as soon as possible. Several bridge projects in Virginia which have been initiated since this research began have already included anchorage zones details redesigned with this approach. The overall cost of several additional stirrups at each end of the beam is minimal, and this design procedure can has proven effective at reducing anchorage zone cracking.

Further research should focus on developing evaluation criteria for the acceptance, repair, or rejection of girders with anchorage zone cracking. While this design method will reduce cracking, it is not likely to completely eliminate anchorage zone cracking. Therefore, guidelines should be established to describe which anchorage

zone cracks should be accepted and which should be repaired or rejected. Some simple guidelines were developed and used for this research; however, a more comprehensive manual is needed to outline acceptable cracks based on final boundary conditions of the in-place girder and environmental conditions. For cracks that do develop, guidelines are needed to describe the appropriate type of repair, if necessary. Finally, clear rejection criteria should also be developed so that owners and fabricators can recognize problems immediately and take action before future beams are cast for a project.

Future research must also focus on quality control issues in precast facilities throughout the nation. Many of the girders used for projects in Virginia are cast at two or three different precast yards. Variability in the manufacturing procedures can be a factor which exacerbates anchorage zone cracking. For example, girders located at the end of a casting line could have wind blowing directly on one anchorage zone which may hinder the curing process. Also, different manufacturers use different release techniques. The girders observed in these field surveys were all flame cut with an acetylene torch. Other states, such as Nebraska, use a gradual release. Research is needed to relate the release method to the magnitude of cracking. Finally, an investigation into the tensile strength of concrete at release is needed. The precast yards observed in this research conduct compression tests on concrete cylinders before transfer, but do not conduct split cylinder tensile tests. The development of tensile strength in early age concrete will have a large impact on anchorage zone cracking.

Changes to the AASHTO LRFD provisions for anchorage zone reinforcement are needed. The changes should include stress limit recommendations based on the materials used and the environmental conditions. Changes to the code should also address large, heavily prestressed girders which are becoming more common in today's bridge construction industry. As rejection criteria are established for crack development, code changes are absolutely necessary since many of the girders observed in this research which developed cracks did meet current code standards. This can put precasters in very difficult and confusing situations.

A final aspect of future research should focus on long-term monitoring of the performance and durability of bridges containing girders with anchorage zone cracks. Structures that contain girders that have been repaired should also be studied to determine

the long-term performance and durability of the repair method. This future research should focus on monitoring changes to cracks once the structure is completed and subjected to live loads. These findings will be helpful to the development of the evaluation, repair, and rejection criteria.

References

AASHTO (1998). *AASHTO LRFD Bridge Design Specifications*, *Second Edition with 2001 Interims*, American Association of State Highway and Transportation Officials, Washington, DC.

AASHTO (2004). *AASHTO LRFD Bridge Design Specifications*, *Third Edition with 2006 Interims*, American Association of State Highway and Transportation Officials, Washington, DC.

AASHTO (2003). *Standard Specifications for Highway Bridges*, *17th Edition*, American Association of State Highway and Transportation Officials, Washington, DC.

ACI (2005). *Building Code Requirements for Structural Concrete, ACI 318-05,* American Concrete Institute, Farmington Hills, Michigan.

Australian Standard (2005). Australian *Bridge Design Code, Section 5: Concrete*. AS5100.5-2004. Sydney, Austrailia.

Canadian Standard Association (CSA). 2000. *Canadian Highway Bridge Design Code*: *A National Standard of Canada*. CAN/CSA-S6-00. Toronto, ON, Canada: CSA.

Castrodale, R. W., Lui, A., and White, C. D., (2002). "Simplified Analysis of Web Splitting in Pretensioned Concrete Girders." *Proceedings, PCI/FHWA/NCBC Concrete Bridge Conference*, Nashville, TN, October 6-9.

Davis, R. T., Buckner, D. C., and Ozyildirim, C., (2005). "Serviceability-Based Design Method for Vertical Beam End Reinforcement." *Proceedings, PCI National Bridge Conference*, Palm Springs, CA, October 16-19.

Foster, S. J., and Rogowsky, D. M. (1997). "Bursting Forces in Concrete Panels Resulting from In-plane Concentrated Loads," *Magazine of Concrete Research*, Vol. 49, No. 180, pp. 231-180.

Gergely, P. and Sozen, M. A. (1967). "Design of Anchorage Zone Reinforcement in Prestressed Concrete Beams," *PCI Journal*, Vol. 12, No. 2, pp. 63-75.

Hengprathanee, S. (2004). "Linear and Nonlinear Finite Element Analyses of Anchorage Zones in Post-Tensioned Concrete Structures," *Doctor of Philosophy Dissertation*, Virginia Polytechnic and State University, Blacksburg, Virginia.

Kannel, J., French, C., and Stolarski, H. (1997). "Release Methodology of Strands to Reduce End Cracking in Pretensioned Concrete Girders," *PCI Journal*, Vol. 42, No. 1, pp. 42-54.

Manual for the Evaluation and Repair of Precast, Prestressed Concrete Bridge Products, Precast/Prestressed Concrete Institute, Chicago, Illinois, 2006.

Marshall, W. T., and Mattock, A. H. (1962). "Control of Horizontal Cracking in the Ends of Pretensioned Prestressed Concrete Girders," *PCI Journal*, Vol. 7, No. 5, pp. 56-74.

Naito, C. J., Parent, G., and Brunn, G. (2006). "Performance of Bulb-Tee Girders Made with Self-Consolidating Concrete," *PCI Journal*, Vol. 51, No. 6, pp. 72-85.

Nilson, A. H. (1987). Design of Prestressed Concrete. John Wiley and Sons, New York.

"North Carolina Department of Transportation Structure Design Unit." <http://www.ncdot.org/doh/preconstruct/highway/structur/strstandards/pdf/> (January 12, 2007).

O'Hagan, D. "Structures Design Office – 2005.2 English Standard Drawings 3/17/05." <http://www.dot.state.fl.us/structures/CADD/standards/2005.2Standards/standards.htm> (January 12, 2007).

Oklahoma Department of Transportation. "Bridge Design Standards Drawings – State Bridges." <http://www.okladot.state.ok.us/bridge/bridge99/sbindex.htm> (January 12, 2007).

Plesha, J. (2002). "Washington State Department of Transportation Bridge Standard Drawings." <http://www.wsdot.wa.gov/eesc/bridge/drawings/> (January 12, 2007).

Schlaich, J., Schafer, K., and Jennewein M., (1987). "Toward a Consistent Design of Structural Concrete," *PCI Journal*, Vol. 32, No. 3, pp. 74-150.

Tuan, C. Y., Yehia, S. A., Jongpitaksseel, N., and Tadros, M., K. (2004). "End Zone Reinforcement for Pretensioned Concrete Girders," *PCI Journal*, Vol. 49, No. 3, pp. 68-82.

Virginia Department of Transportation. (2006). "Volume V – Part 4: Prestressed Concrete Beam Standards." <http://www.vdot.virginia.gov/business/bridge-v5p4.asp> (January 12, 2007).

Wollmann, G. P. and Roberts-Wollmann, C. L. (2000). *Anchorage Zone Design, Reprint of Chapter VIII, Post-Tensioning Manual*, 6th Ed., Post-Tensioning Institute.

Appendix A. Calculations for PCBT-77 Case Study Girder

Virginia PCBT-77 Bridge Girder Data

Depth of girder	h = 77 in.
Area of girder	A_c = 970.7 in^2
Height of centroid	y_b = 37.67 in.
Moment of inertia	I = 788700 in^4
Girder self weight	w_o = 1011 lb/ft
Girder Length	L = 143 ft

Girder Dimensions

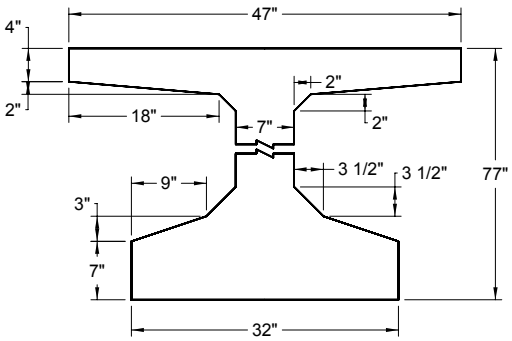

Girder cross section at end

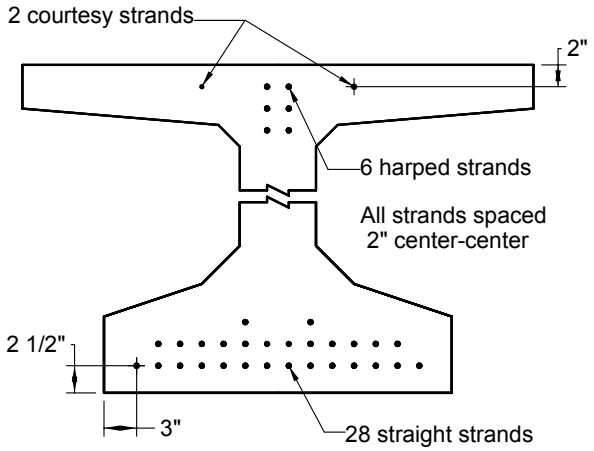

Girder cross section at midspan

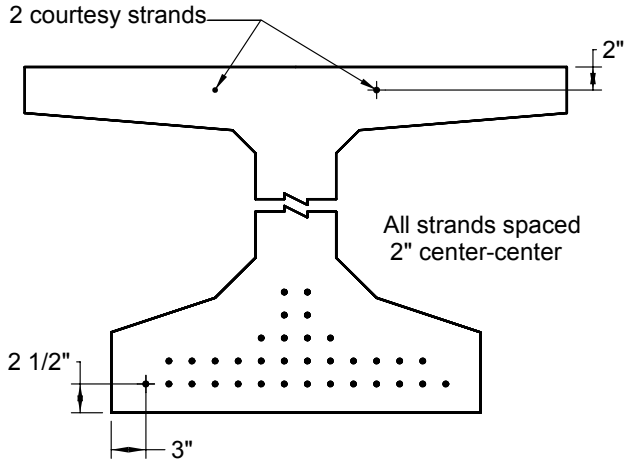

Concrete Material Properties

ω = 150 lb/ft^3
f'_{ci} = 5800 psi
E_{ci} = 4620 ksi

28 Straight and 6 Harped Strand Properties

A_{strand} = 0.217 in^2
f_{pu} = 270 ksi
f_{jack} = 0.75 f_{pu}
E_{ps} = 28500 ksi

2 Courtesy Strand Properties

A_{strand} = 0.217 in^2
f_{pu} = 270 ksi
f_{jack} = 4.61 ksi

Strand location 77 in. from end of beam

Height of centroid of draped strands at beam end = 73 in.
Height of centroid of draped strands at harping point = 8.25 in.
Distance from end to harping point = 0.4L = 0.4(143) = 57.2 ft
Angle of draped strands, θ

$$\theta = a\tan\left(\frac{73-8.25}{12(57.2)}\right) = 5.39°$$

Height of centroid of harped strands 77 in. from end of beam

$$y_{cgs\_draped} = 73 - 77\sin(5.39) = 65.8 \text{ in.}$$

Height of centroid of straight strands 77 in. from end of beam

$$y_{cgs\_harped} = \frac{14(2.25) + 12(4.25) + 2(6.25)}{28} = 3.39 \text{ in.}$$

Height of centroid of courtesy strands 77 in. from end of beam

$y_{cgs\_courtesy} = 73 \text{ in.}$

Properties of all prestressing steel 77 in. from end of beam

	Area (in²)	*y_b (in)*	*I_o (in⁴)*	*P_{jack} (k)*
2 courtesy strands	0.434	75	0	2
6 harped strands	1.30	65.8	3.47	264
28 straight strands	6.08	3.39	9.42	1230
			Total =	1496 kip

Transformed section properties for section 77 in. from end of beam

Section modulus at transfer, n_i

$$n_i = \frac{E_{ps}}{E_{ci}} = \frac{28500}{4620} = 6.17$$

	A_t (in²)	y_b (in)	$A_t y_b$ (in²)	$A_t(y_b-y_t)^2$ (in⁴)	I_{ot} (in⁴)	I_t (in⁴)
Concrete	970.7	37.67	36,570	621	788,700	789,321
Courtesy Strands	2.24	75	168	3,257	0	3,257
Harped Strands	6.72	65.8	443	5,633	17.94	5,651
Straight Strands	31.41	3.39	106.5	35,208	48.7	35,257
Total =	1,011	Total =	37,280		Total =	833,486

$$y_t = \frac{37{,}280}{1{,}011} = 36.87 \text{ in. from bottom of beam}$$

Sample calculations for highlighted values

$$A_t = (n_i - 1)A_{ps\_harped} = (6.17 - 1)(1.30) = 6.72 \text{ in}^2$$

$$I_{ot} = (n_i - 1)I_{o\_harped} = (6.17 - 1)(3.47) = 17.94 \text{ in}^4$$

Stresses from prestress force for section 77 in. from end of beam

$$f_{bot} = \frac{P_{jack\_TOT}}{A_t} + \frac{[P_{courtesy}(y_t - y_{b\_courtesy}) + P_{harped}(y_t - y_{b\_harped}) + P_{straight}(y_t - y_{b\_straight})]y_t}{I_t}$$

$$f_{bot} = \frac{-1{,}496}{1{,}011} + \frac{[-2(36.87 - 75) - 264(36.87 - 65.8) - 1230(36.87 - 3.39)]36.87}{833{,}486}$$

$$f_{bot} = -2.96 \text{ ksi}$$

$$f_{top} = \frac{P_{jack\_TOT}}{A_t} + \frac{[P_{courtesy}(y_t - y_{b\_courtesy}) + P_{harped}(y_t - y_{b\_harped}) + P_{straight}(y_t - y_{b\_straight})](y_t - h)}{I_t}$$

$$f_{top} = \frac{-1{,}496}{1{,}011} + \frac{[-2(36.87 - 75) - 264(36.87 - 65.8) - 1230(36.87 - 3.39)](36.87 - 77)}{833{,}486}$$

$$f_{top} = 0.132 \text{ ksi}$$

Force in the strand groups after transfer

$$f_{cg\_straight} = 0.75 f_{pu} + n_i[f_{bot} + \frac{y_{b\_straight}}{h}(f_{top} - f_{bot})]$$

$$f_{cg\_straight} = 0.75(270) + 6.17[-2.96 + \frac{3.39}{77}(0.132 + 2.96)] = 185.1\,\text{ksi}$$

$$P_{straight} = 185.1(28)(0.217) = 1124\,\text{kip}$$

$$f_{cg\_harped} = 0.75 f_{pu} + n_i[f_{bot} + \frac{y_{b\_harped}}{h}(f_{top} - f_{bot})]$$

$$f_{cg\_harped} = 0.75(270) + 6.17[-2.96 + \frac{65.8}{77}(0.132 + 2.96)] = 200.5\,\text{ksi}$$

$$P_{harped} = 200.5(6)(0.217) = 261.1\,\text{kip}$$

$$f_{cg\_courtesy} = f_{jack} + n_i[f_{bot} + \frac{y_{b\_courtesy}}{h}(f_{top} - f_{bot})]$$

$$f_{cg\_courtesy} = 4.61 + 6.17[-2.96 + \frac{75}{77}(0.132 + 2.96)] = 4.93\,\text{ksi}$$

$$P_{courtesy} = 4.93(2)(0.217) = 2.14\,\text{kip}$$

Integrate stress over concrete area from bottom of girder up until resultant force in concrete equals the applied force in the straight strand group (1124 kip)

Height (in)	*Width (in)*	*Stress (ksi)*	*Force (kip)*	*y_b (in)*	*y_b · Force (in-kip)*	*Σ Force (kip)*
0	32	-2.96	0	0	0	0
7	32	-2.68	-632	3.44	-2,175	-632
10	14	-2.56	-180.8	8.49	-1,535	-812.8
13.5	7	-2.42	-91.5	11.7	-1,071	-904.3
28.3	7	-1.82	-220	20.6	-4,532	-1,124
				Σ =	-9,311	

Sample calculations for highlighted values

$$Force = \frac{(32 + 32)}{2}\frac{(-2.96 - 2.68)}{2}(7 - 0) = -632\,\text{kip}$$

$$y_b = \frac{(7-0)[2(2.68)+2.96]}{3(2.68+2.96)} = 3.44 \text{ in.}$$

Find location of the resultant force in the concrete

$$y_{b\_resul\tan t} = \frac{-9{,}311}{-1{,}124} = 8.28 \text{ in.}$$

Unbalanced internal moment

$$M = (y_{b\_resul\tan t} - y_{b\_straight})P_{straight}$$

$$M = (8.28 - 3.39)(1124) = 5496 \text{ in-k}$$

Note: Integrating the stress over concrete area from top of girder down, will produce the same unbalanced moment within the section

Solve the strut and tie models

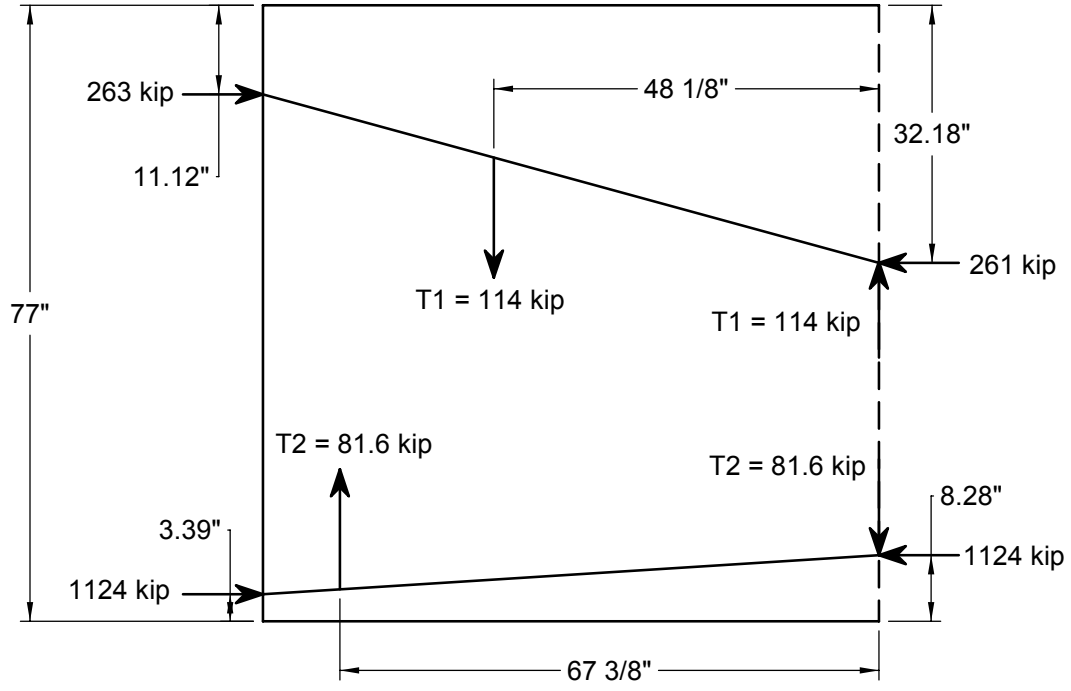

$$T_1 = \frac{5496}{48.125} = 114 \text{ kip} \qquad T_2 = \frac{5496}{67.375} = 81.6 \text{ kip}$$

Design the reinforcement

Select an average operating stress for stirrups based on concrete type and environment

f_s = 18 ksi

Area of steel required for lower strut and tie model

$$A_s = \frac{T_2}{f_s} = \frac{81.6}{18} = 4.53 \text{ in}^2$$

Select 7 No. 5 bars uniformly distributed over $h/4$

Area of steel required for upper strut and tie model

$$A_s = \frac{T_1}{f_s} = \frac{114}{18} = 6.33 \text{ in}^2$$

Note: The model assumes this area of steel is uniformly distributed from the end of the girder to $3h/4$ even though the area of stirrup reinforcement within h/4 will be more densely spaced.

Area of steel required from $h/4$ to $3h/4$

$$A_s = \frac{6.33}{0.75h}(0.5h) = \frac{6.33(0.5)}{0.75} = 4.22 \text{ in}^2$$

Select 7 No. 5 bars uniformly distributed from $h/4$ to $3h/4$

Note: The area of steel required from $h/4$ to $3h/4$ shall be compared to the area of steel required in this region for horizontal shear transfer and the larger requirement will control.

Beam end detailing

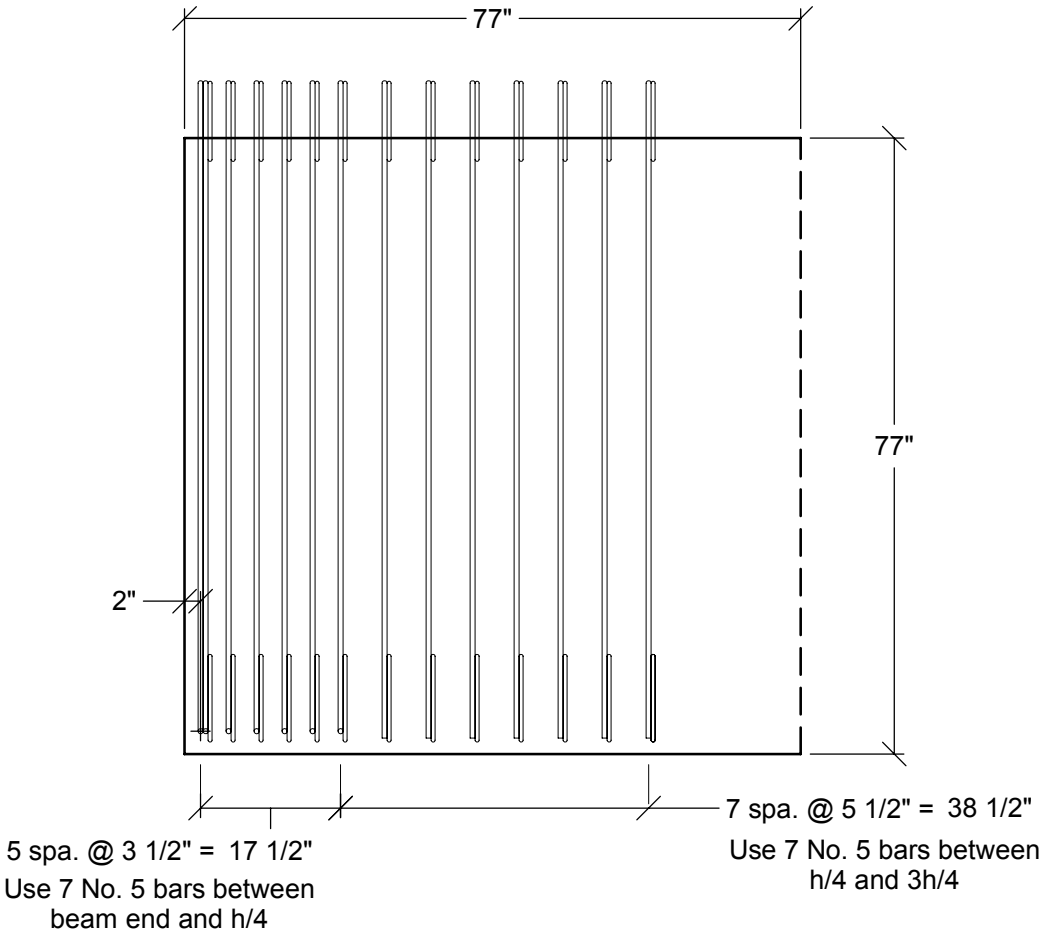

Note: Flanges of beam have been removed for clarity.

Appendix B. Parametric Study Sample Girders and Results

Table B-1. Sample girders - PCBT-29, NWC, ½ in. strand

# of Strands	# Straight	# Draped	P_{jack} (k)	Length (ft)	T_1 (k)	% of P_{jack}	Stirrup area h/4-3h/4 (in^2)	T_2 (k)	% of P_{jack}	Stirrup area End-h/4 (in^2)
14	12	2	438	45	38.6	5.87%	1.43	27.6	6.29%	1.53
16	12	4	500	45	37.2	4.96%	1.38	26.6	5.31%	1.47
18	14	4	562	50	39.0	4.63%	1.44	27.8	4.96%	1.55
20	16	4	624	50	40.3	4.31%	1.49	28.8	4.62%	1.60
22	18	4	686	50	41.7	4.05%	1.54	29.8	4.34%	1.65
24	20	4	748	50	42.9	3.82%	1.59	30.6	4.09%	1.70
26	22	4	810	55	44.5	3.67%	1.65	31.8	3.93%	1.77
28	24	4	872	55	45.7	3.49%	1.69	32.6	3.74%	1.81
30	24	6	933	55	43.1	3.08%	1.60	30.8	3.29%	1.71

Table B-2. Sample girders - PCBT-37, NWC, ½ in. strand

# of Strands	# Straight	# Draped	P_{jack} (k)	Length (ft)	T_1 (k)	% of P_{jack}	Stirrup area h/4-3h/4 (in^2)	T_2 (k)	% of P_{jack}	Stirrup area End-h/4 (in^2)
14	12	2	438	55	37.8	5.76%	1.40	27.0	6.17%	1.50
16	12	4	500	55	36.8	4.91%	1.36	26.3	5.26%	1.46
18	14	4	562	55	38.8	4.60%	1.44	27.7	4.93%	1.54
20	16	4	624	55	40.8	4.36%	1.51	29.1	4.67%	1.62
22	18	4	686	60	42.2	4.20%	1.60	30.9	4.50%	1.71
24	20	4	748	60	45.2	4.03%	1.67	32.3	4.32%	1.79
26	22	4	810	60	47.2	3.89%	1.75	33.7	4.16%	1.87
28	24	4	872	60	49.1	3.76%	1.82	35.1	4.02%	1.95
30	24	6	933	65	47.5	3.39%	1.76	33.9	3.63%	1.88
32	26	6	995	65	45.8	3.07%	1.70	32.7	3.29%	1.82

Table B-3. Sample girders - PCBT-45, NWC, ½ in. strand

# of Strands	# Straight	# Draped	P_{jack} (k)	Length (ft)	T_1 (k)	% of P_{jack}	Stirrup area h/4-3h/4 (in^2)	T_2 (k)	% of P_{jack}	Stirrup area End-h/4 (in^2)
18	14	4	562	65	40.1	4.76%	1.49	28.7	5.10%	1.59
20	16	4	624	70	43.4	4.64%	1.61	31.0	4.97%	1.72
22	18	4	686	70	46.2	4.49%	1.71	33.0	4.82%	1.84
24	20	4	748	70	49.0	4.37%	1.81	35.0	4.68%	1.94
26	22	4	810	70	51.8	4.26%	1.92	37.0	4.57%	2.06
28	24	4	872	75	54.9	4.20%	2.03	39.2	4.50%	2.18
30	24	6	933	75	53.1	3.79%	1.97	37.9	4.06%	2.11
32	26	6	995	75	52.8	3.54%	1.96	37.7	3.79%	2.10
34	28	6	1057	75	52.6	3.32%	1.95	37.6	3.55%	2.09
36	30	6	1119	75	51.7	3.08%	1.92	37.0	3.30%	2.05
38	32	6	1181	80	52.8	2.98%	1.96	37.7	3.19%	2.09
40	34	6	1243	80	52.7	2.82%	1.95	37.6	3.03%	2.09

Table B-4. Sample girders – PCBT-45, NWC, 0.6 in. strand

# of Strands	# Straight	# Draped	P_{jack} (k)	Length (ft)	T_1 (k)	% of P_{jack}	Stirrup area h/4-3h/4 (in^2)	T_2 (k)	% of P_{jack}	Stirrup area End-h/4 (in^2)
22	18	4	971	75	63.8	4.38%	2.36	45.6	4.69%	2.53
24	20	4	1059	75	67.3	4.24%	2.49	48.1	4.54%	2.67
26	22	4	1147	75	70.7	4.11%	2.62	50.5	4.41%	2.81
28	24	4	1234	80	74.6	4.03%	2.76	53.3	4.32%	2.96
30	24	6	1322	80	72.3	3.65%	2.68	51.7	3.91%	2.87
32	26	6	1410	80	71.6	3.38%	2.65	51.1	3.62%	2.84

Table B-5. Sample girders – PCBT-53, NWC, ½ in. strand

# of Strands	# Straight	# Draped	P_{jack} (k)	Length (ft)	T_1 (k)	% of P_{jack}	Stirrup area h/4-3h/4 (in^2)	T_2 (k)	% of P_{jack}	Stirrup area End-h/4 (in^2)
24	20	4	748	80	52.7	4.70%	1.95	37.6	5.03%	2.09
26	22	4	810	85	56.0	4.61%	2.07	40.0	4.95%	2.23
28	24	4	872	85	59.3	4.53%	2.19	42.3	4.86%	2.35
30	24	6	933	85	57.7	4.12%	2.14	41.2	4.42%	2.29
32	26	6	995	85	58.5	3.92%	2.17	41.8	4.20%	2.32
34	28	6	1057	90	59.9	3.78%	2.22	42.8	4.05%	2.38
36	30	6	1119	90	60.7	3.62%	2.25	43.4	3.88%	2.41
38	32	6	1181	90	61.5	3.47%	2.28	44.0	3.72%	2.44
40	34	6	1243	90	59.1	3.17%	2.19	42.2	3.40%	2.35
42	34	8	1305	90	59.9	3.06%	2.22	42.8	3.28%	2.38
44	36	8	1367	90	58.3	2.85%	2.16	41.7	3.05%	2.32

Table B-6. Sample girders – PCBT-53, NWC, 0.6 in. strand

# of Strands	# Straight	# Draped	P_{jack} (k)	Length (ft)	T_1 (k)	% of P_{jack}	Stirrup area h/4-3h/4 (in^2)	T_2 (k)	% of P_{jack}	Stirrup area End-h/4 (in^2)
22	18	4	971	85	67.4	4.63%	2.50	48.2	4.96%	2.67
24	20	4	1059	90	72.3	4.55%	2.68	51.6	4.88%	2.87
26	22	4	1147	90	76.5	4.45%	2.83	54.6	4.77%	3.04
28	24	4	1234	90	80.6	4.35%	2.98	57.6	4.66%	3.20
30	24	6	1322	90	78.7	3.97%	2.92	56.2	4.25%	3.12
32	26	6	1410	90	79.4	3.75%	2.94	56.7	4.02%	3.15

Table B-7. Sample girders – PCBT-61, NWC, ½ in. strand

# of Strands	# Straight	# Draped	P_{jack} (k)	Length (ft)	T_1 (k)	% of P_{jack}	Stirrup area h/4-3h/4 (in^2)	T_2 (k)	% of P_{jack}	Stirrup area End-h/4 (in^2)
26	22	4	810	90	59.6	4.91%	2.21	42.6	5.26%	2.37
28	24	4	872	90	63.4	4.85%	2.35	45.3	5.19%	2.51
30	24	6	933	90	62.0	4.43%	2.30	44.3	4.74%	2.46
32	26	6	995	95	64.2	4.30%	2.38	45.9	4.61%	2.55
34	28	6	1057	95	65.9	4.15%	2.44	47.1	4.45%	2.61
36	30	6	1119	95	67.5	4.02%	2.50	48.2	4.31%	2.68
38	32	6	1181	95	69.1	3.90%	2.56	49.3	4.18%	2.74
40	34	6	1243	100	71.2	3.82%	2.64	50.9	4.09%	2.83
42	34	8	1305	100	69.2	3.53%	2.56	49.4	3.79%	2.75
44	36	8	1367	100	68.8	3.35%	2.54	49.1	3.59%	2.73
46	38	8	1429	100	68.4	3.19%	2.53	48.8	3.42%	2.72
48	38	10	1491	100	65.6	2.93%	2.43	46.8	3.14%	2.60

Table B-8. Sample girders – PCBT-61, NWC, 0.6 in. strand

# of Strands	# Straight	# Draped	P_{jack} (k)	Length (ft)	T_1 (k)	% of P_{jack}	Stirrup area h/4-3h/4 (in^2)	T_2 (k)	% of P_{jack}	Stirrup area End-h/4 (in^2)
26	22	4	1146	95	81.6	4.75%	3.03	58.3	5.09%	3.24
28	24	4	1234	100	86.4	4.67%	3.20	61.7	5.00%	3.43
30	24	6	1322	100	85.5	4.31%	3.17	61.1	4.62%	3.39
32	26	6	1410	100	87.3	4.13%	3.24	62.4	4.42%	3.46
34	28	6	1498	100	89.1	3.97%	3.30	63.7	4.25%	3.54
36	30	6	1586	105	91.6	3.85%	3.39	65.4	4.12%	3.63

Table B-9. Sample girders – PCBT-69, NWC, ½ in. strand

# of Strands	# Straight	# Draped	P_{jack} (k)	Length (ft)	T_1 (k)	% of P_{jack}	Stirrup area h/4-3h/4 (in^2)	T_2 (k)	% of P_{jack}	Stirrup area End-h/4 (in^2)
30	24	6	935	105	67.4	4.81%	2.50	48.1	5.15%	2.68
32	26	6	997	105	69.7	4.67%	2.59	49.8	5.00%	2.77
34	28	6	1059	110	72.6	4.58%	2.69	51.9	4.90%	2.88
36	30	6	1121	110	74.9	4.46%	2.78	53.5	4.78%	2.98
38	32	6	1183	110	77.2	4.36%	2.87	55.1	4.67%	3.07
40	34	6	1245	110	79.4	4.26%	2.95	56.7	4.56%	3.15
42	34	8	1307	115	78.5	4.01%	2.91	56.1	4.29%	3.11
44	36	8	1369	115	79.0	3.85%	2.93	56.4	4.12%	3.13
46	38	8	1431	115	79.4	3.71%	2.95	56.7	3.97%	3.16
48	38	10	1493	115	77.2	3.45%	2.86	55.2	3.70%	3.07

Table B-10. Sample girders – PCBT-69, NWC, 0.6 in. strand

# of Strands	# Straight	# Draped	P_{jack} (k)	Length (ft)	T_1 (k)	% of P_{jack}	Stirrup area h/4-3h/4 (in^2)	T_2 (k)	% of P_{jack}	Stirrup area End-h/4 (in^2)
28	24	4	1236	115	93.9	5.06%	3.48	65.1	5.43%	3.73
30	24	6	1324	115	92.9	4.68%	3.44	66.4	5.02%	3.69
32	26	6	1412	115	95.7	4.53%	3.55	69.4	4.85%	3.80
34	28	6	1500	115	98.5	4.38%	3.65	70.4	4.70%	3.92
36	30	6	1588	115	101	4.25%	3.75	72.3	4.56%	4.02
38	32	6	1676	115	104	4.14%	3.85	74.3	4.43%	4.12

Table B-11. Sample girders – PCBT-77, NWC, ½ in. strand

# of Strands	# Straight	# Draped	P_{jack} (k)	Length (ft)	T_1 (k)	% of P_{jack}	Stirrup area h/4-3h/4 (in^2)	T_2 (k)	% of P_{jack}	Stirrup area End-h/4 (in^2)
38	32	6	1181	115	83.9	4.73%	3.10	59.9	5.07%	3.33
40	34	6	1243	120	87.3	4.68%	3.23	62.3	5.01%	3.46
42	36	8	1305	120	86.0	4.39%	3.18	61.5	4.71%	3.41
44	38	8	1367	120	87.3	4.26%	3.24	62.4	4.56%	3.46
46	38	8	1429	120	88.5	4.13%	3.28	63.2	4.42%	3.51
48	38	10	1491	120	86.7	3.87%	3.21	61.9	4.15%	3.44

Table B-12. Sample girders – PCBT-77, NWC, 0.6 in. strand

# of Strands	# Straight	# Draped	P_{jack} (k)	Length (ft)	T_1 (k)	% of P_{jack}	Stirrup area h/4-3h/4 (in^2)	T_2 (k)	% of P_{jack}	Stirrup area End-h/4 (in^2)
28	24	4	1234	125	100	5.41%	3.71	71.5	5.80%	3.97
30	24	6	1322	125	100	5.03%	3.70	71.2	5.38%	3.96
32	26	6	1410	125	103	4.89%	3.83	73.9	5.24%	4.10
34	28	6	1498	125	107	4.77%	3.97	76.5	5.11%	4.25
36	30	6	1586	130	111	4.68%	4.12	79.5	5.01%	4.42
38	32	6	1674	130	115	4.57%	4.25	82.0	4.90%	4.55
40	32	6	1762	130	118	4.47%	4.37	84.4	4.79%	4.69
42	34	8	1849	130	117	4.21%	4.33	83.5	4.51%	4.64

Table B-13. Sample girders – PCBT-85, NWC, ½ in. strand

# of Strands	# Straight	# Draped	P_{jack} (k)	Length (ft)	T_1 (k)	% of P_{jack}	Stirrup area h/4-3h/4 (in^2)	T_2 (k)	% of P_{jack}	Stirrup area End-h/4 (in^2)
34	28	6	1057	120	82.6	5.21%	3.06	59.0	5.58%	3.28
36	30	6	1119	120	86.0	5.12%	3.18	61.4	5.49%	3.41
38	32	6	1181	120	89.4	5.04%	3.31	63.8	5.40%	3.54
40	34	6	1243	120	92.7	4.97%	3.43	66.2	5.32%	3.67
42	34	8	1305	130	92.9	4.74%	3.44	66.3	5.08%	3.68
44	36	8	1367	130	94.8	4.62%	3.51	67.7	4.95%	3.76
46	38	8	1429	130	96.6	4.51%	3.58	69.0	4.83%	3.83
48	38	10	1491	130	95.1	4.25%	3.52	68.0	4.56%	3.78

Table B-14. Sample girders – PCBT-85, NWC, 0.6 in. strand

# of Strands	# Straight	# Draped	P_{jack} (k)	Length (ft)	T_1 (k)	% of P_{jack}	Stirrup area h/4-3h/4 (in^2)	T_2 (k)	% of P_{jack}	Stirrup area End-h/4 (in^2)
28	24	4	1234	120	104	5.62%	3.85	74.4	6.03%	4.14
30	24	6	1322	120	103	5.20%	3.82	73.7	5.57%	4.09
32	26	6	1410	120	108	5.09%	3.99	76.9	5.45%	4.27
34	28	6	1498	130	113	5.05%	4.20	81.0	5.41%	4.50
36	30	6	1586	130	118	4.95%	4.36	84.1	5.30%	4.67
38	32	6	1674	130	122	4.85%	4.51	87.0	5.20%	4.84
40	34	6	1762	140	127	4.81%	4.71	90.8	5.15%	5.04
42	34	8	1850	140	126	4.55%	4.68	90.2	4.88%	5.01
44	36	8	1937	140	128	4.42%	4.76	91.7	4.73%	5.09

Table B-15. Sample girders – PCBT-93, NWC, ½ in. strand

# of Strands	# Straight	# Draped	P_{jack} (k)	Length (ft)	T_1 (k)	% of P_{jack}	Stirrup area h/4-3h/4 (in^2)	T_2 (k)	% of P_{jack}	Stirrup area End-h/4 (in^2)
38	32	6	1181	125	95.0	5.36%	3.52	67.8	5.74%	3.77
40	34	6	1243	125	98.7	5.29%	3.65	70.5	5.67%	3.92
42	34	8	1305	125	97.7	4.99%	3.62	69.8	5.35%	3.88
44	36	8	1367	125	100	4.88%	3.71	71.6	5.23%	3.97
46	38	8	1429	135	104	4.85%	3.85	74.3	5.20%	4.13
48	38	10	1491	135	103	4.59%	3.80	73.4	4.92%	4.08

Table B-16. Sample girders – PCBT-93, NWC, 0.6 in. strand

# of Strands	# Straight	# Draped	P_{jack} (k)	Length (ft)	T_1 (k)	% of P_{jack}	Stirrup area h/4-3h/4 (in^2)	T_2 (k)	% of P_{jack}	Stirrup area End-h/4 (in^2)
32	26	6	1410	135	115	5.44%	4.26	82.2	5.83%	4.57
34	28	6	1498	135	120	5.35%	4.45	85.8	5.73%	4.77
36	30	6	1586	145	126	5.31%	4.68	90.3	5.69%	5.02
38	32	6	1674	145	131	5.23%	4.86	93.7	5.60%	5.21
40	34	6	1762	145	136	5.14%	5.03	97.1	5.51%	5.40
42	34	8	1850	155	137	4.94%	5.08	97.9	5.29%	5.44
44	36	8	1937	155	140	4.82%	5.19	100	5.16%	5.56
46	38	8	2025	155	143	4.70%	5.29	102	5.04%	5.67
48	38	10	2113	155	141	4.46%	5.24	101	4.78%	5.61

Table B-17. Sample girders – PCBT-28, LWC, ½ in. strand

# of Strands	# Straight	# Draped	P_{jack} (k)	Length (ft)	T_1 (k)	% of P_{jack}	Stirrup area h/4-3h/4 (in^2)	T_2 (k)	% of P_{jack}	Stirrup area End-h/4 (in^2)
14	12	2	438	45	37.9	5.77%	2.10	27.1	6.19%	2.26
16	12	4	500	45	36.5	4.87%	2.03	26.1	5.22%	2.17
18	14	4	562	50	38.2	4.53%	2.12	27.3	4.86%	2.27
20	16	4	624	50	39.4	4.22%	2.19	28.2	4.52%	2.35
22	18	4	686	50	40.7	3.95%	2.26	29.0	4.24%	2.42
24	20	4	748	50	41.7	3.72%	2.32	29.8	3.99%	2.49
26	22	4	810	55	43.3	3.56%	2.40	30.9	3.82%	2.58
28	24	4	872	55	44.3	3.39%	2.46	31.6	3.63%	2.64
30	24	6	933	55	41.7	2.98%	2.32	29.8	3.19%	2.48

Table B-18. Sample girders – PCBT-37, LWC, ½ in. strand

# of Strands	# Straight	# Draped	P_{jack} (k)	Length (ft)	T_1 (k)	% of P_{jack}	Stirrup area h/4-3h/4 (in^2)	T_2 (k)	% of P_{jack}	Stirrup area End-h/4 (in^2)
14	12	2	438	55	37.2	5.67%	2.07	26.6	6.08%	2.22
16	12	4	500	55	36.2	4.83%	2.01	25.8	5.17%	2.15
18	14	4	562	55	38.0	4.51%	2.11	27.2	4.84%	2.27
20	16	4	624	55	39.9	4.27%	2.22	28.5	4.57%	2.38
22	18	4	686	60	42.3	4.11%	2.35	30.2	4.40%	2.51
24	20	4	748	60	44.1	3.93%	2.45	31.5	4.21%	2.62
26	22	4	810	60	45.9	3.78%	2.55	32.8	4.05%	2.73
28	24	4	872	60	47.7	3.65%	2.65	34.1	3.91%	2.84
30	24	6	933	65	46.1	3.29%	2.56	32.9	3.52%	2.74
32	26	6	995	65	44.4	2.97%	2.46	31.7	3.18%	2.64

Table B-19. Sample girders – PCBT-45, LWC, ½ in. strand

# of Strands	# Straight	# Draped	P_{jack} (k)	Length (ft)	T_1 (k)	% of P_{jack}	Stirrup area h/4-3h/4 (in^2)	T_2 (k)	% of P_{jack}	Stirrup area End-h/4 (in^2)
18	14	4	562	65	39.27	4.66%	2.18	28.05	4.99%	2.34
20	16	4	624	70	42.39	4.53%	2.35	30.28	4.85%	2.52
22	18	4	686	70	45.03	4.38%	2.50	32.16	4.69%	2.68
24	20	4	748	70	47.62	4.25%	2.65	34.02	4.55%	2.83
26	22	4	810	70	50.16	4.13%	2.79	35.83	4.43%	2.99
28	24	4	872	75	53.08	4.06%	2.95	37.92	4.35%	3.16
30	24	6	933	75	51.29	3.66%	2.85	36.64	3.92%	3.05
32	26	6	995	75	50.92	3.41%	2.83	36.37	3.65%	3.03
34	28	6	1057	75	50.6	3.19%	2.81	36.14	3.42%	3.01
36	30	6	1119	75	50.3	3.00%	2.80	35.93	3.21%	2.99
38	32	6	1181	80	50.62	2.86%	2.82	36.16	3.06%	3.01
40	34	6	1243	80	50.36	2.70%	2.80	35.97	2.89%	2.99

Table B-20. Sample girders – PCBT-45, LWC, 0.6 in. strand

# of Strands	# Straight	# Draped	P_{jack} (k)	Length (ft)	T_1 (k)	% of P_{jack}	Stirrup area h/4-3h/4 (in^2)	T_2 (k)	% of P_{jack}	Stirrup area End-h/4 (in^2)
22	18	4	971	75	61.54	4.23%	3.42	43.96	4.52%	3.66
24	20	4	1059	75	64.71	4.08%	3.60	46.22	4.37%	3.86
26	22	4	1147	75	67.77	3.94%	3.76	48.41	4.22%	4.03
28	24	4	1234	80	71.26	3.85%	3.96	50.9	4.12%	4.24
30	24	6	1322	80	69	3.48%	3.83	49.29	3.73%	4.11
32	24	8	1410	80	65.77	3.11%	3.65	46.98	3.33%	3.91

Table B-21. Sample girders – PCBT-53, LWC, ½ in. strand

# of Strands	# Straight	# Draped	P_{jack} (k)	Length (ft)	T_1 (k)	% of P_{jack}	Stirrup area h/4-3h/4 (in^2)	T_2 (k)	% of P_{jack}	Stirrup area End-h/4 (in^2)
18	14	4	562	80	41.3	4.90%	2.29	29.5	5.25%	2.46
20	16	4	624	80	44.6	4.77%	2.48	31.9	5.11%	2.66
22	18	4	686	80	47.9	4.66%	2.66	34.2	4.99%	2.85
24	20	4	748	80	51.1	4.56%	2.84	36.5	4.88%	3.04
26	22	4	810	85	54.7	4.50%	3.04	39.1	4.83%	3.26
28	24	4	872	85	57.8	4.42%	3.21	41.3	4.73%	3.44
30	24	6	933	85	56.2	4.02%	3.13	40.2	4.30%	3.34
32	26	6	995	85	56.9	3.81%	3.16	40.7	4.08%	3.38
34	28	6	1057	90	58.2	3.67%	3.23	41.6	3.93%	3.46
36	30	6	1119	90	58.9	3.51%	3.27	42.0	3.76%	3.51
38	32	6	1181	90	59.5	3.36%	3.31	42.5	3.60%	3.54
40	34	6	1243	90	60.2	3.23%	3.35	43.0	3.46%	3.58
42	34	8	1305	90	57.7	2.95%	3.21	41.2	3.16%	3.44
44	36	8	1367	90	56.2	2.74%	3.12	40.1	2.94%	3.35

Table B-22. Sample girders – PCBT-53, LWC, 0.6 in. strand

# of Strands	# Straight	# Draped	P_{jack} (k)	Length (ft)	T_1 (k)	% of P_{jack}	Stirrup area h/4-3h/4 (in^2)	T_2 (k)	% of P_{jack}	Stirrup area End-h/4 (in^2)
22	18	4	971	85	66.1	4.54%	3.67	47.2	4.87%	3.94
24	20	4	1059	90	70.2	4.42%	3.90	50.1	4.73%	4.17
26	22	4	1147	90	74.0	4.31%	4.12	52.9	4.61%	4.40
28	24	4	1234	90	77.8	4.20%	4.32	55.6	4.50%	4.63
30	24	6	1322	90	75.9	3.83%	4.22	54.2	4.10%	4.52
32	26	6	1410	90	76.4	3.61%	4.24	54.5	3.87%	4.55

Table B-23. Sample girders – PCBT-61, LWC, ½ in. strand

# of Strands	# Straight	# Draped	P_{jack} (k)	Length (ft)	T_1 (k)	% of P_{jack}	Stirrup area h/4-3h/4 (in^2)	T_2 (k)	% of P_{jack}	Stirrup area End-h/4 (in^2)
26	22	4	810	90	58.3	4.80%	3.24	41.6	5.14%	3.47
28	24	4	872	90	61.8	4.73%	3.44	44.2	5.07%	3.68
30	24	6	933	90	60.5	4.32%	3.36	43.2	4.63%	3.60
32	26	6	995	95	62.5	4.19%	3.48	44.7	4.49%	3.72
34	28	6	1057	95	64.0	4.04%	3.56	45.7	4.33%	3.82
36	30	6	1119	95	65.5	3.90%	3.64	46.8	4.18%	3.90
38	32	6	1181	95	66.9	3.78%	3.72	47.8	4.05%	3.99
40	34	6	1243	100	68.9	3.69%	3.82	49.2	3.96%	4.10
42	34	8	1305	100	66.9	3.42%	3.72	47.8	3.66%	3.98
44	36	8	1367	100	66.4	3.24%	3.69	47.4	3.47%	3.95
46	38	8	1429	100	65.9	3.07%	3.66	47.1	3.29%	3.92
48	38	10	1491	100	63.1	2.82%	3.50	45.1	3.02%	3.75

Table B-24. Sample girders – PCBT-61, LWC, 0.6 in. strand

# of Strands	# Straight	# Draped	P_{jack} (k)	Length (ft)	T_1 (k)	% of P_{jack}	Stirrup area h/4-3h/4 (in^2)	T_2 (k)	% of P_{jack}	Stirrup area End-h/4 (in^2)
26	22	4	1146	95	79.1	4.60%	4.39	56.5	4.93%	4.71
28	24	4	1234	100	84.1	4.54%	4.67	60.1	4.87%	5.01
30	24	6	1322	100	82.6	4.16%	4.58	59.0	4.46%	4.91
32	26	6	1410	100	84.2	3.98%	4.68	60.1	4.27%	5.02
34	28	6	1498	100	85.7	3.82%	4.77	61.3	4.09%	5.11
36	28	8	1586	105	84.1	3.53%	4.67	60.1	3.79%	5.01

Table B-25. Sample girders – PCBT-69, LWC, ½ in. strand

# of Strands	# Straight	# Draped	P_{jack} (k)	Length (ft)	T_1 (k)	% of P_{jack}	Stirrup area h/4-3h/4 (in^2)	T_2 (k)	% of P_{jack}	Stirrup area End-h/4 (in^2)
30	24	6	933	105	65.8	4.70%	3.66	47.0	5.03%	3.91
32	26	6	995	105	68.0	4.55%	3.77	48.6	4.88%	4.05
34	28	6	1057	110	70.7	4.46%	3.93	50.5	4.78%	4.21
36	30	6	1119	110	72.8	4.34%	4.05	52.0	4.65%	4.34
38	32	6	1181	110	74.9	4.23%	4.16	53.5	4.53%	4.46
40	34	6	1243	110	77.0	4.13%	4.28	55.0	4.42%	4.58
42	34	8	1305	115	76.0	3.88%	4.22	54.3	4.16%	4.52
44	36	8	1367	115	76.4	3.72%	4.24	54.6	3.99%	4.55
46	38	8	1429	115	76.7	3.58%	4.26	54.8	3.84%	4.57
48	38	10	1491	115	74.5	3.33%	4.14	53.2	3.57%	4.44

Table B-26. Sample girders – PCBT-69, LWC, 0.6 in. strarnd

# of Strands	# Straight	# Draped	P_{jack} (k)	Length (ft)	T_1 (k)	% of P_{jack}	Stirrup area h/4-3h/4 (in^2)	T_2 (k)	% of P_{jack}	Stirrup area End-h/4 (in^2)
28	24	4	1234	115	90.8	4.91%	5.05	64.9	5.26%	5.41
30	24	6	1322	115	89.9	4.53%	4.99	64.3	4.86%	5.36
32	26	6	1410	115	92.5	4.37%	5.14	66.1	4.69%	5.51
34	28	6	1498	115	95.0	4.23%	5.28	67.9	4.53%	5.66
36	30	6	1586	115	97.4	4.09%	5.41	69.6	4.39%	5.80
38	30	8	1674	115	95.5	3.80%	5.30	68.2	4.07%	5.68

Table B-27. Sample girders – PCBT-77, LWC, ½ in. strand

# of Strands	# Straight	# Draped	P_{jack} (k)	Length (ft)	T_1 (k)	% of P_{jack}	Stirrup area h/4-3h/4 (in^2)	T_2 (k)	% of P_{jack}	Stirrup area End-h/4 (in^2)
38	32	6	1181	115	81.3	4.59%	4.52	58.0	4.91%	4.84
40	34	6	1243	120	84.4	4.52%	4.68	60.3	4.85%	5.02
42	34	8	1305	120	83.2	4.25%	4.62	59.4	4.55%	4.95
44	36	8	1367	120	84.2	4.11%	4.68	60.2	4.40%	5.01
46	38	8	1429	120	85.3	3.98%	4.74	60.9	4.26%	5.08
48	38	10	1491	120	83.4	3.73%	4.63	59.6	4.00%	4.97

Table B-28. Sample girders – PCBT-77, LWC, 0.6 in. strand

# of Strands	# Straight	# Draped	P_{jack} (k)	Length (ft)	T_1 (k)	% of P_{jack}	Stirrup area h/4-3h/4 (in^2)	T_2 (k)	% of P_{jack}	Stirrup area End-h/4 (in^2)
28	22	6	1234	125	90.7	4.90%	5.04	64.8	5.25%	5.40
30	24	6	1322	125	96.3	4.86%	5.36	68.8	5.20%	5.73
32	26	6	1410	125	99.7	4.71%	5.53	71.2	5.05%	5.94
34	28	6	1498	125	103	4.58%	5.72	73.6	4.91%	6.13
36	30	6	1586	130	107	4.49%	5.93	76.3	4.81%	6.36
38	32	6	1674	130	110	4.38%	6.11	78.5	4.69%	6.54
40	32	8	1762	130	109	4.11%	6.03	77.6	4.40%	6.47
42	34	8	1849	130	112	4.02%	6.20	79.7	4.31%	6.64

Table B-29. Sample girders – PCBT-85, LWC, ½ in. strand

# of Strands	# Straight	# Draped	P_{jack} (k)	Length (ft)	T_1 (k)	% of P_{jack}	Stirrup area h/4-3h/4 (in^2)	T_2 (k)	% of P_{jack}	Stirrup area End-h/4 (in^2)
34	28	6	1057	120	82.6	5.21%	4.59	59.0	5.58%	4.92
36	30	6	1119	120	86.0	5.12%	4.78	61.4	5.49%	5.12
38	32	6	1181	120	89.4	5.04%	4.96	63.8	5.40%	5.32
40	34	6	1243	130	93.8	5.03%	5.21	67.0	5.39%	5.58
42	34	8	1305	130	92.9	4.74%	5.16	66.3	5.08%	5.53
44	36	8	1367	130	94.8	4.62%	5.26	67.7	4.95%	5.64
46	38	8	1429	130	96.6	4.51%	5.37	69.0	4.83%	5.75
48	38	10	1491	130	95.1	4.25%	5.28	68.0	4.56%	5.67

Table B-30. Saple girders – PCBT-85, LWC, 0.6 in. strand

# of Strands	# Straight	# Draped	P_{jack} (k)	Length (ft)	T_1 (k)	% of P_{jack}	Stirrup area h/4-3h/4 (in^2)	T_2 (k)	% of P_{jack}	Stirrup area End-h/4 (in^2)
28	22	6	1234	120	96.6	5.22%	5.37	69.0	5.59%	5.75
30	24	6	1322	120	103	5.20%	5.73	73.7	5.57%	6.14
32	26	6	1410	120	108	5.09%	5.98	76.9	5.45%	6.40
34	28	6	1498	130	113	5.05%	6.30	81.0	5.41%	6.75
36	30	6	1586	130	118	4.95%	6.54	84.1	5.30%	7.00
38	30	8	1674	130	117	4.64%	6.47	83.2	4.97%	6.93
40	32	8	1762	140	122	4.63%	6.80	87.3	4.96%	7.28
42	34	8	1850	140	126	4.55%	7.01	90.2	4.88%	7.52
44	36	8	1937	140	128	4.42%	7.14	91.7	4.73%	7.64

Table B-31. Sample girders – PCBT-93, LWC, ½ in. strand

# of Strands	# Straight	# Draped	P_{jack} (k)	Length (ft)	T_1 (k)	% of P_{jack}	Stirrup area h/4-3h/4 (in^2)	T_2 (k)	% of P_{jack}	Stirrup area End-h/4 (in^2)
38	32	6	1181	150	95.1	5.36%	5.28	67.9	5.75%	5.66
40	34	6	1243	150	98.6	5.29%	5.48	70.4	5.67%	5.87
42	34	8	1305	150	98.3	5.02%	5.46	70.2	5.38%	5.85
44	36	8	1367	155	101	4.93%	5.62	72.2	5.28%	6.02
46	38	8	1429	155	103	4.82%	5.74	73.8	5.17%	6.16
48	38	10	1491	155	103	4.58%	5.69	73.3	4.91%	6.10

Table B-32. Sample girders – PCBT-93, LWC, 0.6 in. strand

# of Strands	# Straight	# Draped	P_{jack} (k)	Length (ft)	T_1 (k)	% of P_{jack}	Stirrup area h/4-3h/4 (in^2)	T_2 (k)	% of P_{jack}	Stirrup area End-h/4 (in^2)
32	26	6	1410	135	112	5.29%	6.22	79.9	5.66%	6.66
34	28	6	1498	135	117	5.18%	6.47	83.2	5.55%	6.93
36	30	6	1586	145	122	5.14%	6.79	87.4	5.51%	7.28
38	30	8	1674	145	122	4.85%	6.77	87.0	5.20%	7.25
40	32	8	1762	145	126	4.78%	7.02	90.1	5.12%	7.51
42	34	8	1850	145	131	4.70%	7.24	93.2	5.04%	7.77
44	36	8	1937	155	135	4.63%	7.48	96.1	4.96%	8.01
46	38	8	2025	155	137	4.51%	7.61	98.0	4.83%	8.16
48	38	10	2113	155	136	4.29%	7.55	97.1	4.60%	8.09

Appendix C. End Zone Design Tables

Table C-1. PCBT-29, Normal Weight Concrete, Beam End Design Table

Normal Weight Concrete					Stirrup Stress = 18 ksi		
		End - h/4			h/4-3h/4		
A	B	C	D	E	F	G	H
No. of ½" strands	A_{ps} (in^2)	$A_{reg'd}$ (in^2)	Quantity and size	Number and spacing size	$A_{reg'd}$ (in^2)	Quantity and size	Number and spacing size
20 or less	3.06	1.60	4 No. 4	2 spa. @ 2.5"	1.49	4 No. 4	4 spa. @ 3.75"
22 or more	3.37	1.65	5 No. 4	2 spa. @ 2.5"	1.54	4 No. 4	5 spa. @ 3"

Table C-2. PCBT-29, Light Weight Concrete, Beam End Design Table

Light Weight Concrete					Stirrup Stress = 12 ksi		
		End - h/4			h/4-3h/4		
A	B	C	D	E	F	G	H
No. of ½" strands	A_{ps} (in^2)	$A_{reg'd}$ (in^2)	Quantity and size	Number and spacing size	$A_{reg'd}$ (in^2)	Quantity and size	Number and spacing size
22 or less	3.37	2.42	4 No. 5	2 spa. @ 2.5"	2.26	4 No. 5	4 spa. @ 3.75"
24 or more	3.67	2.49	5 No. 5	2 spa. @ 2.5"	2.32	4 No. 5	4 spa. @ 3.75"

Table C-3. PCBT-37, Normal Weight Concrete, Beam End Design Table

Normal Weight Concrete					Stirrup Stress = 18 ksi		
		End - h/4			h/4-3h/4		
A	B	C	D	E	F	G	H
No. of ½" strands	A_{ps} (in^2)	$A_{req'd}$ (in^2)	Quantity and size	Number and spacing size	$A_{req'd}$ (in^2)	Quantity and size	Number and spacing size
≤ 18	2.75	1.54	4 No. 4	2 spa. @ 3.5"	1.44	4 No. 4	4 spa. @ 4.5"
≤ 22	3.37	1.71	5 No. 4	2 spa. @ 3.5"	1.60	4 No. 4	4 spa. @ 4.5"
24 or more	3.06	1.62	5 No. 4	2 spa. @ 3.5"	1.51	5 No. 4	5 spa. @ 3.75"

Table C-4. PCBT-37, Light Weight Concrete, Beam End Design Table

Light Weight Concrete					Stirrup Stress = 12 ksi		
		End - h/4			h/4-3h/4		
A	B	C	D	E	F	G	H
No. of ½" strands	A_{ps} (in^2)	$A_{req'd}$ (in^2)	Quantity and size	Number and spacing size	$A_{req'd}$ (in^2)	Quantity and size	Number and spacing size
≤ 20	3.06	2.38	4 No. 5	2 spa. @ 3.5"	2.22	4 No. 5	4 spa. @ 4.5"
≤ 24	3.67	2.62	5 No. 5	2 spa. @ 3.5"	2.45	4 No. 5	4 spa. @ 4.5"
26 or more	3.98	2.73	5 No. 5	2 spa. @ 3.5"	2.55	5 No. 5	5 spa. @ 3.75"

Table C-5. PCBT-45, Normal Weight Concrete, Beam End Design Table

Normal Weight Concrete					Stirrup Stress = 18 ksi		
		End - h/4			h/4-3h/4		
A	B	C	D	E	F	G	H
No. of ½" strands	A_{ps} (in^2)	$A_{req'd}$ (in^2)	Quantity and size	Number and spacing size	$A_{req'd}$ (in^2)	Quantity and size	Number and spacing size
≤ 24	3.67	1.94	5 No. 4	3 spa. @ 3"	1.81	5 No. 4	5 spa. @ 4.5"
26	3.98	2.06	6 No. 4	3 spa. @ 3"	1.92	5 No. 4	5 spa. @ 4.5"
28 or more	4.28	2.18	6 No. 4	3 spa. @ 3"	2.03	6 No. 4	6 spa. @ 3.75"
No. of 0.6" strands	A_{ps} (in^2)	$A_{req'd}$ (in^2)	Quantity and size	Number and spacing size	$A_{req'd}$ (in^2)	Quantity and size	Number and spacing size
≤ 22	4.77	2.53	5 No. 5	3 spa. @ 3"	2.36	4 No. 5	4 spa. @ 5.5"
24 or more	5.21	2.67	5 No. 5	3 spa. @ 3"	2.49	5 No. 5	5 spa. @ 4.5"

Table C-6. PCBT-45, Light Weight Concrete, Beam End Design Table

Light Weight Concrete					Stirrup Stress = 12 ksi		
		End - h/4			h/4-3h/4		
A	B	C	D	E	F	G	H
No. of ½" strands	A_{ps} (in^2)	$A_{req'd}$ (in^2)	Quantity and size	Number and spacing size	$A_{req'd}$ (in^2)	Quantity and size	Number and spacing size
≤ 20	3.06	2.52	5 No. 5	3 spa. @ 3"	2.35	4 No. 5	4 spa. @ 5.5"
≤ 26	3.98	2.99	5 No. 5	3 spa. @ 3"	2.79	5 No. 5	5 spa. @ 4.5"
28 or more	4.28	3.16	6 No. 5	3 spa. @ 3"	2.95	5 No. 5	5 spa. @ 4.5"
No. of 0.6" strands	A_{ps} (in^2)	$A_{req'd}$ (in^2)	Quantity and size	Number and spacing size	$A_{req'd}$ (in^2)	Quantity and size	Number and spacing size
≤ 22	4.77	3.66	6 No. 5	3 spa. @ 3"	3.42	6 No. 5	6 spa. @ 3.75"
≤ 26	5.64	4.03	7 No. 5	3 spa. @ 3"	3.76	7 No. 5	7 spa. @ 3.25"
28 or more	6.08	4.24	7 No. 5	3 spa. @ 3"	3.96	7 No. 5	7 spa. @ 3.25"

Table C-7. PCBT-53, Normal Weight Concrete, Beam End Design Table

Normal Weight Concrete					Stirrup Stress = 18 ksi		
		End - h/4			h/4-3h/4		
A	B	C	D	E	F	G	H
No. of ½" strands	A_{ps} (in^2)	$A_{reg'd}$ (in^2)	Quantity and size	Number and spacing size	$A_{reg'd}$ (in^2)	Quantity and size	Number and spacing size
≤ 24	3.67	2.09	6 No. 4	3 spa. @ 3.75"	1.95	5 No. 4	5 spa. @ 5.25"
≤ 34	5.2	2.38	6 No. 4	3 spa. @ 3.75"	2.22	6 No. 4	6 spa. @ 4.5"
36 or more	5.51	2.41	7 No. 4	3 spa. @ 3.75"	2.25	6 No. 4	6 spa. @ 4.5"
No. of 0.6" strands	A_{ps} (in^2)	$A_{reg'd}$ (in^2)	Quantity and size	Number and spacing size	$A_{reg'd}$ (in^2)	Quantity and size	Number and spacing size
≤ 26	5.64	3.04	5 No. 5	3 spa. @ 3.75"	2.83	5 No. 5	5 spa. @ 5.25"
28 or more	6.08	3.2	6 No. 5	3 spa. @ 3.75"	2.98	5 No. 5	5 spa. @ 5.25"

Table C-8. PCBT-53, Light Weight Concrete, Beam End Design Table

Light Weight Concrete					Stirrup Stress = 12 ksi		
		End - h/4			h/4-3h/4		
A	B	C	D	E	F	G	H
No. of ½" strands	A_{ps} (in^2)	$A_{reg'd}$ (in^2)	Quantity and size	Number and spacing size	$A_{reg'd}$ (in^2)	Quantity and size	Number and spacing size
≤ 24	3.06	3.04	5 No. 5	3 spa. @ 3.75"	2.84	5 No. 5	5 spa. @ 5.25"
26 or more	3.37	3.26	6 No. 5	3 spa. @ 3.75"	3.04	5 No. 5	5 spa. @ 5.25"
No. of 0.6" strands	A_{ps} (in^2)	$A_{reg'd}$ (in^2)	Quantity and size	Number and spacing size	$A_{reg'd}$ (in^2)	Quantity and size	Number and spacing size
≤ 24	5.21	4.17	7 No. 5	3 spa. @ 3.75"	3.9	7 No. 5	7 spa. @ 3.75"
26 or more	5.64	4.4	8 No. 5	3 spa. @ 3.75"	4.12	7 No. 5	7 spa. @ 3.75"

Table C-9. PCBT-61, Normal Weight Concrete, Beam End Design Table

Normal Weight Concrete					Stirrup Stress = 18 ksi		
		End - h/4			h/4-3h/4		
A	B	C	D	E	F	G	H
No. of ½" strands	A_{ps} (in^2)	$A_{req'd}$ (in^2)	Quantity and size	Number and spacing size	$A_{req'd}$ (in^2)	Quantity and size	Number and spacing size
≤ 32	4.9	2.55	7 No. 4	4 spa. @ 3.25"	2.38	6 No. 4	6 spa. @ 5"
≤ 38	5.81	2.74	7 No. 4	4 spa. @ 3.25"	2.56	7 No. 4	7 spa. @ 4.25"
40 or more	6.12	2.83	8 No. 4	4 spa. @ 3.25"	2.64	7 No. 4	7 spa. @ 4.25"
No. of 0.6" strands	A_{ps} (in^2)	$A_{req'd}$ (in^2)	Quantity and size	Number and spacing size	$A_{req'd}$ (in^2)	Quantity and size	Number and spacing size
≤ 26	5.64	3.24	6 No. 5	4 spa. @ 3.25"	3.03	5 No. 5	5 spa. @ 6"
28 or more	6.08	3.43	6 No. 5	4 spa. @ 3.25"	3.2	6 No. 5	6 spa. @ 5"

Table C-10. PCBT-61, Light Weight Concrete, Beam End Design Table

Light Weight Concrete					Stirrup Stress = 12 ksi		
		End - h/4			h/4-3h/4		
A	B	C	D	E	F	G	H
No. of ½" strands	A_{ps} (in^2)	$A_{req'd}$ (in^2)	Quantity and size	Number and spacing size	$A_{req'd}$ (in^2)	Quantity and size	Number and spacing size
≤ 32	4.9	3.72	6 No. 5	4 spa. @ 3.25"	3.48	6 No. 5	6 spa. @ 5"
≤ 38	5.81	3.99	7 No. 5	4 spa. @ 3.25"	3.72	6 No. 5	6 spa. @ 5"
40 or more	6.12	4.1	7 No. 5	4 spa. @ 3.25"	3.82	7 No. 5	7 spa. @ 4.25"
No. of 0.6" strands	A_{ps} (in^2)	$A_{req'd}$ (in^2)	Quantity and size	Number and spacing size	$A_{req'd}$ (in^2)	Quantity and size	Number and spacing size
≤ 26	5.64	4.71	8 No. 5	4 spa. @ 3.25"	4.39	8 No. 5	8 spa. @ 3.75"
28 or more	6.08	5.01	9 No. 5	4 spa. @ 3.25"	4.67	8 No. 5	8 spa. @ 3.75"

Table C-11. PCBT-69, Normal Weight Concrete, Beam End Design Table

Normal Weight Concrete					Stirrup Stress = 18 ksi		
		End - h/4			h/4-3h/4		
A	B	C	D	E	F	G	H
No. of ½" strands	A_{ps} (in^2)	$A_{reg'd}$ (in^2)	Quantity and size	Number and spacing size	$A_{reg'd}$ (in^2)	Quantity and size	Number and spacing size
≤ 32	4.9	2.77	7 No. 4	4 spa. @ 3.75"	2.59	7 No. 4	7 spa. @ 5"
≤ 36	5.51	2.98	8 No. 4	4 spa. @ 3.75"	2.78	7 No. 4	7 spa. @ 5"
38 or more	5.81	3.07	8 No. 4	4 spa. @ 3.75"	2.87	8 No. 4	8 spa. @ 4.25"
No. of 0.6" strands	A_{ps} (in^2)	$A_{reg'd}$ (in^2)	Quantity and size	Number and spacing size	$A_{reg'd}$ (in^2)	Quantity and size	Number and spacing size
≤ 34	7.38	3.92	7 No. 5	4 spa. @ 3.75"	3.65	6 No. 5	6 spa. @ 5.75"
36 or more	7.81	4.02	7 No. 5	4 spa. @ 3.75"	3.75	7 No. 5	7 spa. @ 5"

Table C-12. PCBT-69, Light Weight Concrete, Beam End Design Table

Light Weight Concrete					Stirrup Stress = 12 ksi		
		End - h/4			h/4-3h/4		
A	B	C	D	E	F	G	H
No. of ½" strands	A_{ps} (in^2)	$A_{reg'd}$ (in^2)	Quantity and size	Number and spacing size	$A_{reg'd}$ (in^2)	Quantity and size	Number and spacing size
≤ 30	4.59	3.91	7 No. 5	4 spa. @ 3.75"	3.66	6 No. 5	6 spa. @ 5.75"
≤ 36	5.51	4.34	7 No. 5	4 spa. @ 3.75"	4.05	7 No. 5	7 spa. @ 5"
38 or more	5.81	4.46	8 No. 5	4 spa. @ 3.75"	4.16	7 No. 5	7 spa. @ 5"
No. of 0.6" strands	A_{ps} (in^2)	$A_{reg'd}$ (in^2)	Quantity and size	Number and spacing size	$A_{reg'd}$ (in^2)	Quantity and size	Number and spacing size
≤ 32	6.94	5.51	9 No. 5	4 spa. @ 3.75"	5.14	9 No. 5	9 spa. @ 3.75"
34 or more	7.38	5.66	10 No. 5	4 spa. @ 3.75"	5.28	9 No. 5	9 spa. @ 3.75"

Table C-13. PCBT-77, Normal Weight Concrete, Beam End Design Table

Normal Weight Concrete					Stirrup Stress = 18 ksi		
		End - h/4			h/4-3h/4		
A	B	C	D	E	F	G	H
No. of ½" strands	A_{ps} (in^2)	$A_{req'd}$ (in^2)	Quantity and size	Number and spacing size	$A_{req'd}$ (in^2)	Quantity and size	Number and spacing size
≤ 42	6.43	3.41	9 No. 4	5 spa. @ 3.5"	3.18	8 No. 4	8 spa. @ 4.75"
44 or more	6.73	3.46	9 No. 4	5 spa. @ 3.5"	3.24	9 No. 4	9 spa. @ 4.25"
No. of 0.6" strands	A_{ps} (in^2)	$A_{req'd}$ (in^2)	Quantity and size	Number and spacing size	$A_{req'd}$ (in^2)	Quantity and size	Number and spacing size
≤ 30	6.51	3.96	7 No. 5	5 spa. @ 3.5"	3.7	6 No. 5	5 spa. @ 6.5"
≤ 34	7.38	4.25	7 No. 5	5 spa. @ 3.5"	3.97	7 No. 5	7 spa. @ 5.5"
≤ 38	8.25	4.55	8 No. 5	5 spa. @ 3.5"	4.25	7 No. 5	7 spa. @ 5.5"
40 or more	8.68	4.69	8 No. 5	5 spa. @ 3.5"	4.37	8 No. 5	8 spa. @ 4.75"

Table C-14. PCBT-77, Light Weight Concrete, Beam End Design Table

Light Weight Concrete					Stirrup Stress = 12 ksi		
		End - h/4			h/4-3h/4		
A	B	C	D	E	F	G	H
No. of ½" strands	A_{ps} (in^2)	$A_{req'd}$ (in^2)	Quantity and size	Number and spacing size	$A_{req'd}$ (in^2)	Quantity and size	Number and spacing size
≤ 42	6.43	4.95	8 No. 5	5 spa. @ 3.5"	4.62	8 No. 5	8 spa. @ 4.75"
44 or more	6.73	5.01	9 No. 5	5 spa. @ 3.5"	4.68	8 No. 5	8 spa. @ 4.75"
No. of 0.6" strands	A_{ps} (in^2)	$A_{req'd}$ (in^2)	Quantity and size	Number and spacing size	$A_{req'd}$ (in^2)	Quantity and size	Number and spacing size
≤ 28	6.08	5.4	9 No. 5	5 spa. @ 3.5"	5.04	9 No. 5	9 spa. @ 4.25"
≤ 34	7.38	6.13	10 No. 5	5 spa. @ 3.5"	5.72	10 No. 5	10 spa. @ 3.75"
36 or more	7.81	6.36	11 No. 5	5 spa. @ 3.5"	5.93	10 No. 5	10 spa. @ 3.75"

Table C-15. PCBT-85, Normal Weight Concrete, Beam End Design Table

Normal Weight Concrete					Stirrup Stress = 18 ksi		
		End - h/4			h/4-3h/4		
A	B	C	D	E	F	G	H
No. of ½" strands	A_{ps} (in^2)	$A_{req'd}$ (in^2)	Quantity and size	Number and spacing size	$A_{req'd}$ (in^2)	Quantity and size	Number and spacing size
≤ 38	5.81	3.54	9 No. 4	5 spa. @ 3.75"	3.31	9 No. 4	9 spa. @ 4.75"
40 or more	6.12	3.67	10 No. 4	5 spa. @ 3.75"	3.43	9 No. 4	9 spa. @ 4.75"
No. of 0.6" strands	A_{ps} (in^2)	$A_{req'd}$ (in^2)	Quantity and size	Number and spacing size	$A_{req'd}$ (in^2)	Quantity and size	Number and spacing size
≤ 32	6.94	4.27	7 No. 5	5 spa. @ 3.75"	3.99	7 No. 5	7 spa. @ 6"
≤ 38	8.25	4.84	8 No. 5	5 spa. @ 3.75"	4.51	8 No. 5	8 spa. @ 5.25"
44 or more	9.55	5.09	9 No. 5	5 spa. @ 3.75"	4.76	8 No. 5	8 spa. @ 5.25"

Table C-16. PCBT-85, Light Weight Concrete, Beam End Design Table

Light Weight Concrete					Stirrup Stress = 12 ksi		
		End - h/4			h/4-3h/4		
A	B	C	D	E	F	G	H
No. of ½" strands	A_{ps} (in^2)	$A_{req'd}$ (in^2)	Quantity and size	Number and spacing size	$A_{req'd}$ (in^2)	Quantity and size	Number and spacing size
≤ 42	6.43	5.53	9 No. 5	5 spa. @ 3.75"	5.16	9 No. 5	9 spa. @ 4.75"
44 or more	6.73	5.64	10 No. 5	5 spa. @ 3.75"	5.26	9 No. 5	9 spa. @ 4.75"
No. of 0.6" strands	A_{ps} (in^2)	$A_{req'd}$ (in^2)	Quantity and size	Number and spacing size	$A_{req'd}$ (in^2)	Quantity and size	Number and spacing size
≤ 30	6.51	6.14	10 No. 5	5 spa. @ 3.75"	5.73	10 No. 5	10 spa. @ 4.25"
≤ 34	7.38	6.75	11 No. 5	5 spa. @ 3.75"	6.3	11 No. 5	11 spa. @ 3.75"
40 or more	8.68	7.28	12 No. 5	5 spa. @ 3.75"	6.8	11 No. 5	11 spa. @ 3.75"

Table C-17. PCBT-93, Normal Weight Concrete, Beam End Design Table

Normal Weight Concrete					Stirrup Stress = 18 ksi		
		End - h/4			h/4-3h/4		
A	B	C	D	E	F	G	H
No. of ½" strands	A_{ps} (in^2)	$A_{req'd}$ (in^2)	Quantity and size	Number and spacing size	$A_{req'd}$ (in^2)	Quantity and size	Number and spacing size
≤ 38	5.81	3.77	10 No. 4	6 spa. @ 3.5"	3.52	9 No. 4	9 spa. @ 5"
≤ 44	6.73	3.98	10 No. 4	6 spa. @ 3.5"	3.71	10 No. 4	10 spa. @ 4.75"
46 or more	7.04	4.13	11 No. 4	6 spa. @ 3.5"	3.86	10 No. 4	10 spa. @ 4.75"
No. of 0.6" strands	A_{ps} (in^2)	$A_{req'd}$ (in^2)	Quantity and size	Number and spacing size	$A_{req'd}$ (in^2)	Quantity and size	Number and spacing size
≤ 34	7.38	4.77	8 No. 5	6 spa. @ 3.5"	4.45	8 No. 5	8 spa. @ 5.75"
≤ 38	8.25	5.21	9 No. 5	6 spa. @ 3.5"	4.86	8 No. 5	8 spa. @ 5.75"
≤ 44	9.55	5.56	9 No. 5	6 spa. @ 3.5"	5.19	9 No. 5	9 spa. @ 5"
46 or more	9.98	5.67	10 No. 5	6 spa. @ 3.5"	5.29	9 No. 5	9 spa. @ 5"

Table C-18. PCBT-93, Light Weight Concrete, Beam End Design Table

Light Weight Concrete					Stirrup Stress = 12 ksi		
		End - h/4			h/4-3h/4		
A	B	C	D	E	F	G	H
No. of ½" strands	A_{ps} (in^2)	$A_{req'd}$ (in^2)	Quantity and size	Number and spacing size	$A_{req'd}$ (in^2)	Quantity and size	Number and spacing size
≤ 42	6.43	5.85	10 No. 5	6 spa. @ 3.5"	5.46	9 No. 5	9 spa. @ 5"
46 or more	7.04	6.16	10 No. 5	6 spa. @ 3.5"	5.74	10 No. 5	10 spa. @ 4.75"
No. of 0.6" strands	A_{ps} (in^2)	$A_{req'd}$ (in^2)	Quantity and size	Number and spacing size	$A_{req'd}$ (in^2)	Quantity and size	Number and spacing size
≤ 28	6.08	6.66	11 No. 5	6 spa. @ 3.5"	6.22	11 No. 5	11 spa. @ 4.25"
≤ 34	7.38	7.25	12 No. 5	6 spa. @ 3.5"	6.77	11 No. 5	11 spa. @ 4.25"
≤ 38	8.25	7.77	13 No. 5	6 spa. @ 3.5"	7.24	12 No. 5	12 spa. @ 3.75"
40 or more	8.68	8.01	14 No. 5	6 spa. @ 3.5"	7.48	13 No. 5	13 spa. @ 3.5"

Appendix D. Derivation for Alternate Strut-and-Tie Model

Generic Model Layout

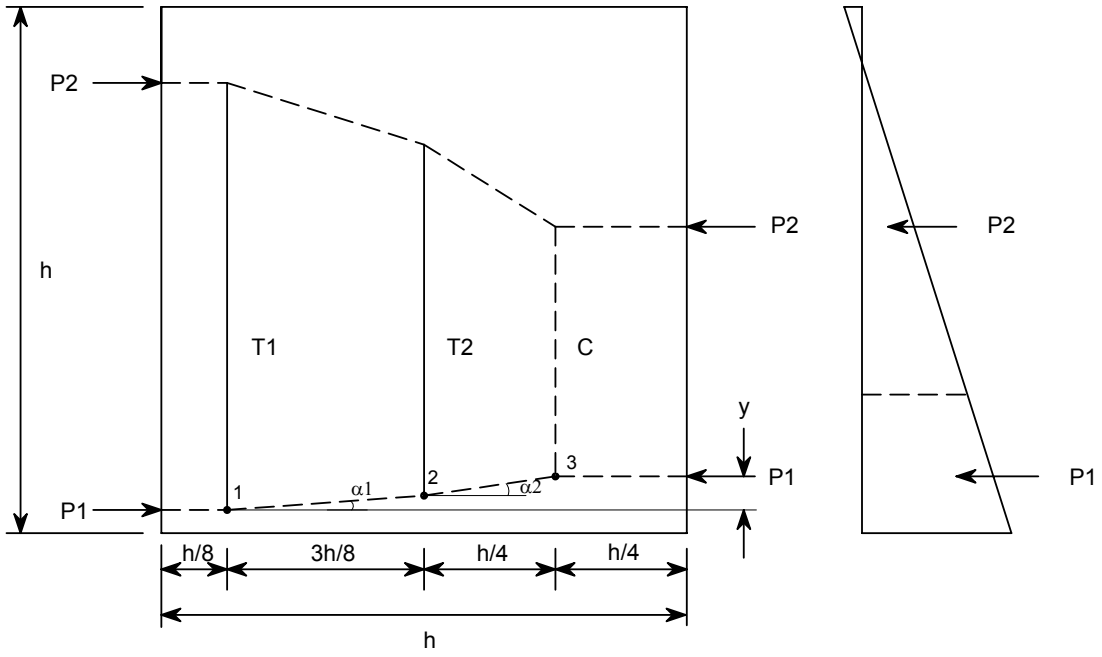

Set T1 = T2 and solve for the corresponding angles, α_1 and α_2

From equilibrium in the vertical direction:

$T_1 + T_2 = C$ and therefore: $2T_1 = C$

Given the geometry of the model, the following is also true:

$$y = \frac{3h}{8}\tan\alpha_1 + \frac{h}{4}\tan\alpha_2$$

Let: $\tan\alpha_1 = a$ and $\tan\alpha_2 = b$

$$y = \frac{3h}{8}a + \frac{h}{4}b \qquad (1)$$

From equilibrium of node 3:

$P_1 \tan\alpha_2 = C$ or $P_1 b = 2T_1$

Which simplifies to:

$$T_1 = \frac{P_1 b}{2} \qquad (2)$$

From equilibrium of node 1:

$$T_1 = P_1 \tan\alpha_1$$

This simplifies to:

$$T_1 = P_1 a \qquad (3)$$

Equation (3) can be re-written:

$$\tan\alpha_1 = a = \frac{T_1}{P_1}$$

Setting equation (2) and (3) equal to each other:

$$2a = b$$

Insert this into equation (1) and simplify:

$$y = \frac{7ha}{8} = \frac{7hT_1}{8P_1}$$

Solve for T1:

$$T_1 = T_2 = \frac{8P_1 y}{7h}$$

Appendix E. Calculations for PCBT-53 Experimental Girder

Virginia PCBT-53 Bridge Girder Data

Depth of girder	h = 53 in.
Area of girder	A_c = 802.7 in^2
Height of centroid	y_b = 26.06 in.
Moment of inertia	I = 312400 in^4
Girder self weight	w_o = 669 lb/ft
Girder Length	L = 65 ft

Girder Dimensions

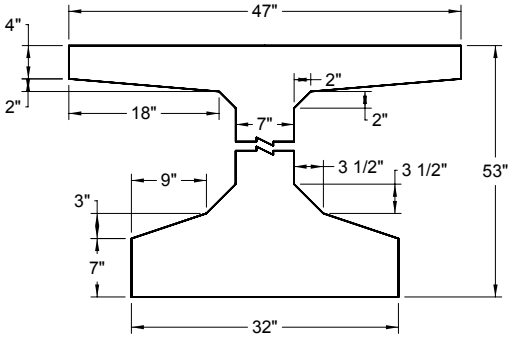

Girder cross section at end

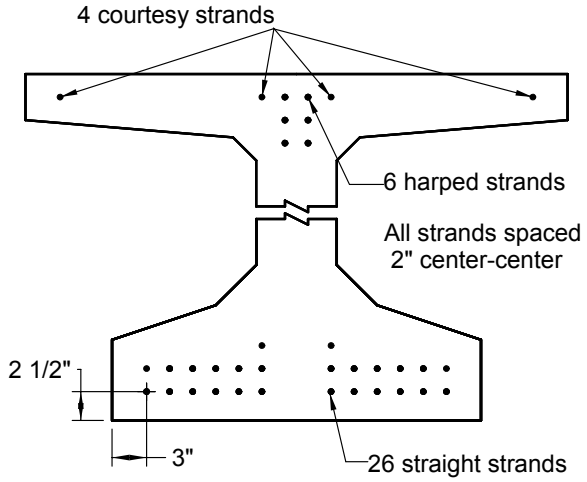

Girder cross section at midspan

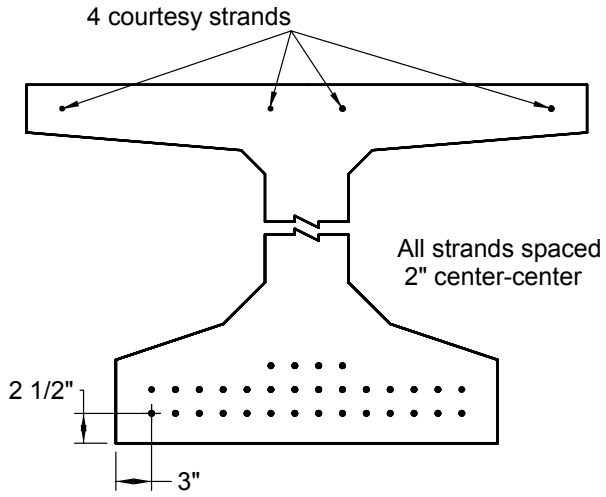

Concrete Material Properties

ω = 120 lb/ft^3
f'_{ci} = 5,500 psi
E_{ci} = 3,217 ksi

26 Straight and 6 Harped Strand Properties

A_{strand} = 0.153 in^2
f_{pu} = 270 ksi
f_{jack} = 0.75 f_{pu}
E_{ps} = 28,500 ksi

4 Courtesy Strand Properties

A_{strand} = 0.153 in^2
f_{pu} = 270 ksi
f_{jack} = 26.2 ksi

Strand location 53 in. from end of beam

Height of centroid of harped strands at beam end = 49 in.
Height of centroid of harped strands at harping point = 4.25 in.
Distance from end to harping point = 32.5 ft – 2.5 ft = 30 ft
Angle of draped strands, θ

$$\theta = a\tan\left(\frac{49-4.25}{12(30)}\right) = 7.09°$$

Height of centroid of harped strands 53 in. from end of beam

$$y_{cgs\_draped} = 49 - 53\sin(7.09) = 42.4\,\text{in.}$$

Height of centroid of straight strands 53 in. from end of beam

$$y_{cgs\_harped} = \frac{12(2.25)+12(4.25)+2(6.25)}{26} = 3.48\,\text{in.}$$

Height of centroid of courtesy strands 53 in. from end of beam

$y_{cgs\_courtesy} = 51\,\text{in.}$

Properties of all prestressing steel 53 in. from end of beam

	Area (in²)	*y_b (in)*	*I_o (in⁴)*	*P_{jack} (k)*
4 courtesy strands	0.612	51	0	16
6 harped strands	0.918	42.4	2.45	186
26 straight strands	3.98	3.48	6.21	806
			Total =	1,008 kip

Transformed section properties for section 53 in. from end of beam

Section modulus at transfer, n_i

$$n_i = \frac{E_{ps}}{E_{ci}} = \frac{28500}{3217} = 8.86$$

	A_t (in²)	y_b (in)	$A_t y_b$ (in²)	$A_t(y_b-y_t)^2$ (in⁴)	I_{ot} (in⁴)	I_t (in⁴)
Concrete	802.7	26.06	20,920	252	312,400	312,652
Courtesy Strands	4.81	51	245	3,128	0	3,128
Harped Strands	7.22	42.4	306	2,062	19.3	2,081
Straight Strands	31.3	3.48	109	15,180	48.8	15,229
Total =	846	Total =	21,580		Total =	333,090

$$y_t = \frac{21{,}580}{846} = 25.5\,\text{in. from bottom of beam}$$

Sample calculations for highlighted values

$$A_t = (n_i - 1)A_{ps\_harped} = (8.86 - 1)(0.918) = 7.22\,\text{in}^2$$

$$I_{ot} = (n_i - 1)I_{o\_harped} = (8.86 - 1)(2.45) = 19.3\,\text{in}^4$$

Stresses from prestress force for section 53 in. from end of beam

$$f_{bot} = \frac{P_{jack\_TOT}}{A_t} + \frac{[P_{courtesy}(y_t - y_{b\_courtesy}) + P_{harped}(y_t - y_{b\_harped}) + P_{straight}(y_t - y_{b\_straight})]y_t}{I_t}$$

$$f_{bot} = \frac{-1{,}008}{846} + \frac{[-16(25.5-51) - 186(25.5-42.4) - 806(25.5-3.48)]25.5}{333{,}090}$$

$$f_{bot} = -2.28\,\text{ksi}$$

$$f_{top} = \frac{P_{jack\_TOT}}{A_t} + \frac{[P_{courtesy}(y_t - y_{b\_courtesy}) + P_{harped}(y_t - y_{b\_harped}) + P_{straight}(y_t - y_{b\_straight})](y_t - h)}{I_t}$$

$$f_{top} = \frac{-1{,}008}{846} + \frac{[-16(25.5-51) - 186(25.5-42.4) - 806(25.5-3.48)](25.5-53)}{333{,}090}$$

$$f_{top} = -0.019\,\text{ksi}$$

Force in the strand groups after transfer

$$f_{cg\_straight} = 0.75 f_{pu} + n_i[f_{bot} + \frac{y_{b\_straight}}{h}(f_{top} - f_{bot})]$$

$$f_{cg\_straight} = 0.75(270) + 8.86[-2.28 + \frac{3.48}{53}(-0.019 + 2.28)] = 184 \text{ ksi}$$

$$P_{straight} = 184(26)(0.153) = 731 \text{kip}$$

$$f_{cg\_harped} = 0.75 f_{pu} + n_i[f_{bot} + \frac{y_{b\_harped}}{h}(f_{top} - f_{bot})]$$

$$f_{cg\_harped} = 0.75(270) + 8.86[-2.28 + \frac{42.4}{53}(-0.019 + 2.28)] = 198 \text{ ksi}$$

$$P_{harped} = 198(6)(0.153) = 182 \text{ kip}$$

$$f_{cg\_courtesy} = f_{jack} + n_i[f_{bot} + \frac{y_{b\_courtesy}}{h}(f_{top} - f_{bot})]$$

$$f_{cg\_courtesy} = 26.2 + 8.86[-2.28 + \frac{51}{53}(-0.019 + 2.28)] = 25.3 \text{ ksi}$$

$$P_{courtesy} = 25.3(4)(0.153) = 15.5 \text{ kip}$$

Integrate stress over concrete area from bottom of girder up until resultant force in concrete equals the applied force in the straight strand group (731 kip)

Height (in)	*Width (in)*	*Stress (ksi)*	*Force (kip)*	*y_b (in)*	*y_b · Force (in-kip)*	*Σ Force (kip)*
0	32	-2.28	0	0	0	0
7	32	-1.98	-477	3.42	-1630	-477
10	14	-1.85	-132	8.48	-1120	-609
13.5	7	-1.70	-65.3	11.7	-764	-674
18.5	7	-1.49	-56.2	16.0	-896	-731
				Σ =	-4410	

Sample calculations for highlighted values

$$Force = \frac{(32 + 32)}{2}\frac{(-2.28 - 1.98)}{2}(7 - 0) = -477 \text{ kip}$$

$$y_b = \frac{(7-0)[2(1.98)+2.28]}{3(2.28+1.98)} = 3.42 \text{ in.}$$

Find location of the resultant force in the concrete

$$y_{b\_resul\tan t} = \frac{-4410}{-731} = 6.03 \text{ in.}$$

Unbalanced internal moment

$$M = (y_{b\_resul\tan t} - y_{b\_straight})P_{straight}$$

$$M = (6.03 - 3.48)(731) = 1864 \text{ in-k}$$

Note: Integrating the stress over concrete area from top of girder down, will produce the same unbalanced moment within the section

Solve the strut and tie models

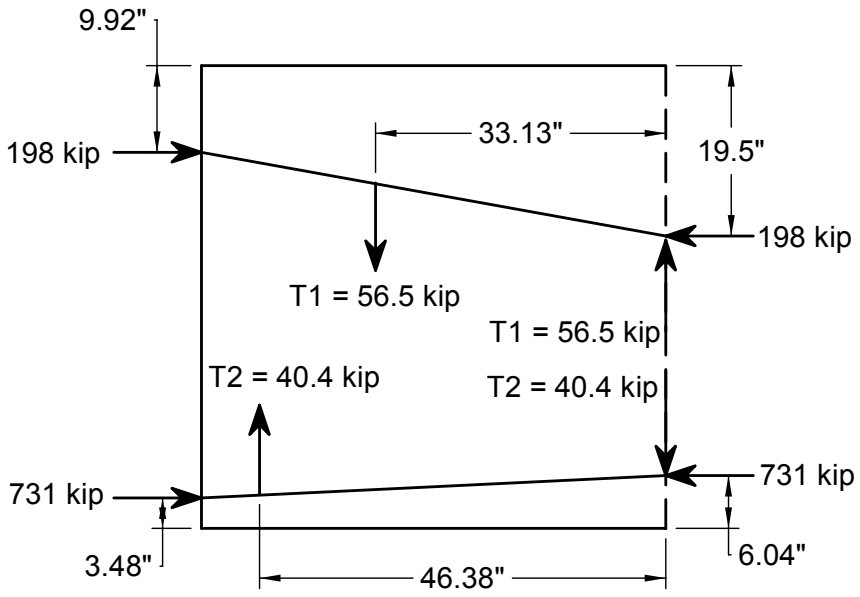

$$T_1 = \frac{1864}{33.1} = 56.3 \text{ kip} \qquad T_2 = \frac{1864}{46.4} = 40.2 \text{ kip}$$

Design the reinforcement

Control anchorage zone – stirrup working stress = 18 ksi

f_s = 18 ksi

Area of steel required for lower strut and tie model

$$A_s = \frac{T_2}{f_s} = \frac{40.2}{18} = 2.23 \text{ in}^2$$

Select 4 No. 5 bars uniformly distributed over $h/4$, $A_{s\_provided} = 2.48$ in^2

Area of steel required for upper strut and tie model

$$A_s = \frac{T_1}{f_s} = \frac{56.3}{18} = 3.13 \text{ in}^2$$

Note: The model assumes this area of steel is uniformly distributed from the end of the girder to $3h/4$ even though the area of stirrup reinforcement within h/4 will be more densely spaced.

Area of steel required from $h/4$ to $3h/4$

$$A_s = \frac{3.13}{0.75h}(0.5h) = \frac{3.13(0.5)}{0.75} = 2.09 \text{ in}^2$$

Select 4 No. 5 bars uniformly distributed from $h/4$ to $3h/4$, $A_{s\_provided} = 2.48$ in^2

Note: The spacing for 4 No. 5 bars between $h/4$ and $3h/4$ is 8.83 in. which exceeds the minimum spacing in this region for horizontal shear transfer of 7 in. The minimum spacing for stirrups for horizontal shear transfer will control.

Experimental anchorage zone – stirrup working stress = 12 ksi

f_s = 12 ksi

Area of steel required for lower strut and tie model

$$A_s = \frac{T_2}{f_s} = \frac{40.2}{12} = 3.35 \text{ in}^2$$

Select 5 No. 5 bars uniformly distributed over $h/4$, $A_{s\_provided} = 3.1$ in^2

Area of steel required for upper strut and tie model

$$A_s = \frac{T_1}{f_s} = \frac{56.3}{12} = 4.69 \text{ in}^2$$

Note: The model assumes this area of steel is uniformly distributed from the end of the girder to 3*h*/4 even though the area of stirrup reinforcement within h/4 will be more densely spaced.

Area of steel required from *h*/4 to 3*h*/4

$$A_s = \frac{4.69}{0.75h}(0.5h) = \frac{4.69(0.5)}{0.75} = 3.13 \text{ in}^2$$

Select 5 No. 5 bars uniformly distributed from *h*/4 to 3*h*/4, $A_{s\_provided} = 3.1 \text{ in}^2$

Beam end detailing

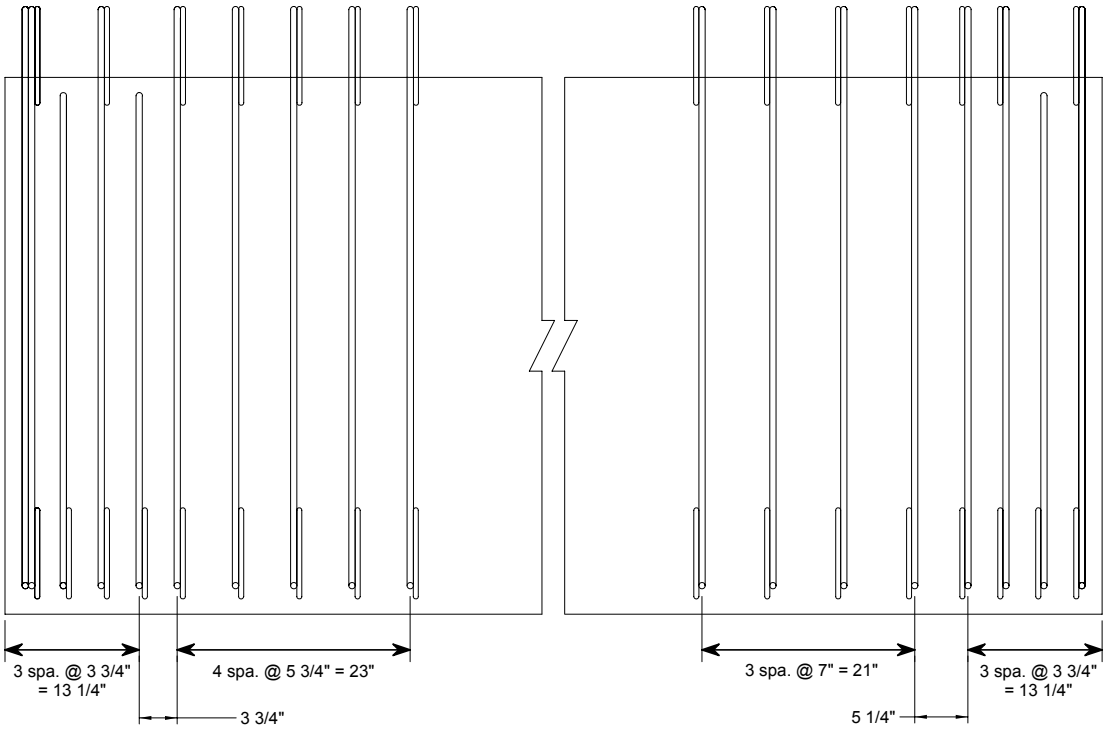

12 ksi Beam End Reinforcement Detail

18 ksi Beam End Reinforcement Detail

Note: Flanges of beam have been removed for clarity.

Vita

Eric D. Crispino is a native of Southington, Connecticut. He received his commission from the United States Military Academy in May 1998 and holds a Bachelor of Science degree in Civil Engineering.

Eric's first assignment was as a Troop Fire Support Officer with Howitzer Battery, 1st Squadron, 3rd Armored Cavalry Regiment at Fort Carson, Colorado in January 1999. He also served as a Battery Fire Direction Officer, Platoon Leader, Executive Officer, and as the Squadron Adjutant. Following this tour at Fort Carson, Eric attended the Captain's Career Course at Fort Sill, Oklahoma.

In October 2002, Eric was assigned to the 3rd Battalion, 6th Field Artillery at Fort Drum, New York. He served as the Battalion Fire Direction Officer and deployed to JRTC in December 2002. He then served as the Battalion Fire Support officer for 2nd Battalion, 22nd Infantry where he deployed to Operation Enduring Freedom IV. On 5 February 2004, Eric took command of Charlie Battery at Orgun-E, Afghanistan. The battery redeployed to Fort Drum in May 2004 and began the transformation process. As part of this transformation the battery was redesignated as Alpha Battery and moved to the new platoon-based battery concept.

In 2005, Eric accepted a position as an instructor within the Civil and Mechanical Engineering Department at West Point, NY. In preparation for this assignment he completed studies at Virginia Polytechnic and State University from 2005 to 2007 where he received a Master of Science degree in Civil Engineering.

Eric is married to the former Amy White of Southington, Connecticut. They have a son, Patrick, age 4 and a daughter, Anna, age 10 months.